

Final Report

"An MHD Heat Source Based on Intermetallic Reactions"

June 15, 1991

from

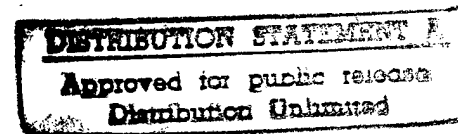
General Sciences, Inc.
205 Schoolhouse Road
Souderton, PA 18964

submitted to

U.S. Department of Energy
Pittsburgh Energy Technology Center

as a requirement of

Contract No. DE-AC22-87PC79679



PLEASE RETURN TO:

BMD TECHNICAL INFORMATION CENTER
BALLISTIC MISSILE DEFENSE ORGANIZATION
7100 DEFENSE PENTAGON
WASHINGTON D.C. 20301-7100

19980309 184

U 4457

Accession Number: 4457

Publication Date: Jun 15, 1991

Title: MHD Heat Source Based on Intermetallic Reactions

Personal Author: Sadjian, J.; Marston, C.H.

Corporate Author Or Publisher: General Sciences, Inc., 205 Schoolhouse Road, Souderton, PA 18964

Report Prepared for: US Department of Energy, Pittsburgh Energy Technology Center, P.O.Box 10940, Pittsburgh, PA 15236-0940

Descriptors, Keywords: Space Power Technology Transfer MHD Heat Source Intermetallic Reaction Ion Release

Pages: 00072

Cataloged Date: Apr 19, 1993

Contract Number: DE-AC22-87PC79679

Document Type: HC

Number of Copies In Library: 000001

Record ID: 26691



Department of Energy
Pittsburgh Energy Technology Center
P.O. Box 10940
Pittsburgh, Pennsylvania 15236-0940

July 8, 1991

Mr. Charles Sharn
SDIO/SY
Washington, DC 20301-7100

Dear Mr. Sharn:

The Pittsburgh Energy Technology Center (PETC) entered into an interagency agreement with the Strategic Defense Initiative Organization (SDIO) for the purpose of developing and implementing a program titled "Feasibility Assessment Program for Space-Based, Multi-Megawatt, MHD Power System." PETC awarded eight contracts resulting from a PRDA that solicited proposals for innovative, fundamental/applied research approaches complementing the feasibility assessment program.

The SDIO Space Power Program Manager, Richard L. Verga, requested that PETC implement a Technology Transfer Program. As part of our response to this request, I have attached the final report for Contract No. DE-AC22-87PC79679 with General Sciences, Inc. This report is one of the eight contracts implementing innovative, fundamental/applied research.

Sincerely,

A handwritten signature in cursive script, reading "Leo E. Makovsky", is positioned below the word "Sincerely,".

Leo E. Makovsky
Advanced Power Generation and
Fundamental Research Division

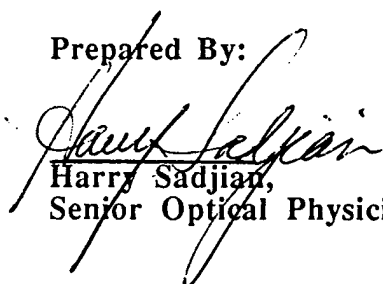
Enclosure

cc w/o enclosure:
G. Staats, PETC
H. Chambers, PETC

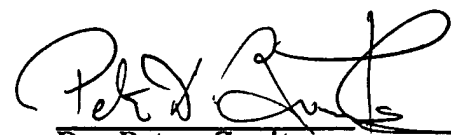
cc w/enclosure:
R. Verga, SDIO

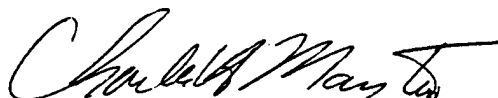
AN MHD HEAT SOURCE BASED ON
INTERMETALLIC REACTIONS

Prepared By:


Harry Sadjian,
Senior Optical Physicist

Approved By:


Dr. Peter Zavitsanos,
President, GSI



Dr. Charles H. Marston,
Associate Professor,
Villanova University
Villanova, PA

ABSTRACT

The main objective of this program was the development of an MHD heat source for potential use in Space - Based Multi Megawatt, MHD Power Systems.

The approach is based on extension of high temperature chemical/ion release technology developed by the General Sciences, Incorporated (GSI) team and successfully applied in other Space Applications. The relevance to the SDIO/MHD objectives is a natural one in that solid state reactions have been identified which can deliver energy densities and electrons in excess of those from high energy explosives as well as other conventional fuels.

The use of intermetallic reactions can be used to generate hot hydrogen plasma from the reaction, to create a high level of seedant ionization, can be packaged as cartridge type fuels for discrete pulses. The estimated weight for energizing a (100 MW - 1000 sec) Pulsed MHD Power System can range from 12 to 25×10^3 kg depending on reaction system and strength of the magnetic field.

The program consisted of two major tasks with eight subtasks designed to systematically evaluate these concepts in order to reduce fuel weight requirements.

Laboratory measurements on energy release, reaction product identification and levels of ionization were conducted in the first task to screen candidate fuels. The second task addressed the development of a reaction chamber in which conductivity, temperature and pressure were measured. Instrumentation was developed to measure these parameters under high temperature pulsed conditions in addition to computer programs to reduce the raw data.

Measurements were conducted at GSI laboratories for fuel weights of up to 120 grams and at the Franklin Research Center* for fuel weights up to 1 kilogram.

The results indicate that fuel weight can be scaled using modular packaging. Estimates are presented for fuel weight requirements for SDIO pulsed power applications.

* Located at Elverson, PA.

TABLE OF CONTENTS

<u>Section</u>	<u>Page</u>
A. BACKGROUND AND SCOPE	1
B. PROGRAM PLAN AND TECHNICAL PLAN	7
B. 1. BOMB CALORIMETER TESTS	7
B. 2. DTA MEASUREMENTS	9
B. 3. IONIZATION MEASUREMENTS	9
C. SMALL REACTION CHAMBER AND INSTRUMENTATION	13
C. 1. REACTION CHAMBER	13
C. 2. INSTRUMENTATION	16
D. TEST RESULTS FROM SMALL REACTION CHAMBER	21
E. SCALED-UP TESTING (250 grams to 1 kg)	38
F. CONCLUSIONS AND RECOMMENDATIONS	43
G. ESTIMATION OF FUEL WEIGHT REQUIREMENTS FOR SDIO APPLICATIONS	46
ACKNOWLEDGEMENTS	46
REFERENCES	48
APPENDIX A. EVALUATION OF THE POTENTIAL OF HEATED HYDROGEN AS THE WORKING FLUID IN A LARGE, SPACE BASED, MHD POWER GENERATION SYSTEM	50
APPENDIX B. CALCULATION OF CONDUCTIVITY AND PROGRAM LISTING	53
APPENDIX C. PROGRAM LISTING FOR CALCULATING TEMPORAL CONDUCTIVITY FROM VOLTAGE VS. CURRENT DATA	64
APPENDIX D. LARGE SCALE TEST FACILITY	65
APPENDIX E. PHOTOMETRIC MEASUREMENT OF TEMPERATURE	71

A. BACKGROUND AND SCOPE

The advantages of MHD for large scale pulsed power have long been recognized. The most notable example is the Avco Mark V self-excited "rocket generator" (Reference 1) which produced 23.5 MJ net output for a few seconds as early as 1964 at a specific energy of approximately 0.5 MW/kg and an enthalpy extraction of about 8%.

In the 1970's attention shifted to commercial power generation, with the emphasis on high efficiency and control of air pollutants. While much valuable technology work was accomplished, including a deeper understanding of the complex behavior of an MHD generator, little or no overall cost advantage was shown relative to conventional coal fired power plants (Reference 2).

Probably the most significant results of this era applicable to large scaled pulsed power came from the tests of the High Performance Demonstration Experiment (HPDE) at Arnold Engineering Development Center (AEDC). The HPDE produced 30.5 MW at a specific energy of .61 MJ/kg and an enthalpy extraction of about 11% (Reference 3).

The AEDC work was important both for what was accomplished and for the difficulties encountered. While never operated at full power, generator performance was up to expectations as far as it was tested. HPDE testing ended when the magnet support structure suffered a catastrophic brittle failure as a result of unanticipated local stresses at cryogenic temperature (Reference 4). The failure underscores the critical role of magnet design in any large scale MHD power system.

Enthalpy extraction as a function of the principal design variables is shown for both the Mark V and the HPDE in Figure A.1 (Reference 5). The parameter has the dimensions of reciprocal velocity because Mach Number was used to represent velocity. Since the value of the parameter depends on how one computes average values, an error bar rather than a precise point would probably better represent the data. Nevertheless the plot can provide some guidance in estimating potential performance of large scale units.

Also relevant to the objectives of this program are, the reports by the University of Tennessee Space Institute (UTSI) (Reference 7 and 8). The review on the "Status of Explosive MHD Technology in the Soviet Union" suggests that the explosive concept is capable of producing high energy pulses of several 100 MW for short durations of (10 - 100) μ sec. It offers the advantages of repetitive and high stored energy densities (~ 5 MJ/kg or 1.2 Kcal/g) and with improvements could be applied to potential military applications. In fact, if one could extend the pulse duration by one or two orders of magnitude without compromising power, the concept could have a profound effect in SDI weapon systems.

The conclusions of the second UTSI publication (Reference 8) can be summarized as follows:

1. The future for explosive MHD generators in terms of SDI objectives can be enhanced only by increasing the (low $<5\%$) conversion efficiency and consequently their effective low energy density.
2. Combustion driven MHD pulse generators, on the other hand, appear more promising partly due to demonstrated increase of efficiency with increasing scale. This is not to say that the SDI objectives are easily obtainable.

The main objective of the SDIO/MHD Program is the development of a multi-megawatt (MMW) MHD power system which can be positioned in space to provide power to a variety of space weapons such as Electromagnetic Launches, Lasers and Particle Beams. The required power levels exceed 100 MW in bursts of 1 - 5 seconds for cumulative time periods of 1000 seconds or more. Fuel mass in the vicinity of 25 - 50 tons are required at conversion efficiencies of 15%. Due to the large numbers involved, significant improvements must be made in the following important parameters before a space based systems become feasible. These are:

1. power conditioning.
2. highly efficient magnetic designs
3. heat source improvements

Other ancillary problems, are minimization of the weight and volume of the device, minimization of the contamination of space optics and thrust control.

Power density for an MHD generator can be approximated as,

$$(\text{Power}/\text{Volume}) P_v \propto \sigma (v B)^2$$

That is, that power per unit volume is proportional to conductivity of the plasma times the product of gas velocity and magnetic field squared.

This work has addressed the problem of developing an efficient pulsed heat source which minimizes fuel weight while maximizing power output. In addition, the fuel mixture developed was designed to maximize conductivity in order to generate the optimum power density.

The approach used in this work centers on the use of a new heat source which can generate more energy per unit weight and volume than other propellants or solid fuels. The heat generated provides the vehicle to ionize seedants in a high velocity plasmas. The GSI heat source, called Hi-Therm, can be controlled as to its duration and output and serves to produce H₂ gas in-situ in one reaction.

The GSI method of generating a hot plasma in the form of a solid state reaction has important advantages. The Hi-Therm material has long-term stability, instant availability and can be packaged as disposable cartridges or modules with the potential for rapid reloading. In addition, Hi-Therm has been found to be environmentally safe (i.e. no toxins produced) and safe to handle under a variety of conditions of heat, impact and electrical discharge.

The final configuration developed under this program consisted of a mixture of Hi-Therm with Cesium seeded hydride which produced an ionized hydrogen plasma of nearly 3000°K. Theoretical calculations had indicated that such a plasma would produce a conductivity on the order of 100 Siemens/meter at static temperature of 3000°K. See Figure A.2 and Appendix B. Measurements of conductivity indicated values in excess of 100 Siemens/meter with durations of 1/2 to 1 second.

For a Space Based MHD generator a high energy density heat source is desired. For this reason a careful search was performed on available fuel candidates. Table I shows the heats of combustion in kcal/g for a variety of reactions. As expected, hydrogen heads the list followed by beryllium (Be) and boron (B). Since Be - powders represent a serious source of toxicity, it was discarded as a candidate. Boron is an attractive candidate because of its high heat of combustion

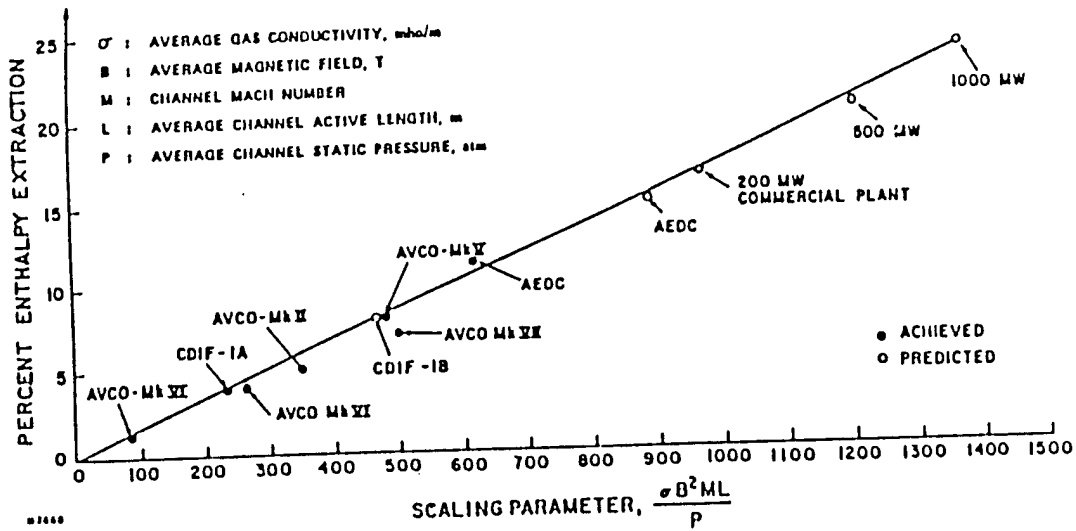


FIGURE A.1. SCALING OF MHD CHANNEL ENTHALPY EXTRACTION (REFERENCE 5)

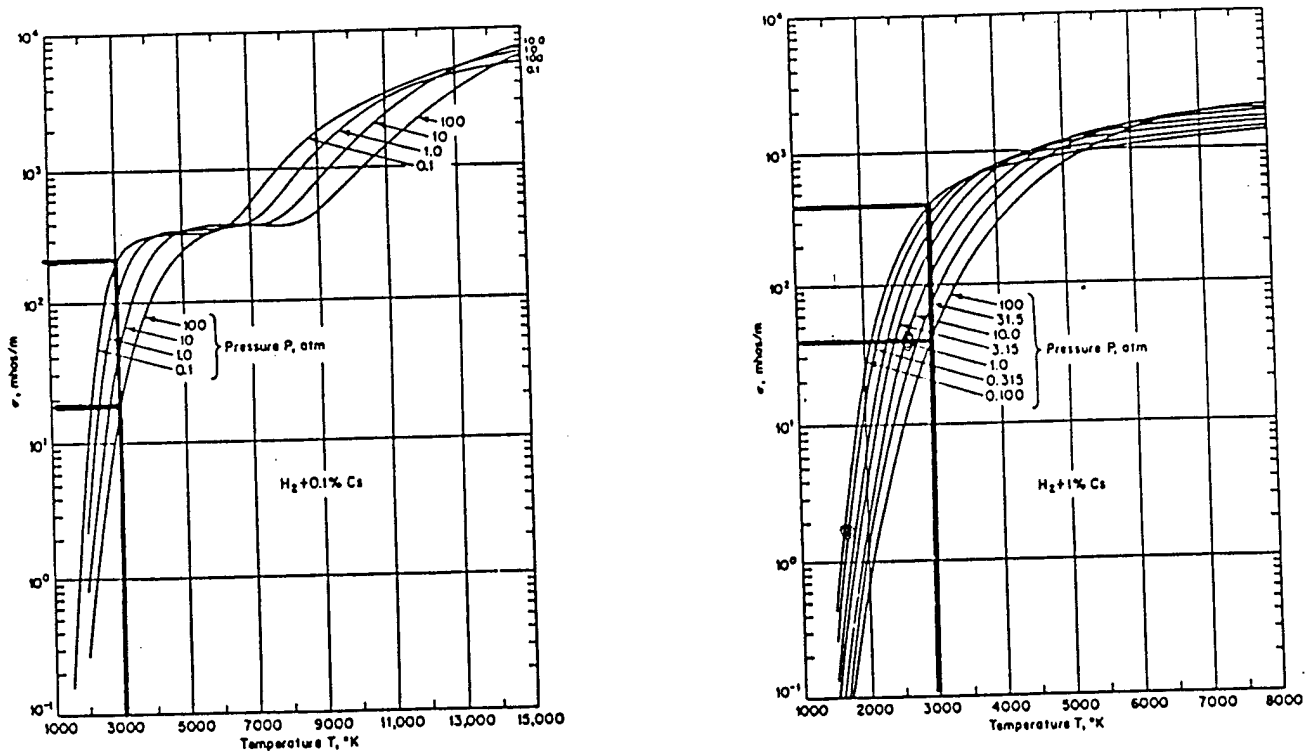


FIGURE A.2. ELECTRICAL CONDUCTIVITY OF CESIUM SEEDDED HYDROGEN (REFERENCE 1)

(a) HYDROGEN + 1.0E-3 CESIUM
 (b) HYDROGEN + 1.0E-2 CESIUM

TABLE 1
HEAT OF COMBUSTION OF VARIOUS MATERIALS

MATERIALS	Kcal/g	Kcal/cc
HYDROGEN = H_2	28.7	--
BERYLLIUM - Be	16.2	29
BORON - B	14.0	33
LITHIUM - Li	10.3	
CARBON - C	7.8	--
ALUMINUM - Al	7.4	20
SILICON - Si	7.3	18
MAGNESIUM - Mg	5.9	10
PHOSPHORUS - P	5.8	11
TITANIUM - Ti	4.6	20
CALCIUM - Ca	3.8	6
ZIRCONIUM - Zr	2.8	18
NIOBIUM - Nb	2.5	21
SULFUR - S	2.2	5
MOLYBDENUM - Mo	1.9	19
IRON - Fe	1.8	14
MANGANESE - Mn	1.7	12
CERIUM - Ce	1.7	11
TANTALUM - Ta	1.4	23
THORIUM - Th	1.3	14
ZINC - Zn	1.3	9
WOLFRAM - W	1.1	21
NICKEL - Ni	1.0	9
PARAFFIN & HYDROCARBONS	~ 10.3	
POLYSTYRENE	9.9	
PARAFFIN	9.8	
ASPHALT	9.5	
WOOD CHARCOAL	8.1	
LAMINAC	7.0	
GUANIDINE	4.2	
FLOUR, SUGARS, STARCHES, ETC.	3.6-4.0	
NITROCELLULOSE (COMBUSTION)	2.2-2.6	
NITROCELLULOSE (EXPLOSION)	1.0	

(14kcal/g). From the practical standpoint however, people have experienced a great deal of difficulty in trying to exploit this element as a high energy fuel, because the formation of B_2O_3 on the boron particles "chokes" the reaction.

Limited success was achieved by Max Planck Institute in this area by using reactive additives. More encouraging data were generated by Zavitsanos (Ref. 9-12) and his group at G.E. and later at GSI: In an effort to utilize the Ti/B reaction (now called Hi-Therm) as a heat source for Aerospace Applications and Materials Synthesis, this reaction was studied under many different conditions, one of which involved "pre-conditioned"* samples reacting in static air. Under this condition it was found that two exothermic processes take place. The first is the formation of TiB_2 i.e. $Ti + 2B \rightarrow TiB_2 + 1.2 \text{ kcal/g}$, the second is the combination of TiB_2 i.e. $TiB_2 + O_2 \rightarrow TiO_2 + B_2O_3 + 6.42 \text{ kcal/g}$. Figure A.3 shows typical DTA (Differential Thermal Analysis) and TGA (Thermogravimetric Analysis) response. At 928°K the steep rise in the DTA trace denotes the reaction of Ti with B to form TiB_2 . A second spike denotes the combustion of TiB_2 with air to form TiO_2 and B_2O_3 . The weight increases as noted of 91% and 88% compare favorably with the theoretical increase of 115%. The ratio of the area under the exotherm for combustion versus reaction is found to be 4.9 versus the theoretical ratio of 6.3.

When a comparison is made on that basis the order is as follows:

Be (5.82 kcal/g), B (4.4 kcal/g), Ti/2B/Li (4.18 kcal/g), Ti/2B/8B (4.12 kcal/g), Al (3.91 kcal/g), H_2 (3.19 kcal/g), H/C (Hydrocarbons) (2.79 kcal/g); aluminized propellants would somewhat be somewhere between aluminum and hydrocarbons.

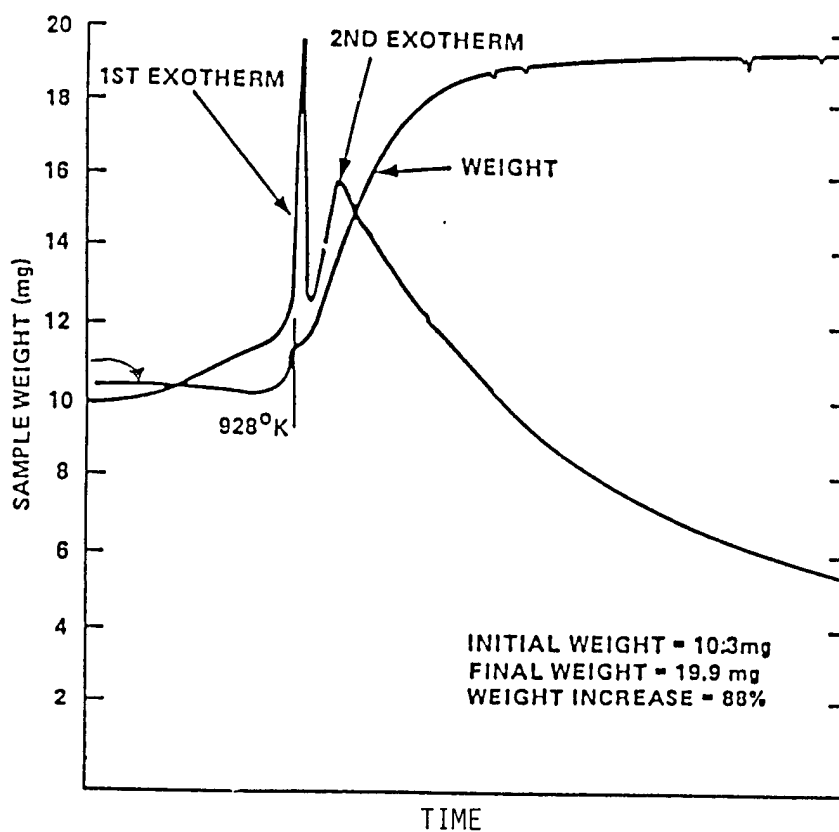
Other chemical reactions which proceed in the condensed phase are the conventional pyrothermites. The thermites constitute a class of reactions which have been used for many heat related applications, including atmospheric releases of barium/metal from canisters on sounding rockets. The intermetallic systems, however, have outperformed this conventional technology (originally developed by Max Planck) due to superior energy content and versatility. GSI was given the task of the Chemical Canister and Heat Development of the CRRES (Combined Radiation and Release Satellite) Program. This program was completed at GSI and 52 multi-kg canisters and 20 heaters were delivered. The canisters are designed to release ionized Li and Ba in space and the heaters will transfer heat to SF_6 for release in the ionosphere.

The development most pertinent to the program is the pioneering work of Dr. Zavitsanos on the development of highly exothermic solid state compositions which surpass other chemical reactions in this category in terms of energy density, temperature, level of ionization, ability to store, initiate, dispense, seed and Scale-up. This work was originally supported by the Air Force (Rome Air Development Center), and ARPA and a portion was patented as a "Metal Vapor Generator" by P. D. Zavitsanos U.S. Patent #4092,263 May 30, 1978. (Ref. 9). Subsequent to this effort this particular chemical system has been used as a "clean", manageable, energy source in

* Proprietary Process at GSI.

Use of disclosure of this data is subject to the restriction on the title page of this document.

General Sciences, Incorporated
Proprietary Information



NOTES

1ST EXOTHERM
DUE TO TiB_2
FORMATION

2ND EXOTHERM
DUE TO TiB_2
COMBUSTION
(TiO_2 & B_2O_3)

TOTAL ENERGY
RELEASED
6.2 kcal/g
(82%
THEORETICAL)

FIGURE A.3. TWO-STEP EXOTHERMIC RELEASE

General Sciences, Incorporated
Proprietary Information

many aerospace applications (replacing conventional thermite and pyrotechnics technology) as a metal vapor/ion generator for Al, Nd, Sm, Ca, Sr, Ba/Ba⁺, Li⁺, Cs⁺ these released quantities range from 20kg to small .1 gm size Cs - seeded pellets to be released as decoys using ionization enhancement.

Another area which was explored for the Air Force (Ballistic Missile Office) is the development of a Cs - seeded fuel in a pellet form (.2 cm diam). Upon initiation with 600°K source, each pellet acts as a high temperature spherical micro-furnace ($T > 3200^{\circ}\text{K}$) releasing a plasma consisting of cesium ions and electrons while the reacting components remain in the solid form in essentially the original spherical shape: $\text{Ti(c)} + 2\text{B(c)} + \text{Cs - Salt} \rightarrow \text{TiB}_2\text{(c)} + \text{Cs}^+ + \text{e}^-$. Seeding levels as high as 8% (by weight) have been tested at GSI and at the Delco Ballistic Range facility and very high levels of ionization efficiency have been verified (50 - 80% in many cases). The same pellets large or small which can be used to eject ions (without movement) can be moved by a flow provided either externally or by a decomposing binder internal to the fuel charge.

Based on the above analysis, it was concluded that the Ti/2B reaction (Hi-Therm) represented the optimum reaction in terms of maximizing the stated goals of this effort.

An evaluation of heated hydrogen as a working fluid in a large, space based, MHD power generation system was presented in our original proposal. For completeness, it is reproduced as Appendix A.

B. PROGRAM PLAN AND TECHNICAL PROGRAM

This development program was divided into two tasks with multiple sub-tasks for each task. The initial task involved the analysis, design and measurements of candidate reaction schemes for down-selection and selections of the most promising for subsequent testing and evaluation under task 2. In task 2, the design and fabrication of the reaction chamber and measurements of conductivity and pressure evolved from the small vacuum chamber (~ 2' x 4') testing involving low mass fuel charges used in task 1 to large mass fuel charge testing in a large vacuum tank facility (~7' x 40'). Along the development process, instrumentation and reaction chamber configurations were modified to reflect the results of measurements of temperature, pressure and conductivity.

Modification of the original program plan were made during the development phase and final selection of the fuel charge mixture measurements made early in the program dictated certain changes in program direction.

B.1 Bomb Calorimeter Tests

In order to assess the effect of additives to the basic Hi-Therm material (Ti/2B in stoichiometric proportions), a series of bomb calorimeter tests were conducted. The requirement for producing a hot ionized hydrogen plasma dictated the evaluation of additives on the overall energy output of Hi-Therm.

The results of these tests are indicated on Table II. As expected, the addition of substantial amounts of TiH₂ or Cs compound does not affect the energy output substantially. The addition of

TABLE II. BOMB CALORIMETER TEST DATA
HEAT RELEASE IN KCALS/GM

TEST NUMBER	MATERIAL	GAS ENVIRONMENT	HEAT RELEASED
1	Ti/2B	N ₂	1.08
2	Ti/2B	N ₂	1.09
3	Ti/2B	O ₂	6.39
4	Ti/2B (50%) + TiH ₂ /2B (50%)	N ₂	1.03
5	Same as 4	N ₂	1.03
6	Ti/2B (95%) + Cs ₂ CO ₃ (5%)	N ₂	1.21
7	Same as 6	N ₂	1.17
8	Ti/3B	N ₂	1.1
9	Ti/3B	N ₂	1.11
10	Ti/4B	N ₂	1.04
11	Ti/4B	N ₂	1
12	Ti/2B + 2.12% K ₂ CO ₃	N ₂	1.25
13	Same as 12	N ₂	1.22
14	Ti/2B + 5/4 LiClO ₄ *	N ₂	1.71
15	Same as 14 *	N ₂	1.65

* The lithium perchlorate was kept anhydrous until the test

perchlorates, although increasing energy output, requires special handling and the increased output is not large enough to warrant their use due to the increase in the safety hazard. The presence of O_2 increases the output many-fold but the methodology of introducing O_2 into the Hi-Therm material is a difficult one and could have required an substantial development effort.

Based on the calorimetric results, the use of Hi-Therm with TiH_2 and cesium compounds appeared to be the best combination to produce a hot ionized hydrogen plasma.

B.2. DTA Measurements

Differential Thermal Analysis (DTA) was conducted on candidate mixtures to augment the calorimetric results and additionally to determine,

1. reaction temperature
2. speed of reaction
3. relative safety of the reaction

The DTA measurements were made with a Eberback DTA Apparatus in ambient air. While the measurement of the temperature at which reactions took place are within the accuracy of the apparatus, the absolute calorific values calculated from these runs are only semi-quantitative. In some cases, scans showed two peaks with a shoulder due to the reaction of the materials and subsequent oxidation.

The results are tabulated in Table III. The test samples that contained lithium perchlorate are not included as this material reacted too violently during the test and was rejected based on safety considerations.

The Hi-Therm material was assigned a value of 1.2 Kcal/gm and was used as the standard for the equipment and test samples. As the results indicate, the addition of TiH_2 and cesium compounds do not materially effect energy output or the reaction temperature. Based on these results, the 50 : 50 mix of $Ti/2B$ and $TiH_2/2B$ was chosen as a starting point for initiating the ionization testing.

B.3 Ionization Measurements

The feasibility of producing MHD power depends on the ability to produce a stream of hot H_2 gas seeded with ionized potassium or cesium ions etc. using the intermetallic reaction $Ti + 2B$ as the heat source. Accordingly, GSI devised an ionization apparatus shown schematically in Figure B.1 and pictorially in Figure B.2. In this apparatus a pressed pellet of the intermetallic mixture containing the seed compound is enclosed in a cylindrical brass test chamber approximately 3.0 inches in diameter and 6.0 inches long which is evacuated. The pellet is housed in a small basket of Molybdenum wire which is supported on a pair of insulated feedthroughs. A 12.6 volt, 10.0 ampere transfer is connected to these feedthroughs to supply power for pellet ignition. This transfer is connected to a "Variac" which is normally set to about half the line voltage. The test chamber is polarized, by means of a small power supply, so that it is 20 volts positive with respect to the pellet. (It was experimentally determined that polarizing voltage is not critical). A 2.0 ohm precision resistor is connected in series with the power supply to measure

TABLE III

SAMPLE	WEIGHT mg	TEMP* C	PEAK AREA	CALORIES	Kcal/gm	
Ti/2B	9.79	440	3123	11.75	1.20	
From the above run 1 calorie was calculated to be equal to 266 area units.						
Ti/2B w 5%CsCO ₃	10.06	465	1134	4.26	0.43	
Ti/2B w 2.1%K ₂ CO ₃	2.90	615	1470	5.52	1.90	
TiH ₂ /2B	7.05	590	1950	7.33	1.04	
TiH ₂ /2B w 5%CsCO ₃	6.40	500	1365	5.13	0.80	
TiH ₂ /2B w 2.1%K ₂ CO ₃	5.13	555	1845	6.93	1.35	
Ti/3B	7.14	440	372	1.40	0.20	} 1.1
		585	1700	6.39	0.89	
Ti/2B50% TiH ₂ /2B50%	6.50	460	474	1.78	0.27	} 1.02
		550	1292	4.86	0.75	

*Temp. at peak maximum

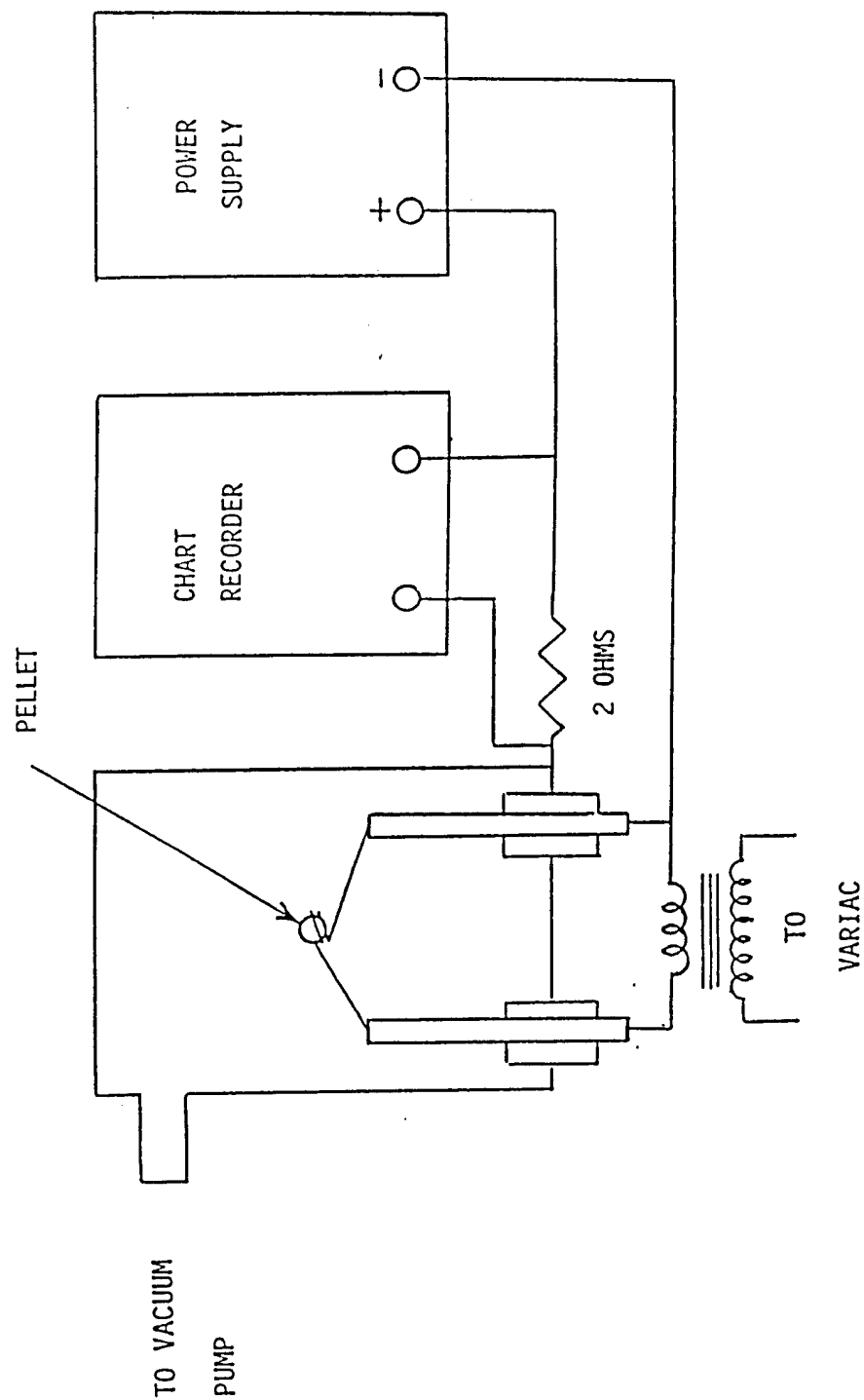


FIGURE B.1. SCHEMATIC OF IONIZATION APPARATUS

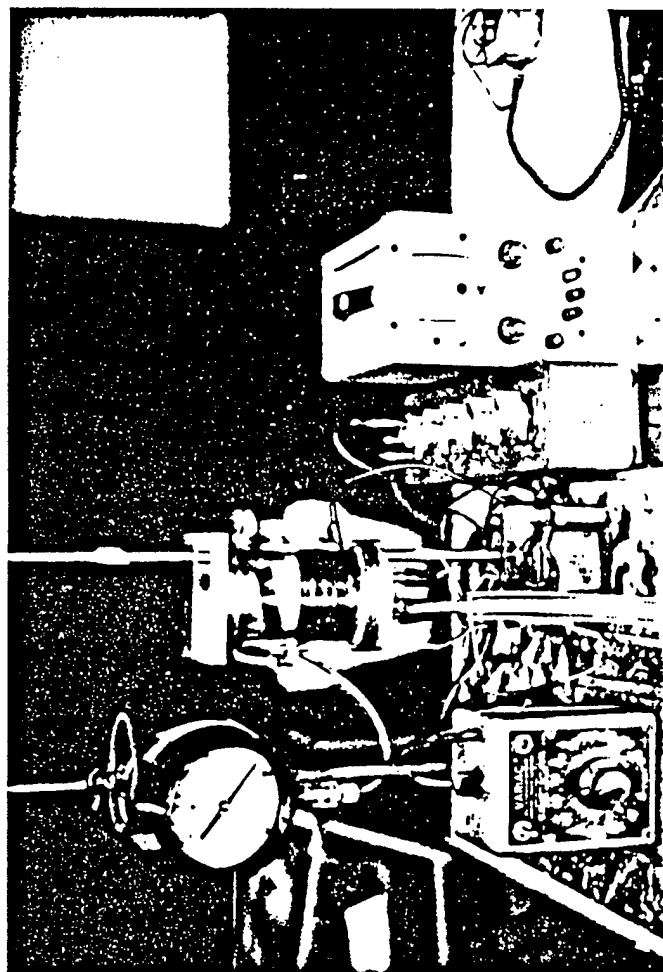


FIGURE B.2. PHOTOGRAPH OF IONIZATION APPARATUS

current flow. A Fisher Recordall Series 5000 Omniscribe Chart Recorder is connected across the resistor to record the current.

Tests were run with the recorder set for 1.0 volts full scale and with a chart speed up to 2.6 cm per minute. Unfortunately, this system has limitations in that the response time of the recorder was not fast enough to fully resolve the pulse shape even when running at the maximum chart speed. Tests at the high chart speed seem to indicate a pulse duration in the order of 1/2 second, as all the pulses seem to look alike, except for amplitude and it has become fairly common to run tests with a chart speed of 2.5 cm per minute.

Figure B.3 show a typical electron density trace for $\text{Ti} + 2\text{B} + 5\% \text{CsNO}_3$ and $.7 \text{TiH}_2 + 3\text{Ti} + 2\text{B} + 5\% \text{CsNO}_3$. Note that both currents peak at near the same value indicating that the presence of hydrogen has a negligible effect on electron output. Former work* had shown that for the experimental conditions of chamber pressure at $\sim .02$ atmospheres, the electron output using these materials is about 45 percent of theoretical maximum.

It was concluded from these results that there was a choice in the seeding methods available for rendering the hot hydrogen gas stream conductive. Easily ionized compounds can be added in situ to the hydrogen source as was demonstrated here, or alternatively, injected downstream in a more conventional manner.

C. SMALL REACTION CHAMBER AND INSTRUMENTATION

C.1 Reaction Chamber

The initial testing was carried out in the GSI (2' x 3') vacuum tank fitted with a chamber designed to hold up to a 100 gram charge. Figure C.1 shows diagrammatically the experimental arrangement. The reaction chamber consisted of a combustion chamber which holds the charge, a diaphragm and a wire screen. The test cell which housed the conductivity cell, pressure sensor and optical window was fitted with an expansion nozzle which allow the generated gases to flow into the vacuum tank (dump tank). The charge was initiated electronically.

During the course of testing, different thickness diaphragms were used (to control duration of release) usually of polyethylene ranging from 2 mils to 25 mils. The wire screen was fine mesh molybdenum wire initially used to reduce particle flow. The optical window was used in the initial testing to record the spectra of the flow in order to determine temperature in the test cell (also called measurement chamber).

In the later testing, the wire screen and diaphragms were removed and replaced with 10 mil grafoil as the results indicated extensive heat loss to the surroundings.

In addition, a burst disc port was incorporated in the measurement chamber to act as a relief valve if the pressure exceeded 10 atmospheres (relief port set for 15 atmospheres). On the early experiments it was found that the burst disc would thermally degrade due to the hot particulates. Subsequent tests incorporated the burst disc at the end of elbow tubing to prevent this.

* Zavitsanos, PD & Semon, H. "Exothermic Pellet Development for Wake Augmentation" - Final Report. GSI, Plymouth Meeting PA November 1986.

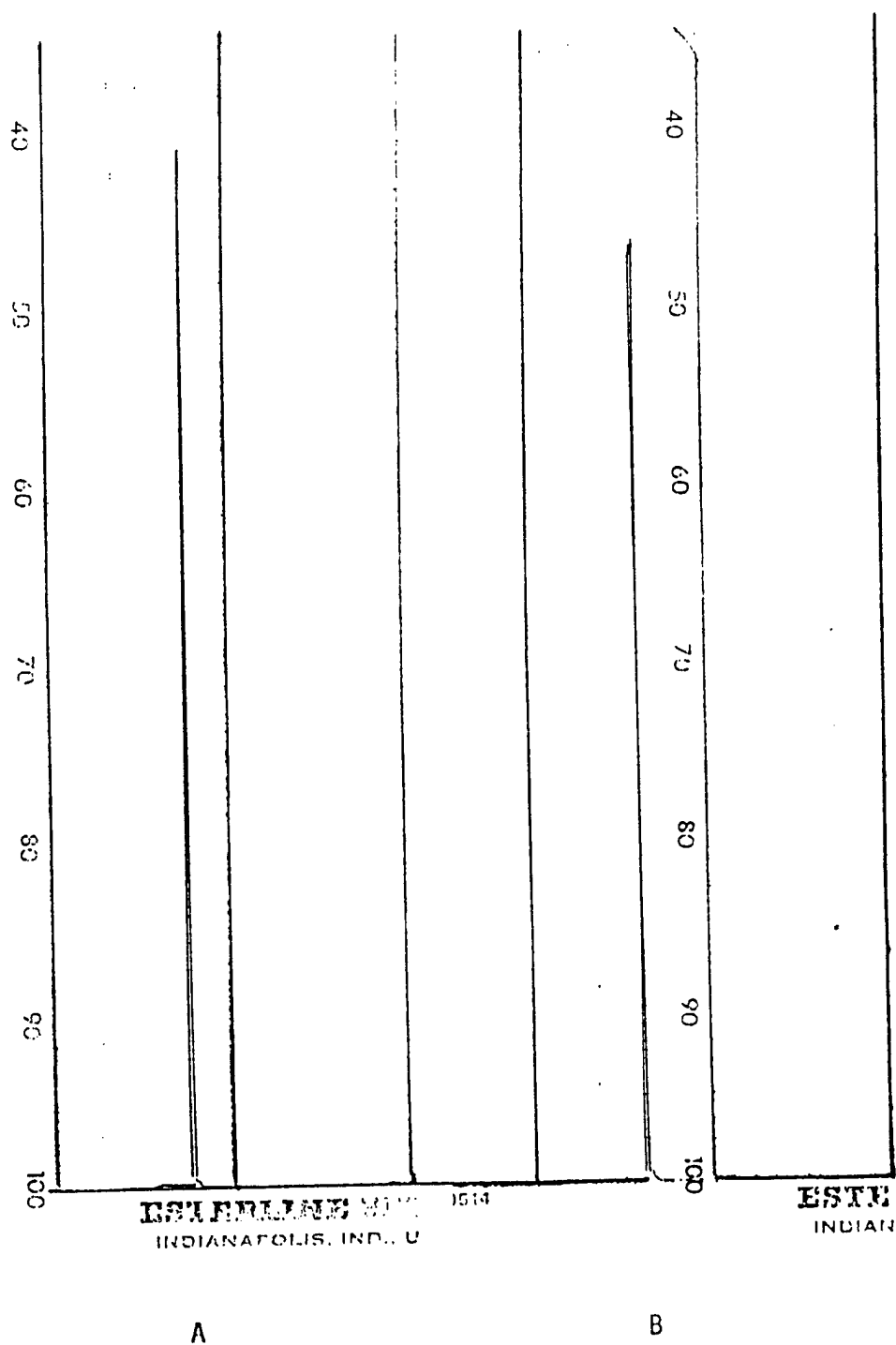


FIGURE B.3. ELECTRON DENSITY TRACE

FOR (A) $T_1 + 2B + 5\% \text{CsNO}_3$ AND (B) $.7\text{TiH}_2 + .3\text{Ti} + 2B + 5\% \text{CsNO}_3$
 SHOWING NEGLIGIBLE (IF ANY) EFFECT ON ELECTRON OUTPUT DUE TO THE
 PRESENCE OF HYDROGEN.

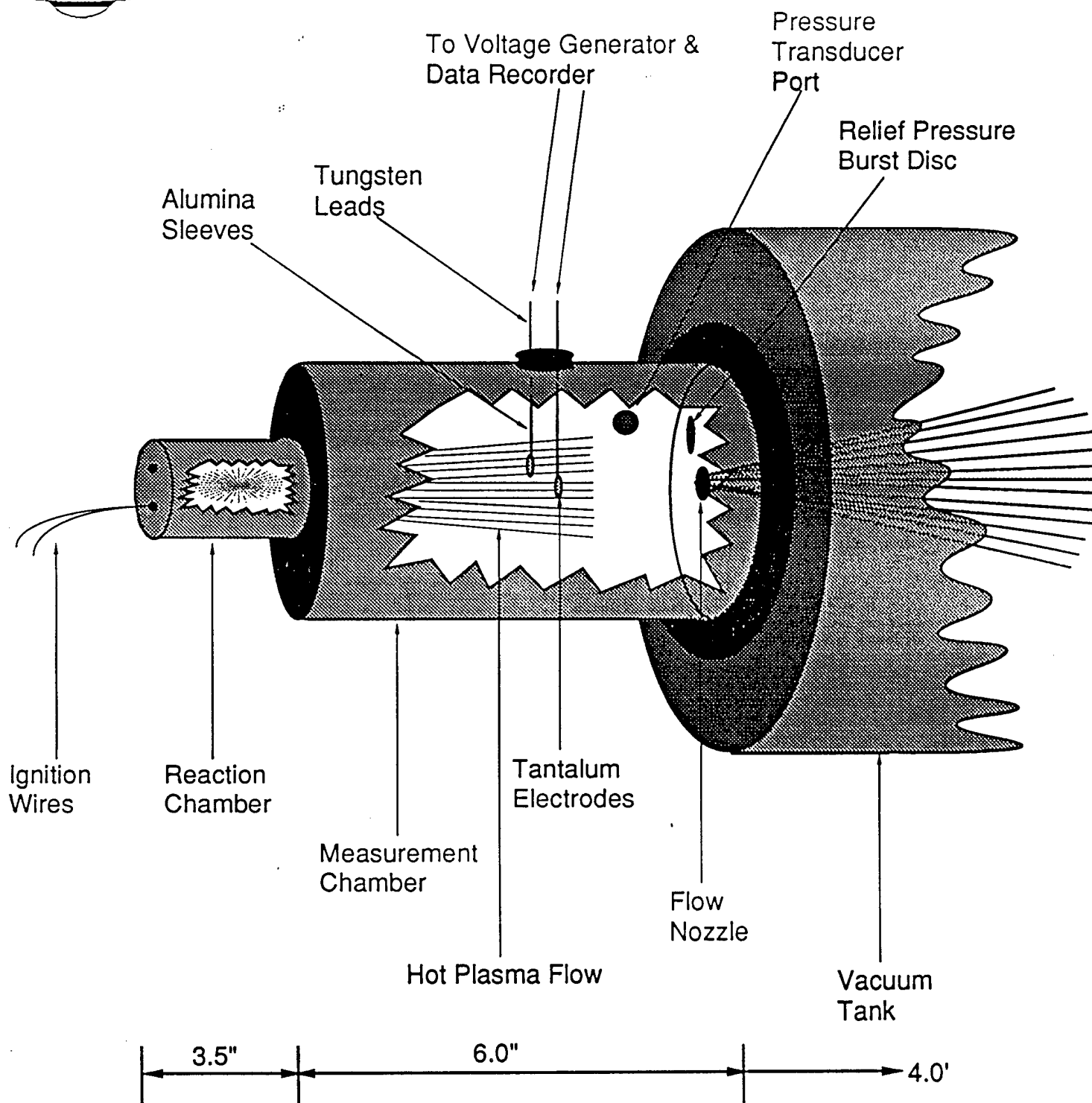


FIGURE C.1. DIAGRAM OF PULSED HEAT SOURCE GENERATOR ATTACHED TO VACUUM TANK

In Figure C.2a is shown a picture of the reaction chamber and combustion chamber assembled and the attachment to the wall of the vacuum chamber through the expansion nozzle and the burst disc port (melted by the hot particulates).

C.2 Instrumentation

The goal of this program was to develop a pulsed ionized gas source of high velocity. From theoretical consideration (see Appendix B), it was determined that conductivities approaching 100 S/M at pressures of 10 atmospheres were attainable. Consequently, instrumentation was developed to measure temperature, pressure and conductivity.

For the pressure measurements, the measurement chamber was fitted with a pressure port connected to a coiled copper tubing ending in a Setra pressure transducer (Figure C.2b). The coiled copper tubing was necessary to allow the gas to cool before reaching the transducer. A photograph of the plasma flow in the vacuum tank is shown in Figure C.3.

The measurement of conductivity in a high temperature pulsed flow presented a challenge as existing probe configurations would not be usable. Our initial attempts at measuring conductivity utilized a high temperature conductivity probe described in Reference 13. A drawing of the RF high temperature probe is shown in Figure C.4. Enameled copper wire is wound around an alumina tube which is encased in a boron nitride cylinder to protect against the high temperature plasma. A low power RF frequency is applied to the coil.

The method is based on the interaction of a small R.F. field with a conducting fluid. The created RF magnetic field, B , of the coil (Figure C.4) also creates a perpendicular electric field, $E(t)$, which in turn produces in the plasma small R.F. currents of density $j(t) = \sigma E(t)$. The ohmic dissipated energy density $j E^2$ is proportional to the plasma conductivity σ . When the dissipated power is measured external to the probe, σ can be determined. One of the difficulties of this probe is due to the attenuation of the dissipated power density varying as r^{-4} from the coil. Consequently, the size of the casing and distance from the coil was an important consideration. In addition, the impressed frequency must be much less than the collision frequency of the electrons; otherwise D.C. conductivity is not measured (valid at high pressure).

The probe was calibrated against known conductivity values of KCl solutions. Initially calibrations were made before and after each run.

In our attempts to use this probe, it was found that it was not sensitive enough to produce meaningful dissipation measurements. After several attempts to use this conductivity probe, it was abandoned.

A conventional double electrode probe was used to measure the conductivity of the remaining tests. Initial operational tests used two tungsten wire electrodes which proved successful. A modification was made by incorporating tantalum electrodes (to define the area of measurement more precisely) and shielding the tungsten wire with alumina tubes. A diagram of the tantalum double probe is shown in Figure C.5. This probe was used for a substantial number of tests until it appeared that the tantalum electrodes became non-responsive (i.e. lost sensitivity)

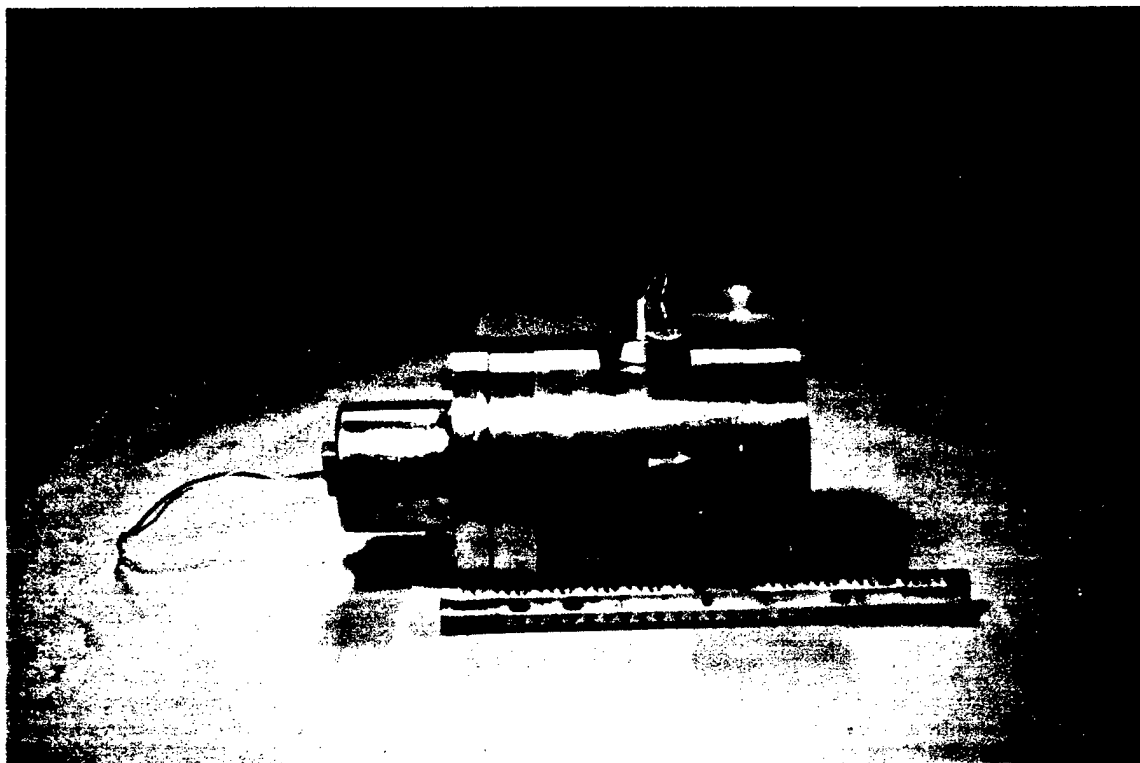


**FIGURE C.2a. MHD COMBUSTION CHAMBER AND
MEASUREMENT CHAMBER ASSEMBLED**



**FIGURE C.2.b. MHD REACTOR CELL ATTACHED TO VACUUM TANK
SHOWING THE COUPLED COPPER TUBING**

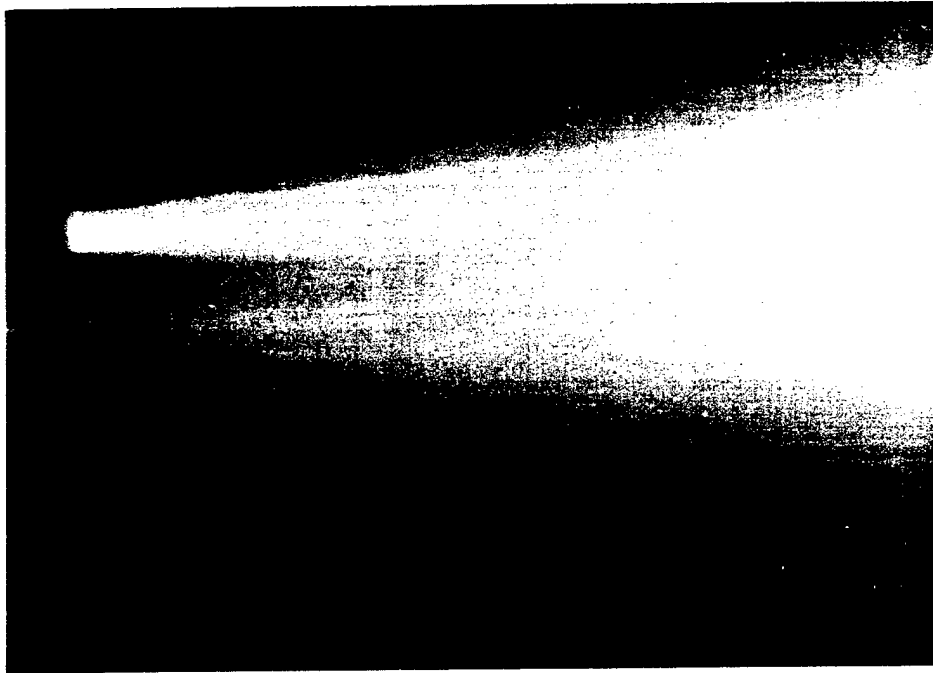


FIGURE C.3. VIEW IN VACUUM TANK SHOWING PLASMA FLOW FROM NOZZLE AND BURST DISC PORT

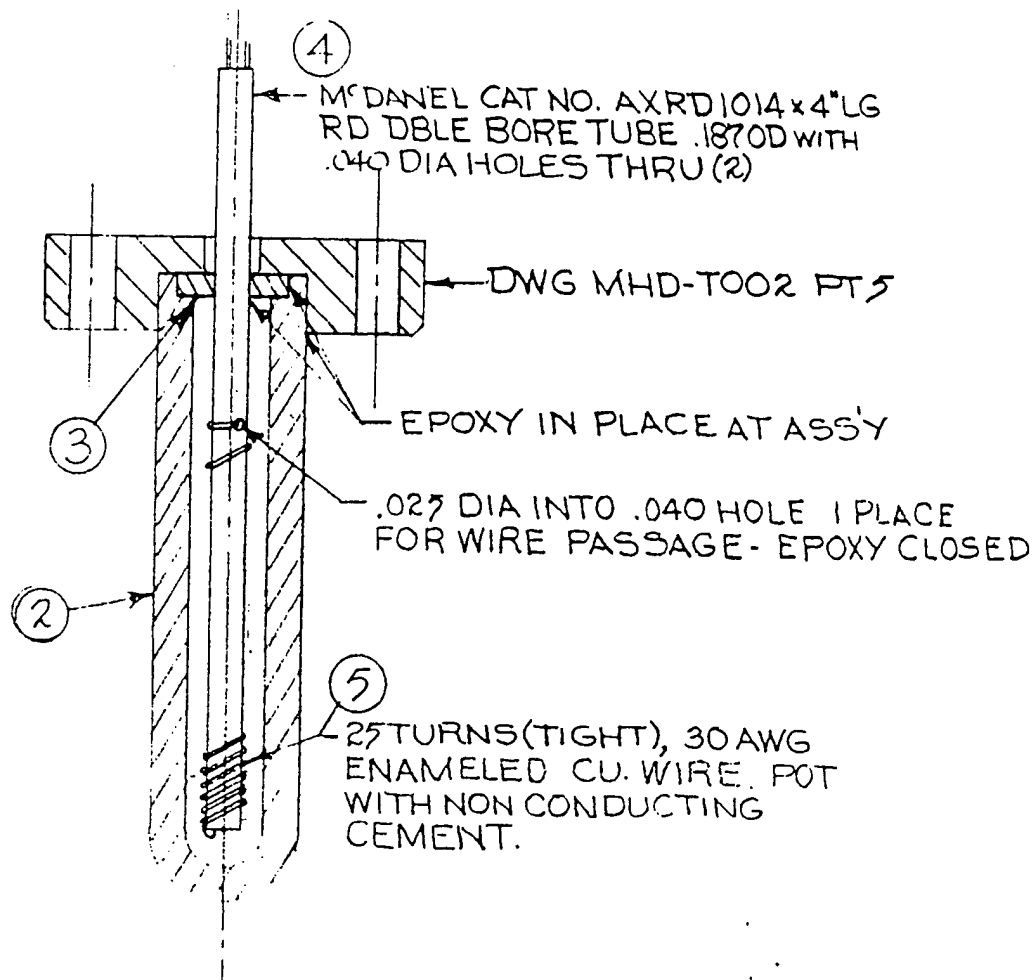


FIGURE C.4. DRAWING OF RF CONDUCTIVITY PROBE USED IN INITIAL MEASUREMENTS

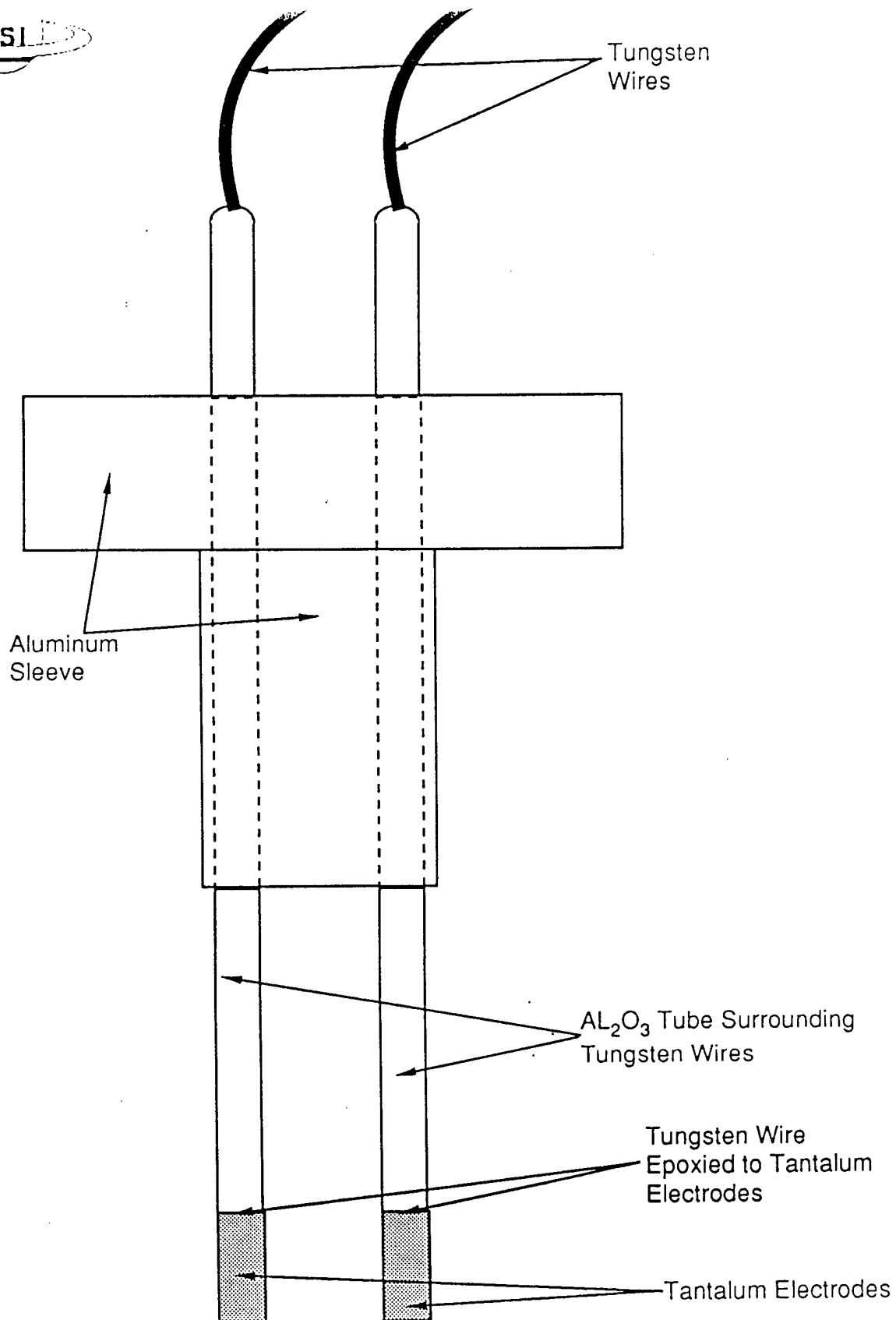


FIGURE C.5. DIAGRAM OF TANTALUM DOUBLE PROBE USED FOR MEASURING CONDUCTIVITY--SCALE 2X

probably due to hydrogen "poisoning". For the remainder of the tests a conventional tungsten electrode double probe was used without the tantalum electrodes.

The double probe was excited by 60 Hz voltage with a peak of 20 volts. The resulting current change was recorded during the test and an effective resistance was obtained. The probe was calibrated against known conductivity KCl solutions (certified by Fischer Scientific) and an effective cell constant was derived. The final conductivity was obtained from,

$$\sigma = \frac{A \text{ (probe constant in meter}^{-1}\text{)}}{R \text{ (ohms)}}$$

The probe was calibrated before and after each test. The raw data was recorded on a conventional stereo tape recorder by converting the raw voltage signals to frequency. The process was reversed and presented to the computer for processing. The overall recording scheme developed under this program is diagramed in Figure C.6. In order to reduce the labor of data reduction, a computer program was also written. In this program, the average resistance is determined (i.e. from the V-I profile) every 20 milliseconds. The conductivity is then obtained from the probe constant and measured resistance to produce a temporal conductivity profile. The overall procedure used on all our tests is diagramed in Figure C.7. A listing of the program used to reduce the raw voltage and current data to temporal conductivity is reproduced in Appendix C.

D. TEST RESULTS FROM SMALL REACTION CHAMBER

The results of the first series of tests are shown in Table IV. Initially a 50 : 50 mixture of Ti/2B and TiH₂ with a 50 gram total charge were used. We employed a fiber optic photometer to measure the light output from the hot particulates in the measurement chamber fitted with an optical window. The correlation between light output and temperature is shown in Figure D.1. Using this curve an estimate of temperature could be made in order to determine the efficiency of conversion of heat of combustion of the reaction to temperature. For these tests pressure measurements were made with a typical pressure profile shown in Figure D.2.

The first three tests indicated a great loss of energy based on the low temperature. It was decided to confirm this by using the RF probe to measure conductivity and an optical spectrograph (1.5 Meter Bausch and Lomb) to determine what species may be contributing to the low temperature. The spectra confirmed the low temperature by the presence of TiH molecule (a low temperature species) and by the calcium reversal method. The RF probe failed to produce meaningful results; however, the low temperature ~1500°K indicated unexpected energy losses in the system. In tests 8 and 9, the ratio of TiB₂ to TiH₂ was increased as was the amount of charge to allow a more efficient energy transfer to the TiH₂. This increased the temperature by about 500°K but still too slow to obtain substantial conductivities (see curve in Appendix B).

In Table V is shown the second series of tests (number 10 to 15) in which the RF probe was abandoned and replaced by the double tungsten probe with tantalum electrodes. As the table indicates, the difference between seeded and unseeded flow showed a factor of 10 change in conductance (mhos). Although, the results were encouraging, the conductance values were still too low.

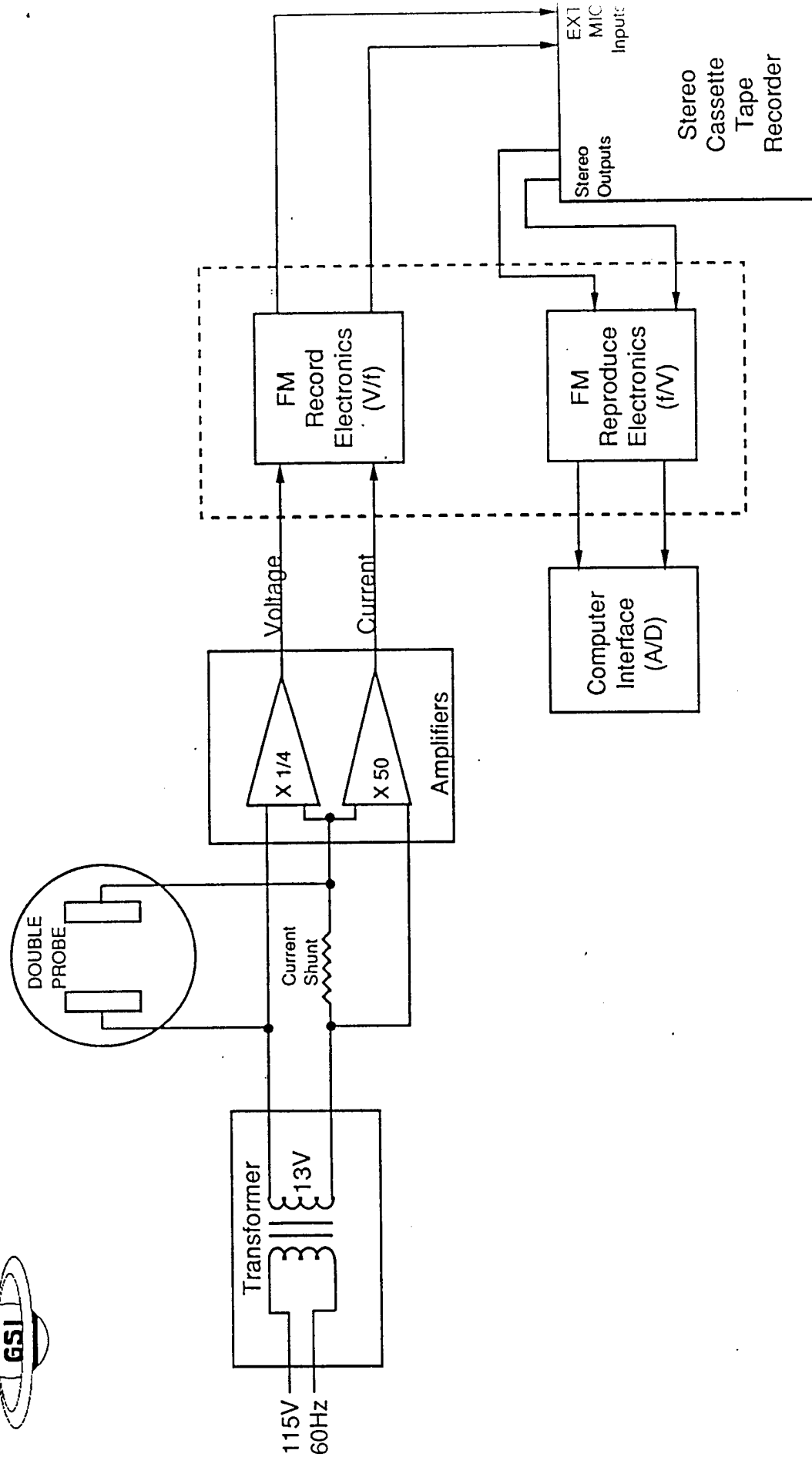


FIGURE C.6. BLOCK DIAGRAM OF VOLTAGE GENERATOR AND DATA RECORDER USED TO MEASURE CONDUCTIVITY OF PULSED HEAT SOURCE GENERATOR

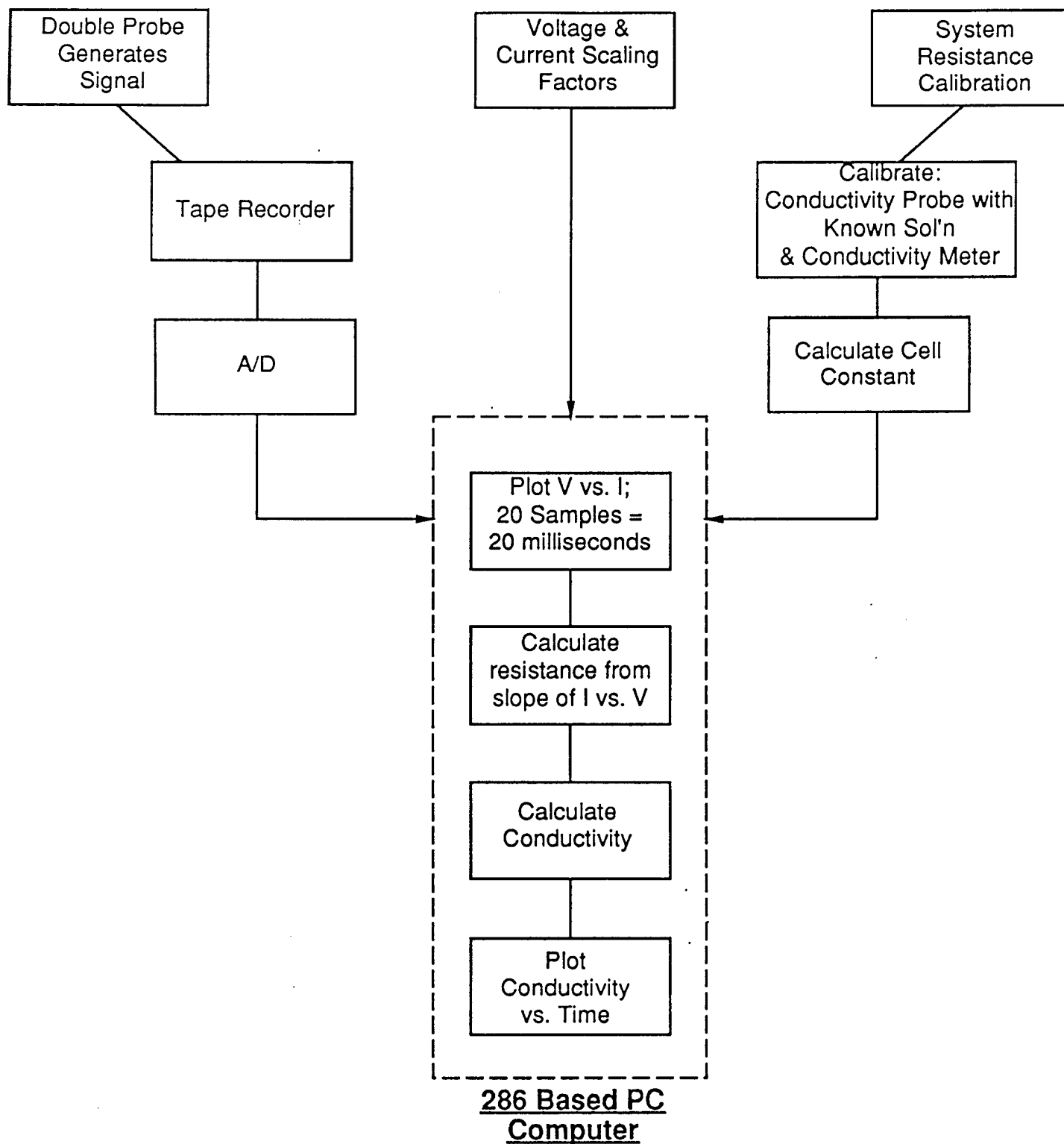


FIGURE C.7. FLOW CHART OF PROCEDURE USED TO GENERATE TEMPORAL CONDUCTIVITY PLOTS FROM DOUBLE PROBE DATA

TABLE IV.
CONDITIONS AND INITIAL TEST REQUIREMENTS OF MHD HEATER

NO.	DATE	TOTAL CHARGE (grams)	NOMINAL CHARGE COMPOSITION % BY WEIGHT					% MASS EJECTED	INSTRUMENTATION DEPLOYED		SPECTROGRAPH	LIGHT PROBE (LUX)	EFFECTIVE BLACKBODY TEMP. BASED ON LIGHT PROBE
			Ti/2B	B	TiH2	CsN03	Ca0		PEAK PRESSURE (PSIA)	RF PROBE			
1	11/21/88	50	28	20	46	6	-	NR	61	-	-	-	-
2	11/23/88	50	29	22	49	-	-	NR	40	-	-	768(3)	1540 K
3	11/30/88	50	29	22	49	-	-	NR	39	-	-	432(3)	1480 K
4	12/07/88	50	29	22	49	-	-	38	43	AIP	-	-	-
5	12/09/88	50	28	20	46	6	-	26	-	AIP	TiH Spectral (Low Temp).	-	-
6	12/16/88	50	28	20	46	6	(1)	50	-	AIP	Heavy Red Continuum	-	-
7	12/21/88	50	29	21	48.5	-	1.5(2)	50	53	AIP	No Spectra	-	-
8	12/28/88	75	67	9	20	5	-	45	97(5)	AIP	2020 K Ca Line Reversal (7)	4 Pulses(6); (684), (606), (204), (30)	>1500 K
9	12/30/88	75	65	9	20	5	1.0(2)	61	52	AIP	No Spectra; window power covered	Single Pulse 33,000	1940 K

NR: NOT RECORDED AIP: ANALYSIS IN PROGRESS - = NOT USED OR FAILED TO RECORD

- (1) Ca0 DRIED ON MOLYBDENUM SCREEN
- (2) Ca0 MIXED WITH TOTAL CHARGE
- (3) RECORDER VALUES (COMPUTER GAVE SATURATED VALUES >1200 LUX)
- (4) LIGHT PROBE POSITIONED EXTERNAL TO OPTICAL WINDOW
- (5) COMPUTER READING (RECORDER VALUE WAS 68 PSIA)
- (6) COMPUTER READINGS (>1200, 500, AND 100)
- (7) REPRESENTS EFFECTIVE PLASMA TEMPERATURE

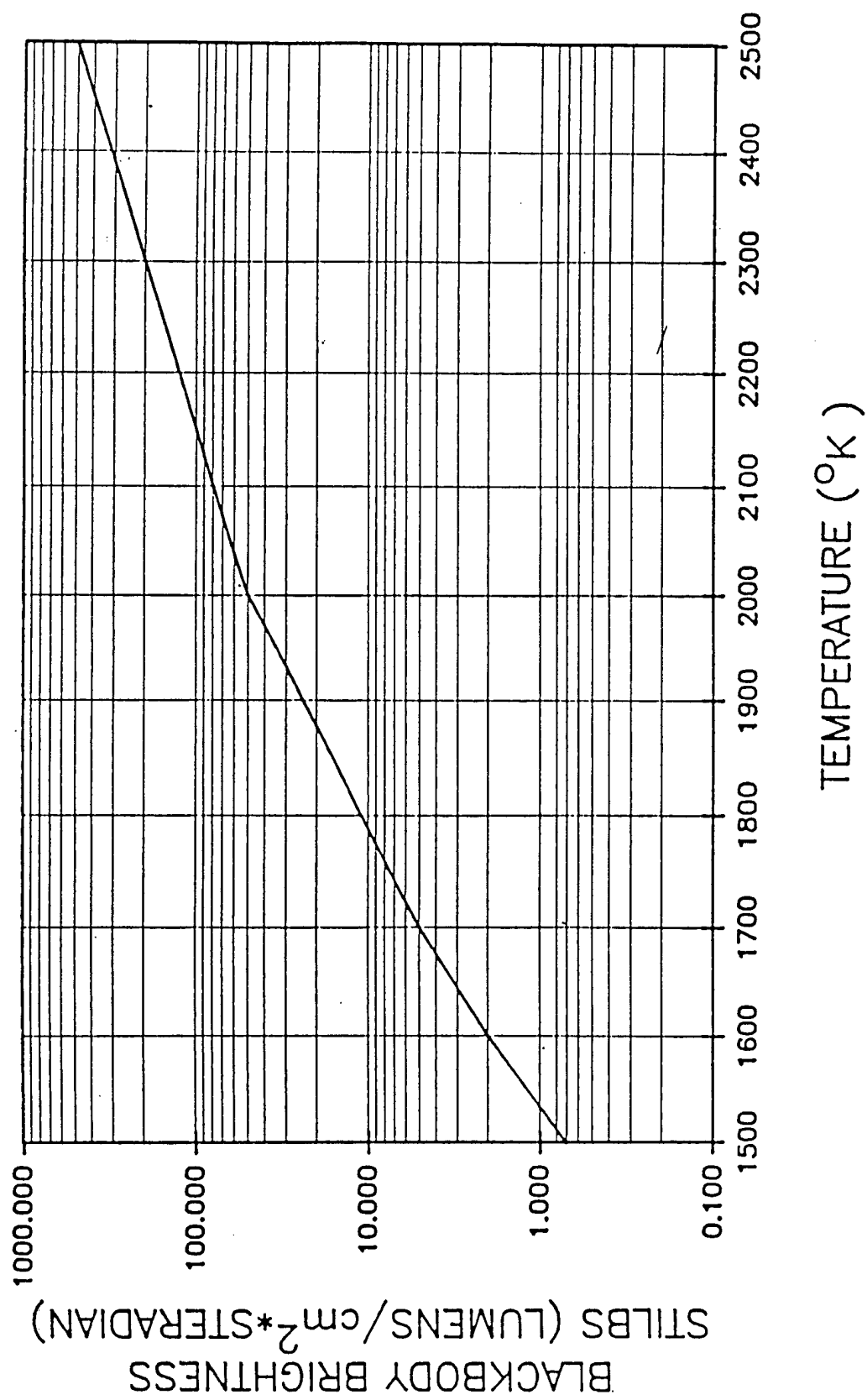
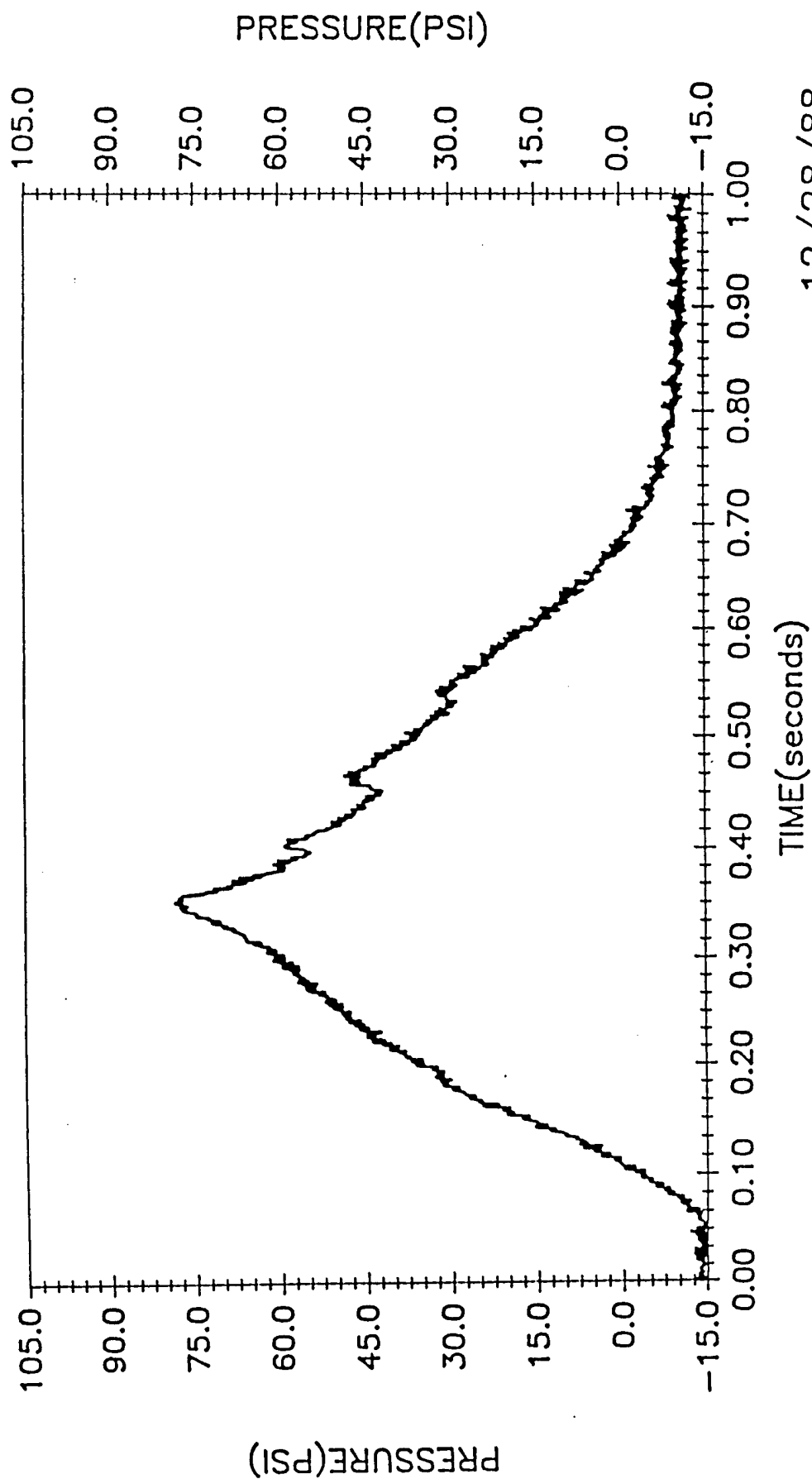


FIGURE D.1. VARIATION OF BLACKBODY BRIGHTNESS WITH TEMPERATURE

MHD CELL ASSEMBLY
PRESSURE VS TIME

DE-17



12/28/88

FIGURE D.2. TYPICAL PRESSURE PROFILE OF INITIAL MHD HEATER TESTS

TABLE V.
SECOND SERIES OF TESTS OF SMALL MHD HEATER CHAMBER

NOMINAL COMPOSITION OF CHARGE BY WEIGHT %										INSTRUMENTATION DEPLOYED			
TEST NO.	DATE	TOTAL CHARGE (gms).	Ti/2B	B	Ti/H2	CsN03	CaH2	%MASS EJECTED	PEAK PRESSURE (PSIA)	DOUBLE PROBE RESISTANCE (OHMS)	SPECTRO- GRAPH	PEAK LIGHT PROBE (LUX)	ESTABLISHED PEAK TEMPERATURE (KELVIN)
10	1/9/91	75	65	9	20	5	1	45	105	N/A	NO SPECTRA	16000	1800
(LIGHT PROBE)													
11	1/13/89	75	65	9	20	5	1	73	35	2500 (3)	HEAVY CONTINUUM	>50,000 Ca & Cs LINE	1950 (LIGHT PROBE) 1900
REVERSALS (SPECTRO- GRAPH)													
12	1/18/89	75	70	9	21	0	1	20(2)	25	100,000(1)	EMISSION LINES NOT IDENTIFIED	8000	1500
13	1/20/89	75	65	9	20	5	0	47(2)	95	3100(1)	NONE TAKEN	90000	1800
14	1/25/89	75	65	9	20	5	0	48(2)	80	4100(1)	NONE TAKEN	NOT USED	N/A
15	1/31/89	75	70	9	21	0	0	5	87	42000	NONE TAKEN	NOT USED	N/A

1 RESULTS ARE COMPUTER AVERAGED OVER DURATION BY REGRESSION PLOT
(RESISTANCE OBTAINED FROM SLOPE OF VOLTAGE VERSUS CURRENT CURVE)

2 SCREEN COATED WITH MgO TO BLOCK SOME OF THE PARTICLE FLOW

At this point in the program, we instituted the computer program to obtain temporal conductivity from the raw voltage/current data instead of just recording conductance. Runs #14 and #15 were evaluated in terms of conductivity. For run #16 our instrumentation failed and only pressure data was recorded. Run #17 was conducted as a replacement for #16.

In Figures D.3 and D.4, are shown the pressure profiles for runs #16 and #17 indicating some variance between runs. In Figure D.5 and D.6 are shown the calibration procedure used in the remainder of the runs. In D.5, a system check was always made before the run with a known resistor between the tantulum electrodes. In D.6 is shown the calibration curve using $45\mu\text{mhos/cm}$ KCl solution from which the probe constant is determined (i.e. in this case $K = .285\text{ cm}^{-1}$).

In Figure D.7 is shown the composite curve of the measured conductivities for seeded and unseeded flows. Although the conductives were still low, the difference was very sizable.

Starting with run #18 and running to #21 the ratio of $\text{Ti}/2\text{B}$ to TiH_2 was maintained but the charge increased to 100 grams as it was felt that the low fuel mass contributed to heavy losses to the environment. In addition, changes were made to the diaphragm and screens to allow freer particle flow. The conductivity profiles are shown in Figure D.8. As the flow became less restricted the conductivity increased although erratically. Note the change of conductivity scale in run #21. At this stage of development program, conductivities of about .1 to 1 S/M were being achieved but still erratic.

During this period, our tantulum double probe failed (i.e. lost sensitivity) and it was decided to revert back to the double tungsten probe insulated partly with an alumina sleeve. It was additionally decided to compact the fuel (similar to solid rocket fuel) and remove all diaphragms except the screen. Additional tests were conducted at 200g fuel weight. Pressures in excess of 20 atmospheres were recorded with subsequent destruction of the double probe. After several attempts at the higher fuel weight, destroying several probes in the process, the fuel weight was scaled back to 120 grams with only the screen present in the chamber. The runs between #22 and #26 were operational tests in which the probes were destroyed. The result of the compacted fuel with screen is shown in Figure D.9 (run #27). With the compacted fuel, the conductivity appears to be less erratic and has increased by a factor of 10 over previous tests. In addition, it is noted that the peak pressure slightly exceeds 10 atmospheres. Tests #28 and #29 were additional operational tests to improve the performance over #27; however, #27 seemed optimum.

A final sequence of tests were conducted in which the screen was removed maintaining 120 grams of compacted fuel. Tests were run with and without the seedant (CsNO_3). The conductivity results are shown in Figure D.10. Although still somewhat erratic, the conductivity increased by almost another factor of 10.

In Figure D.11 is shown an overview of all the small scale tests. This is indicated by the dotted rectangles against the theoretical predictions of a cesium seeded hydrogen plasma at 10 atmospheres. For all the tests conducted, the mole percent ranged from .01 to .06. As can be seen from Figure D.11, as the restrictions (diaphragms) were removed there appeared to be more efficient transfer of the heat of the reaction to hydrogen.

At this point, it was felt that the highest conductivity was achieved for the small scale testing. It was then prudent to scale the fuel weight up to reduce the loss of energy to the

MHD CELL ASSEMBLY PRESSURE VS TIME

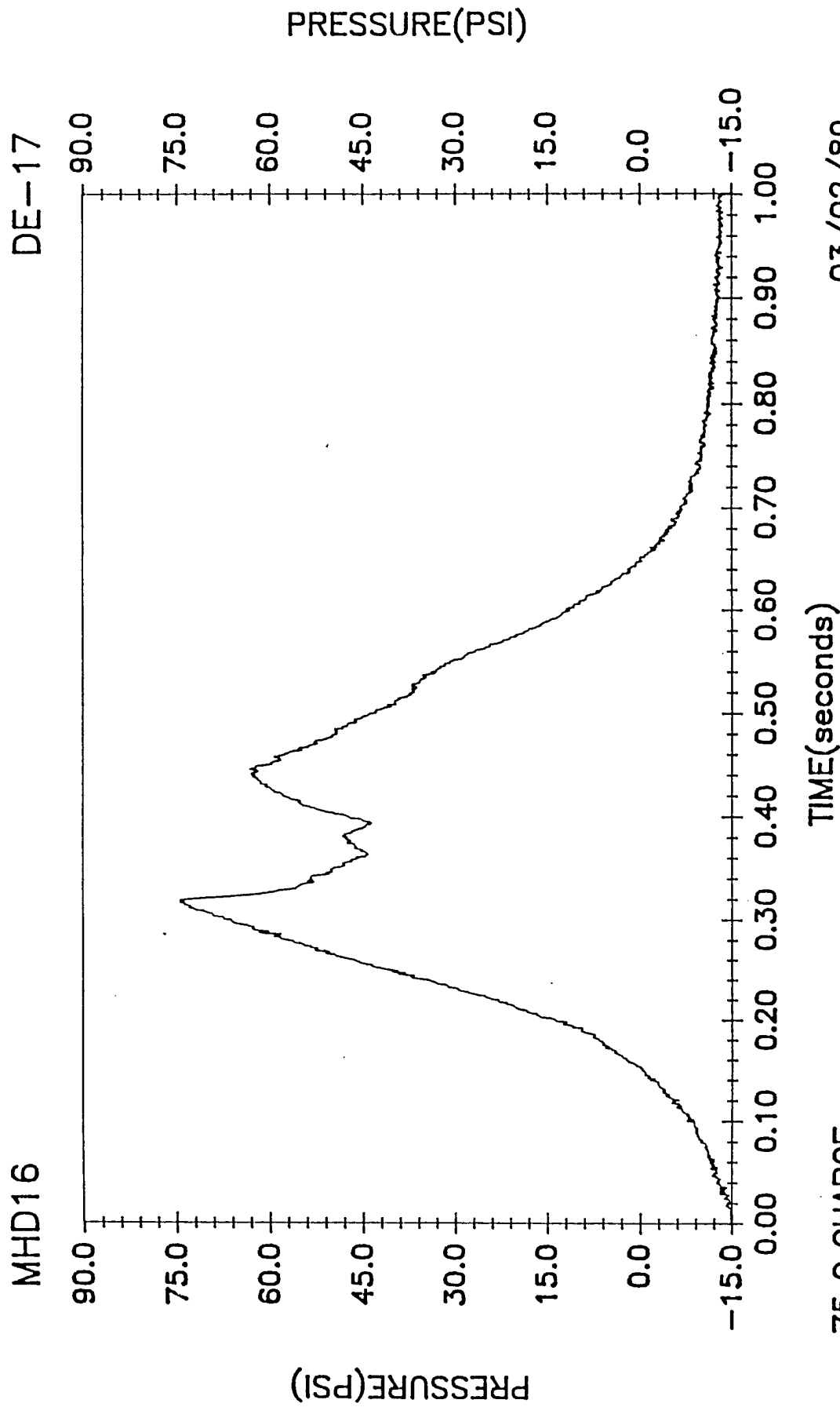
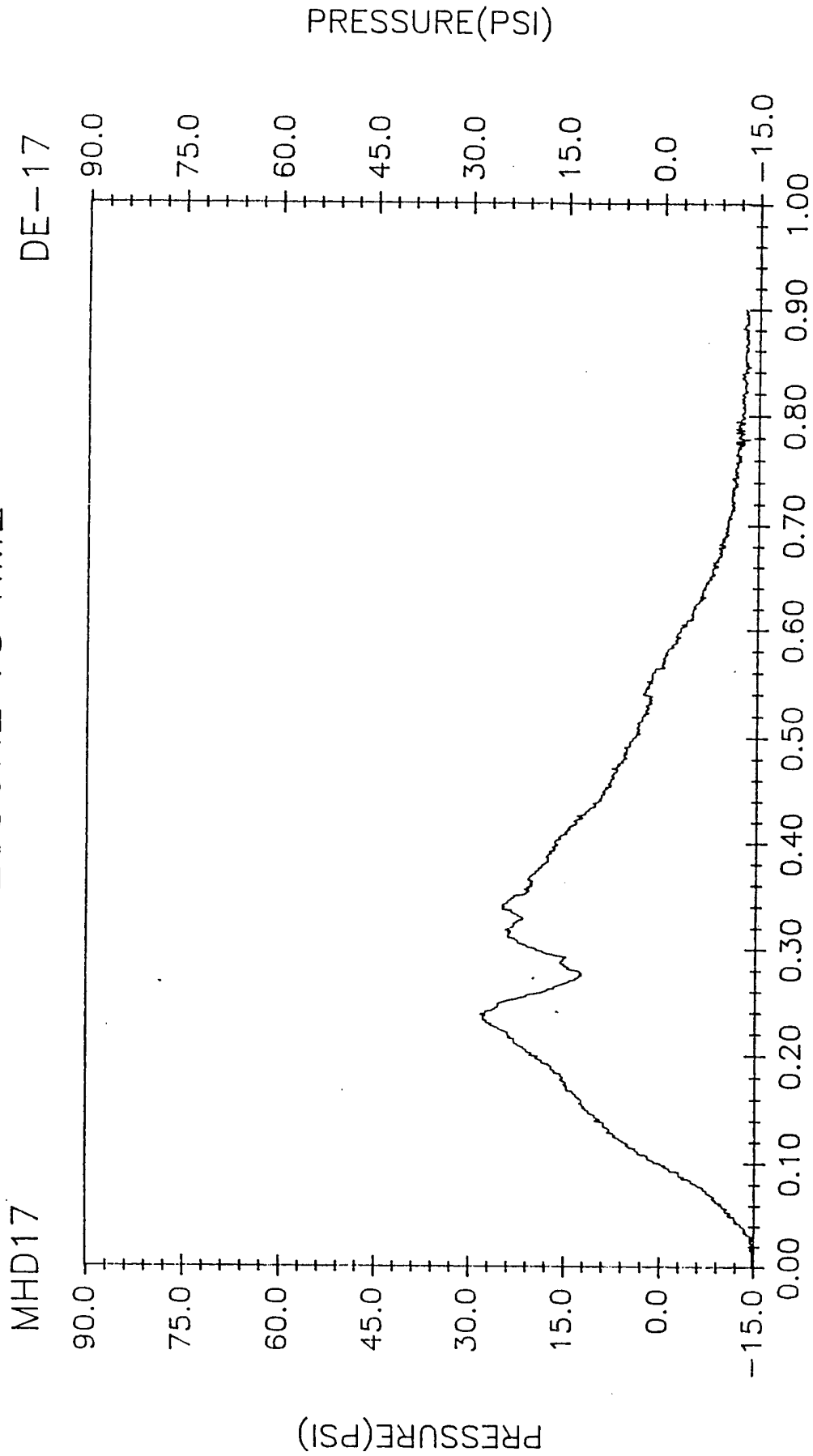


FIGURE D.3. TEMPORAL PRESSURE PROFILE RUN NO. 16

03/02/89

75 G CHARGE

MHD CELL ASSEMBLY PRESSURE VS TIME



03/22/89

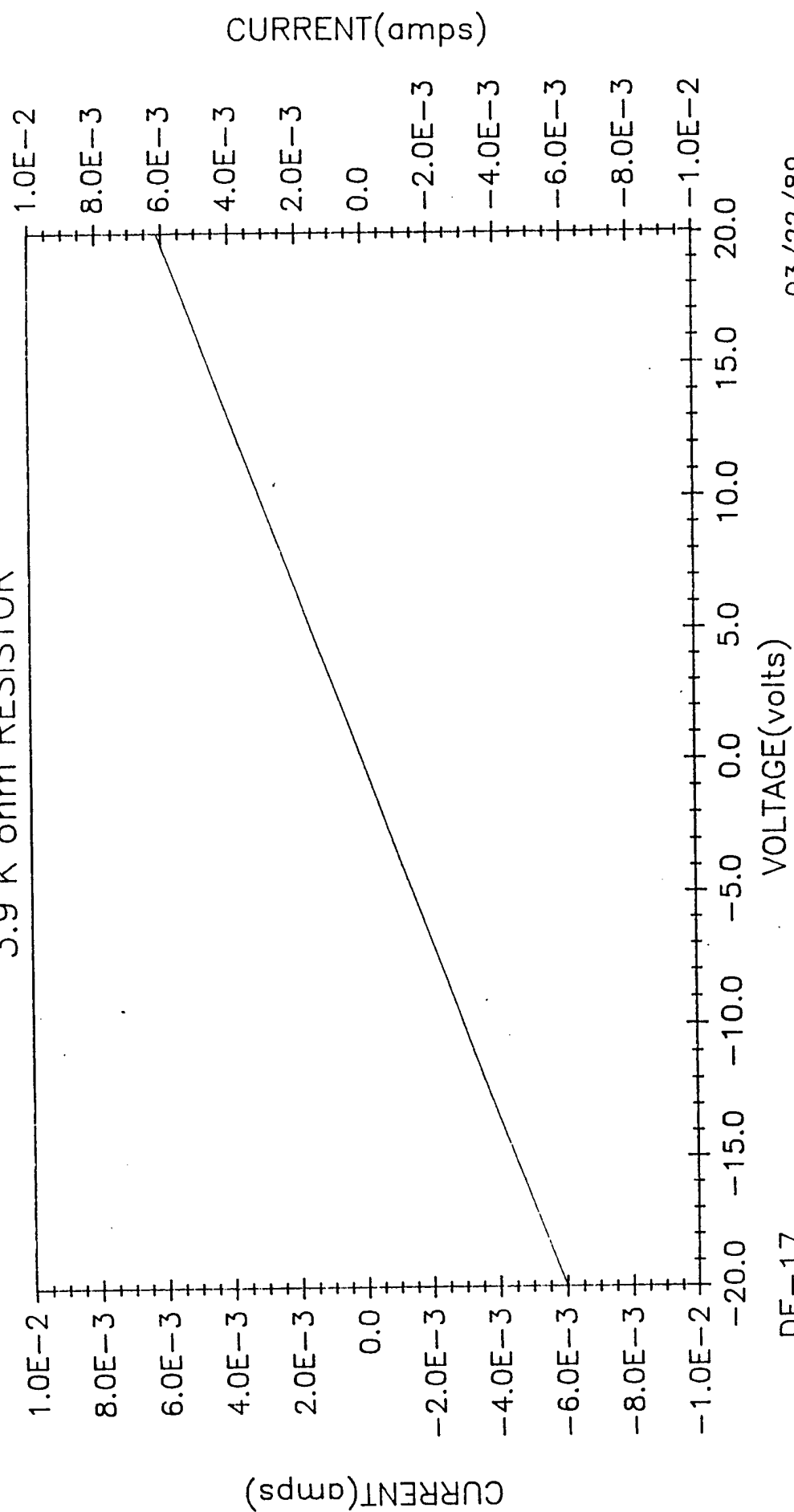
TIME(seconds)

75 G CHARGE

FIGURE D.4. TEMPORAL PRESSURE PROFILE RUN NO. 17

MHD17P.

SYSTEM CALIBRATION PLOT REGRESSION of VOLTAGE VS CURRENT 3.9 K ohm RESISTOR



03/22/89

DE-17

MHD17 PRE-RUN

DE3900C1

FIGURE D. 5. SYSTEM CHECK WITH 3900 ohm RESISTOR.

DOUBLE PROBE DATA

PLOT REGRESSION of VOLTAGE VS CURRENT

CALIBRATION OF NEW DOUBLE PROBE PRIOR TO RUN MHD-17

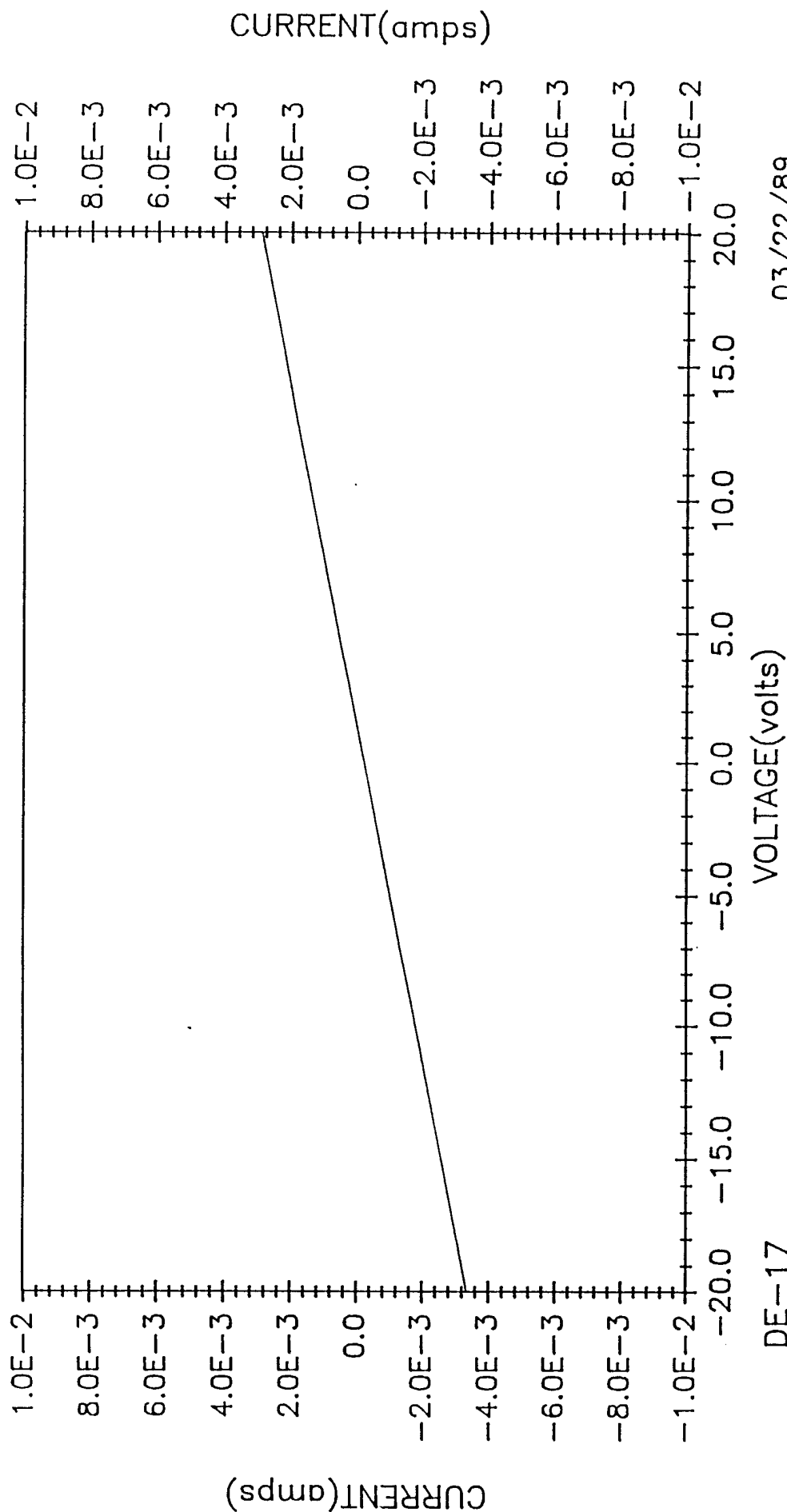
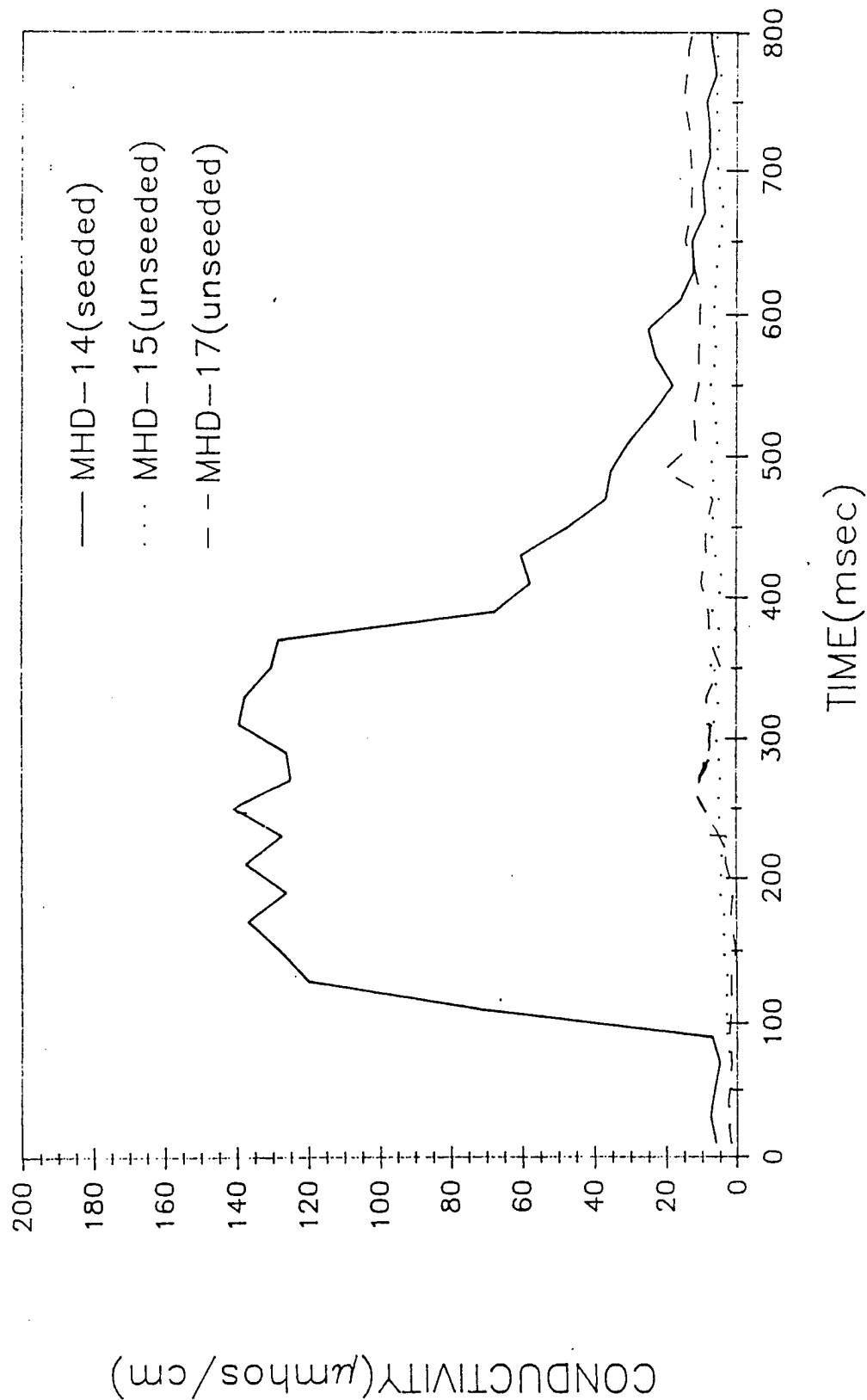


FIGURE D.6. CALIBRATION OF TANTALUM DOUBLE PROBE WITH KCl SOLUTION TO OBTAIN PROBE CONSTANT K.

CONDUCTIVITY vs TIME

COMPARISON OF SEEDED vs UNSEEDED FLOW



MHDCVT02

FIGURE D.7. COMPARISON OF CONDUCTIVITIES OF SEEDED AND UNSEEDED FLOWS

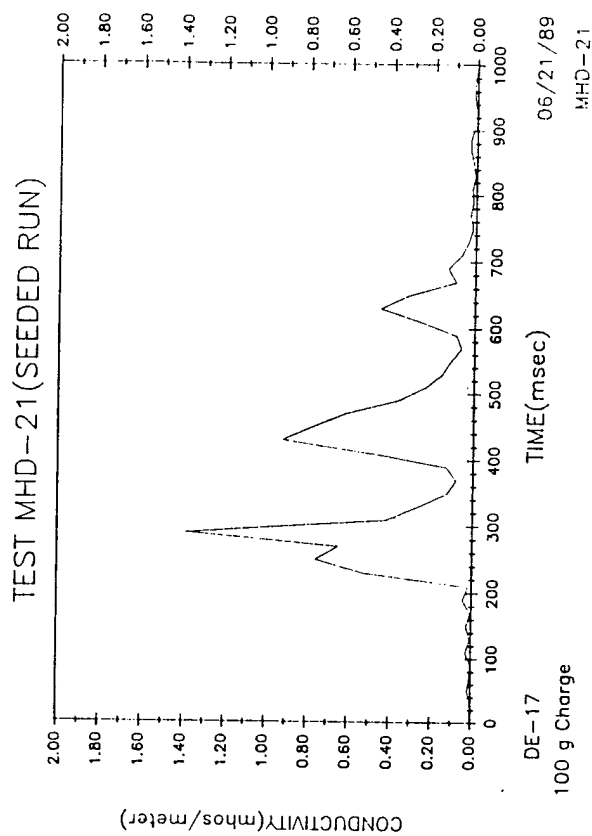
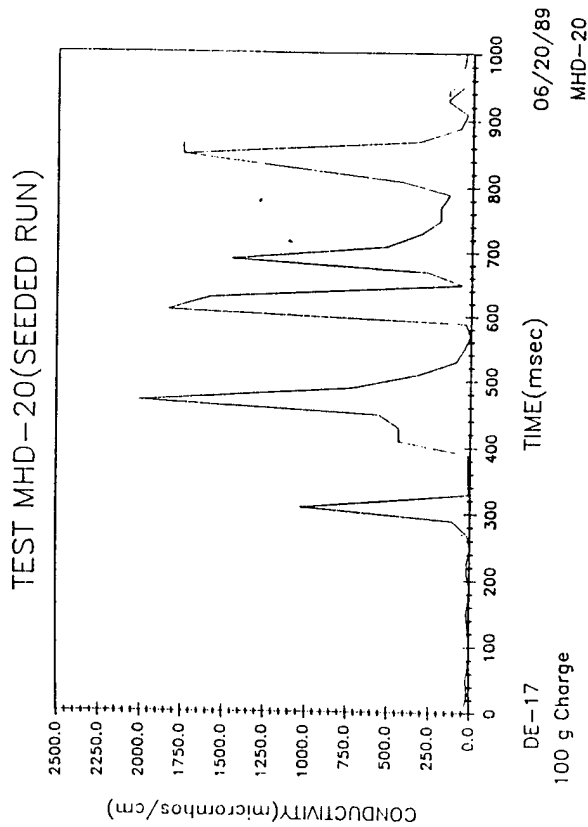
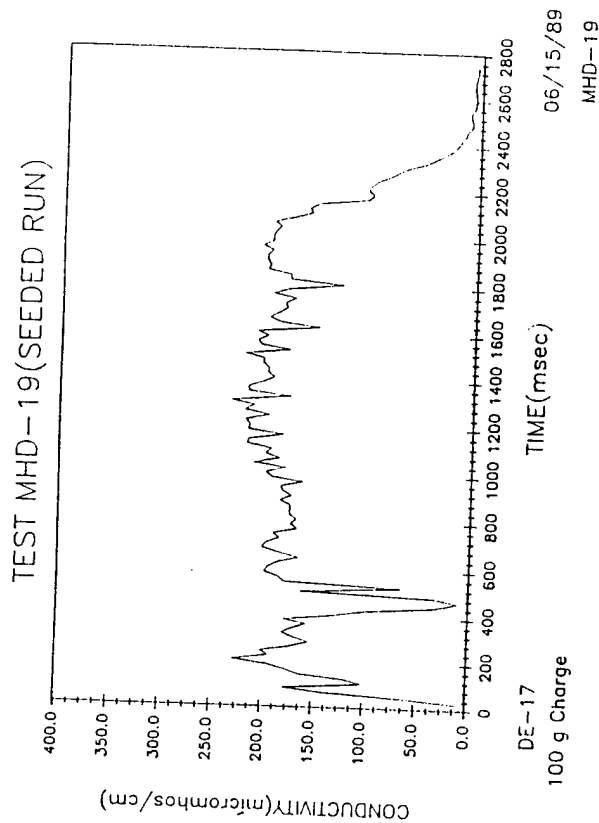
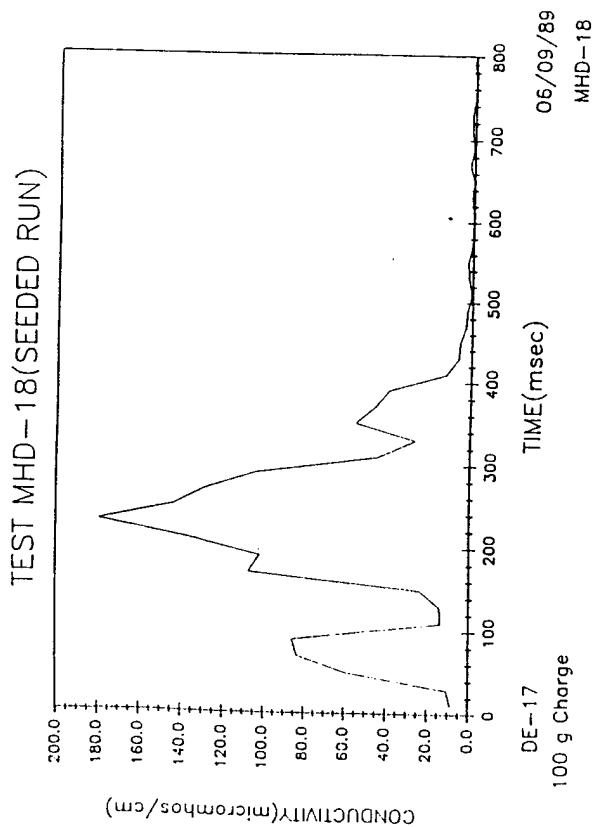
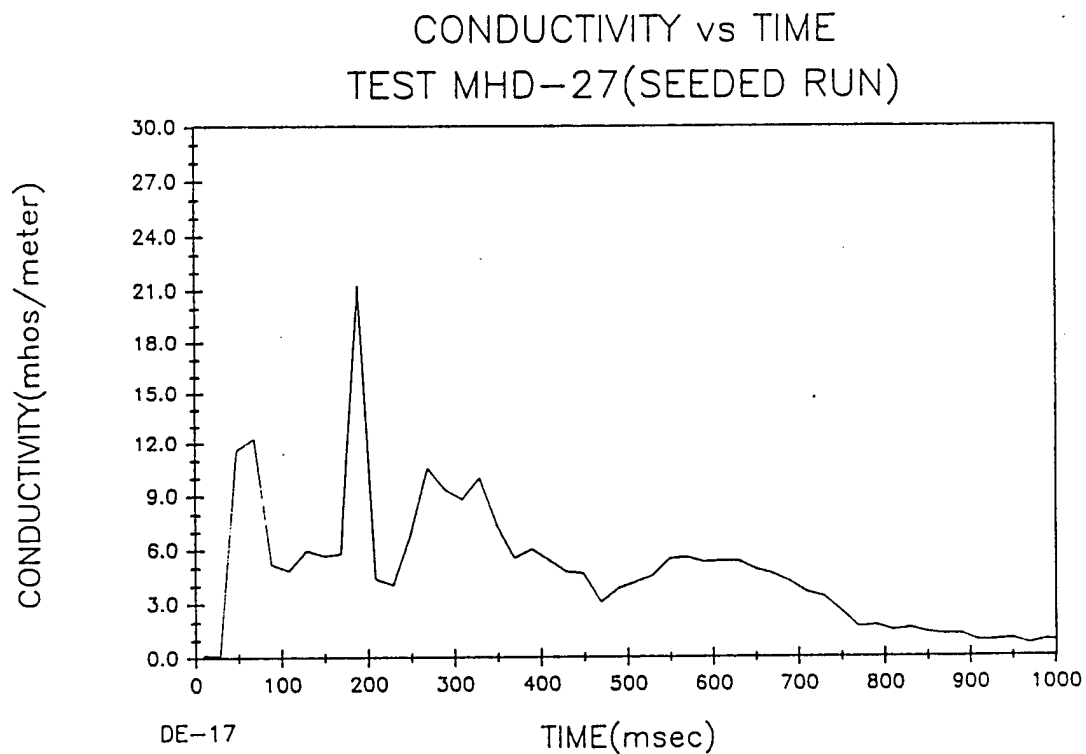
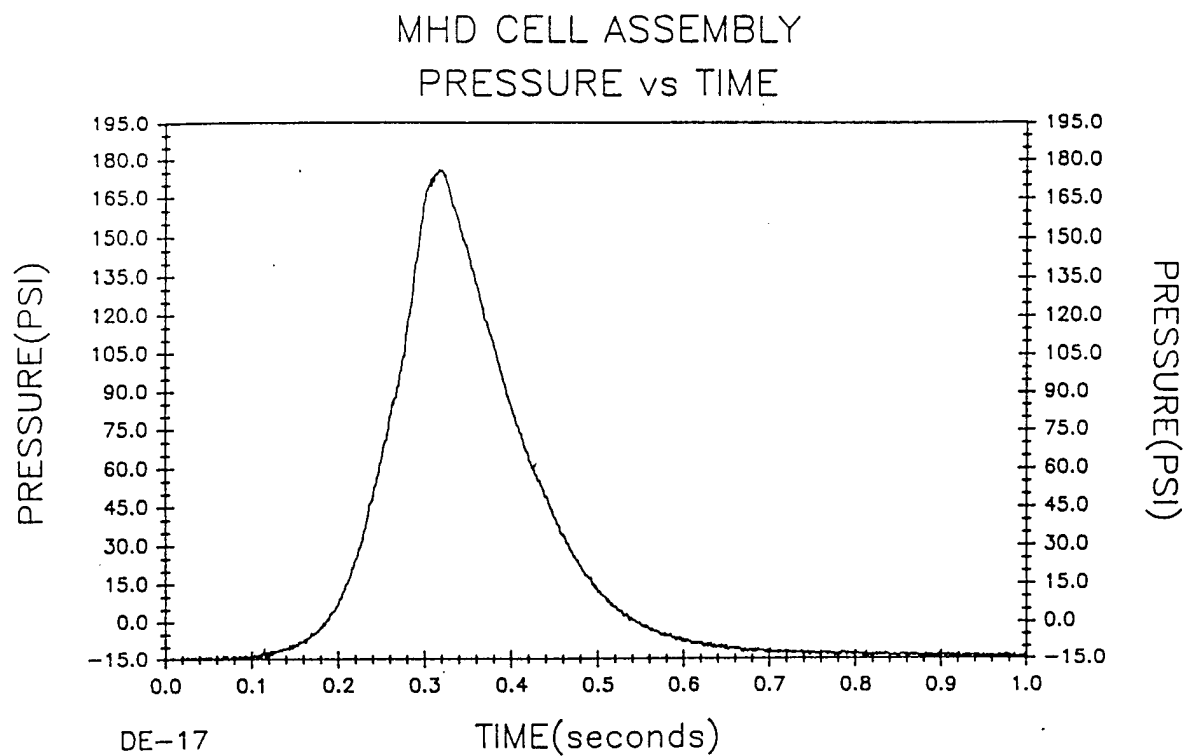


FIGURE D. 8. COMPOSITE CONDUCTIVITY PROFILES OF RUNS 18, 19, 20 AND 21
SEEDED WITH 5% BY WEIGHT CsNO₃



TEMPORAL CONDUCTIVITY FOR RESTRICTED FLOW(SCREEN ONLY)

**FIGURE D. 9. PRESSURE AND CONDUCTIVITY PROFILES OF COMPACTED FUEL
TEST WITH SCREEN ONLY. RUN # 27**

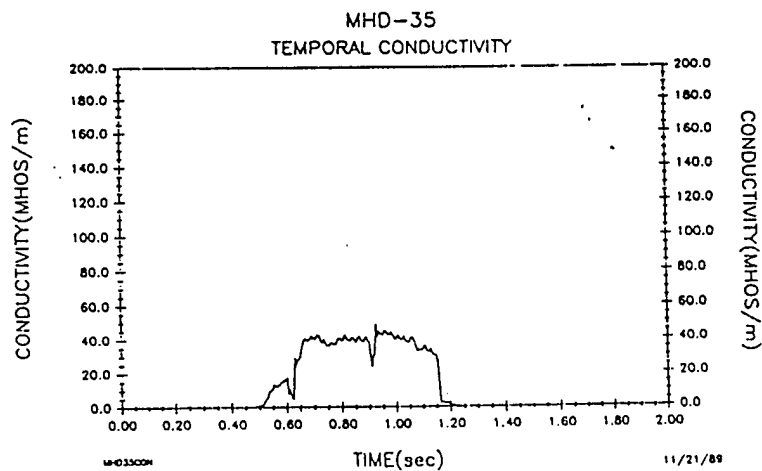
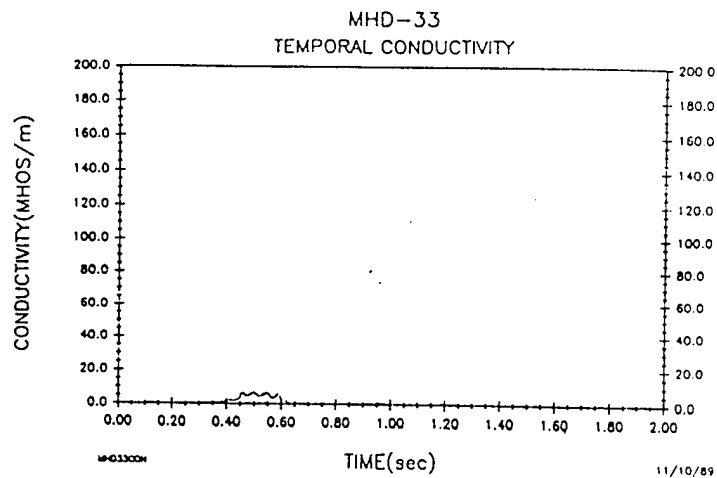
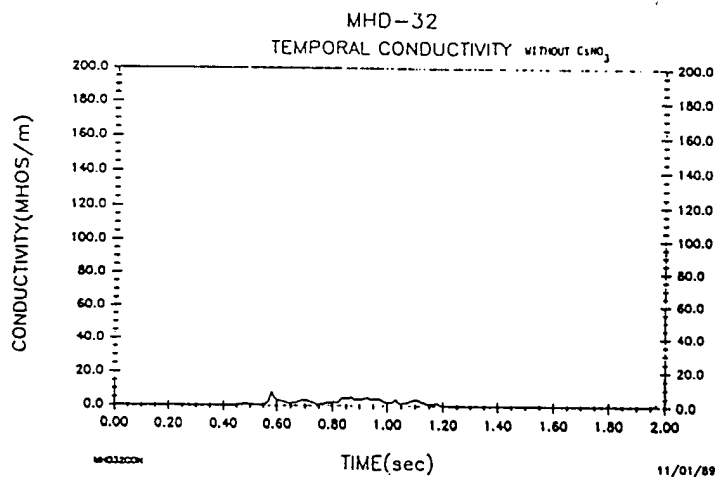
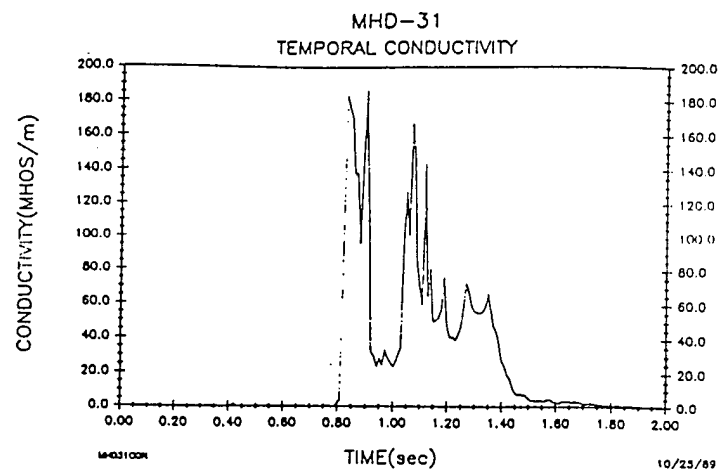
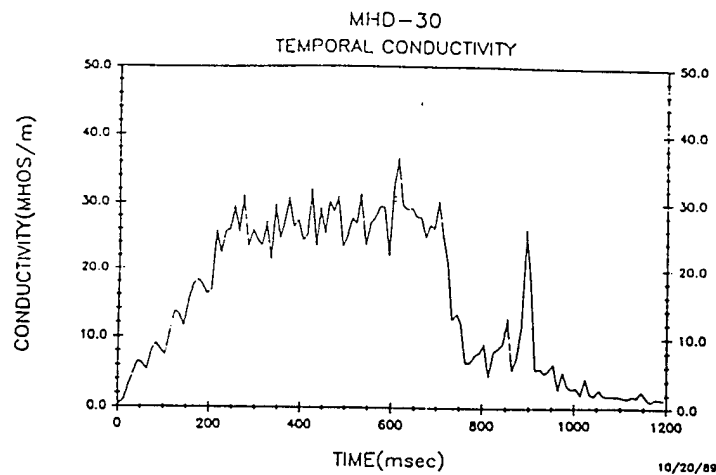


FIGURE D. 10. FINAL SEQUENCE OF SMALL SCALES TESTS WITH 120g COMPACTED FUEL AND SCREEN REMOVED. MIDDLE ROW CONDUCTIVITY PROFILES ARE WITHOUT CsNO_3 SEEDANT

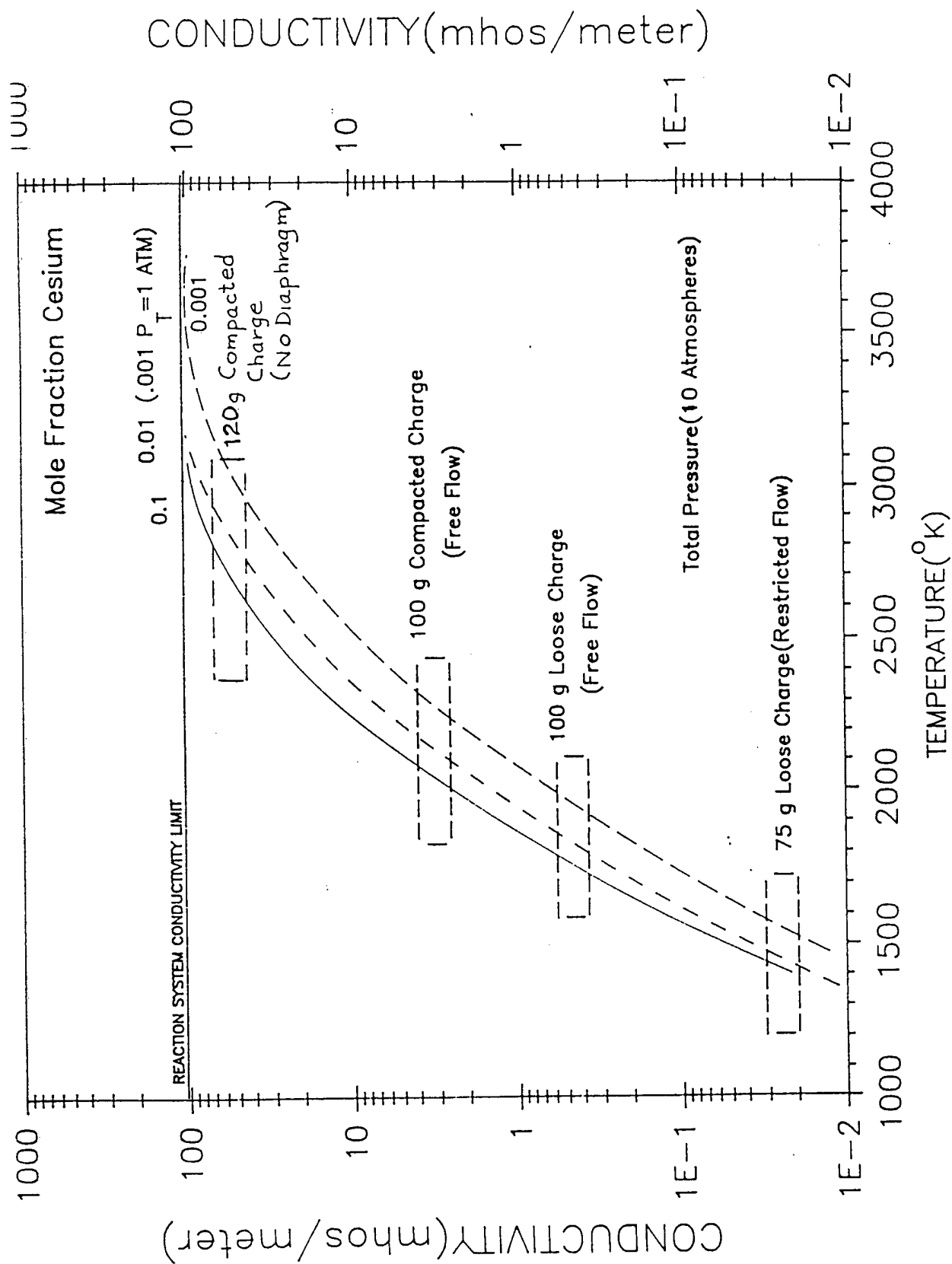


FIGURE D. 11. OVERVIEW OF THE SMALL SCALE TESTING AGAINST THEORETICAL SEEDED-HYDROGEN PLASMA

environment and reduce edge effects. This scaled up series of tests are discussed in the next section.

E. SCALED-UP TESTING (250 grams to 1 Kilogram)

The series of small scale testing established the optimum charge to TiH_2 ratio and provided the data necessary to increase the charge weight high enough to provide a significant reduction in the edge effects (i.e. loss of energy to the canister).

A theoretical analysis was performed by Dr. Charles Marston in which he established the relationship between the length/diameter ratio of the reaction chamber and nozzle area. The calculations are presented in Appendix D.

Based on these results a new reaction chamber was designed and fabricated. The goal was to test the system entirely in vacuum using three double tungsten probes situated near the center of the reaction chamber, one located at the end of the chamber and one located at the exit expansion nozzle. In addition, a fiber-optic cabled photometer was located at the end of the reaction chamber (i.e. stagnation region). The purpose of the photometer was to correlate the measured temperature with measured conductivity at the stagnation region. The method of correlating the photometric measurements with temperature is described in Appendix E.

A drawing of the scaled-up system is shown in Figure E.1. The overall size of the combustion chamber was 5.5 inches in diameter and about 7" long. The reaction chamber was about 11.5" in diameter and about 30" long.

The entire unit was placed in a 7 foot diameter by 40 foot long vacuum chamber located at the Franklin Research Center, Elverson, PA. This facility has been used in the past to test GSI and CRESS canisters for space flight releases.

The operating vacuum for this test facility is about 300 microns. It has the capacity to test fuel charges up to 15 kilograms.

The combustion chamber was designed to take up to a kilogram charge. Lower charges were used initially, filling the remainder of the space with fire brick. In addition, diaphragms of 25 mil grafoil sandwiched between 10 mil mylar sheets were used.

In the first test a total charge of 250 grams was used containing 70% by weight of Ti/2B, 25% by weight of TiH_2 /2B and 5% by weight of CsNO_3 . Calibrations of the three probes were the same as carried out as in the small scale tests.

In Figure E.2 is shown the assembled unit, the combustion chamber, the tungsten probes and the conductivity profile obtained from a 250 gram fuel charge test. In addition to the pressure and light measurements, video were also taken from the side of the Franklin Research vacuum tank of the flow from the nozzle and end-on video were taken 40 feet from the nozzle.

The conductivity profile of this configuration and charge was very uniform from the stagnation probe. The center probe was destroyed during the test while the probe at the expansion nozzle showed a drop of a factor of 50 as expected (Figure E.3). The light probe data and pressure data are shown in Figure E.4. The light probe data indicated temperatures in excess of 2500°K (probe data off scale) and pressure at its peak of about 6 atmospheres. The duration of the pulse as indicated by E.2d was about 1/2 second.

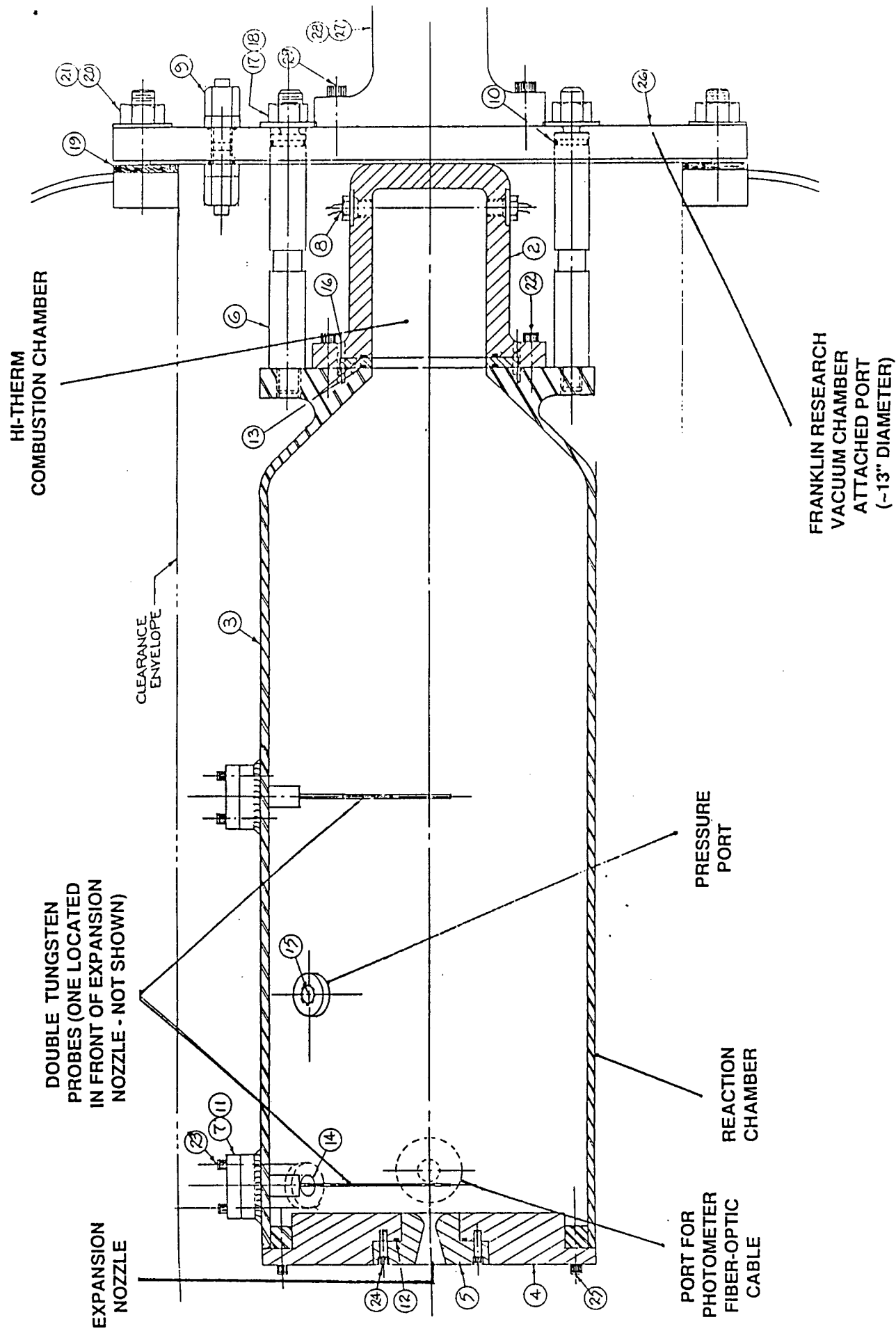
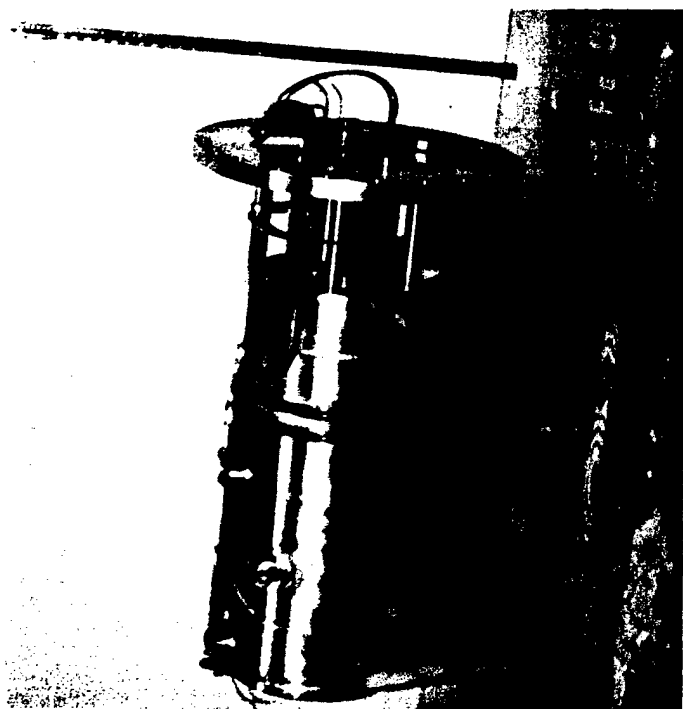


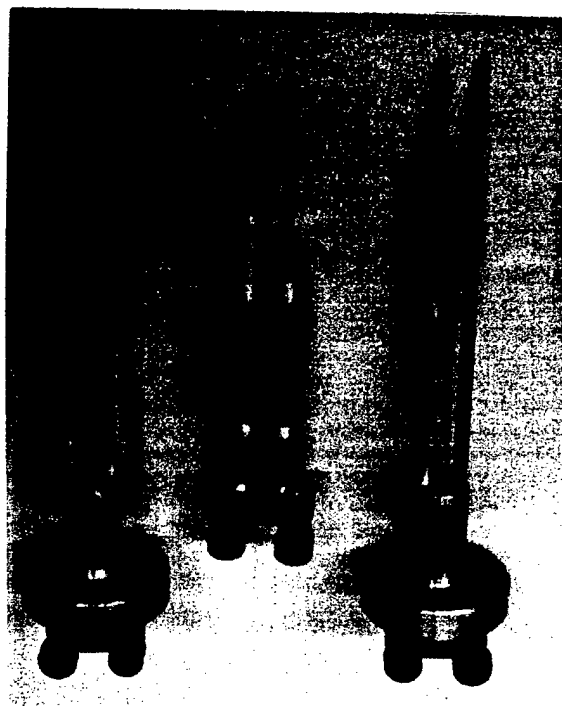
FIGURE E.1. DRAWING OF MHD HEATER FOR SCALED-UP TESTING AT THE FRANKLIN RESEARCH CENTER (SEE TEXT)



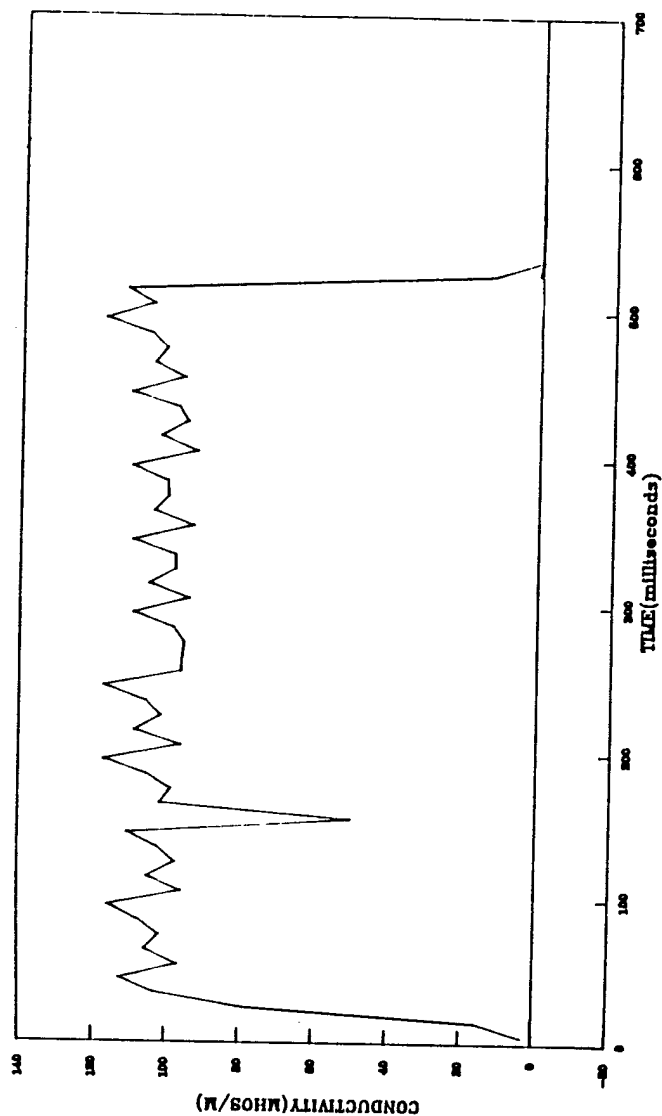
A. ASSEMBLED UNIT



B. FUEL CANISTER



C. CONDUCTIVITY PROBES



D. PLASMA CONDUCTIVITY BY 250g CHARGE (500 msec)

FIGURE E.2. PHOTOGRAPHS OF ASSEMBLED MHD HEATER (A), THE COMBUSTER CHAMBER (B), THREE DOUBLE TUNGSTEN PROBES (C) AND RESULTING CONDUCTIVITY PROFILE FROM A 250 gram FUEL CHARGE

CONDUCTIVITY PROFILE MHD TEST #1

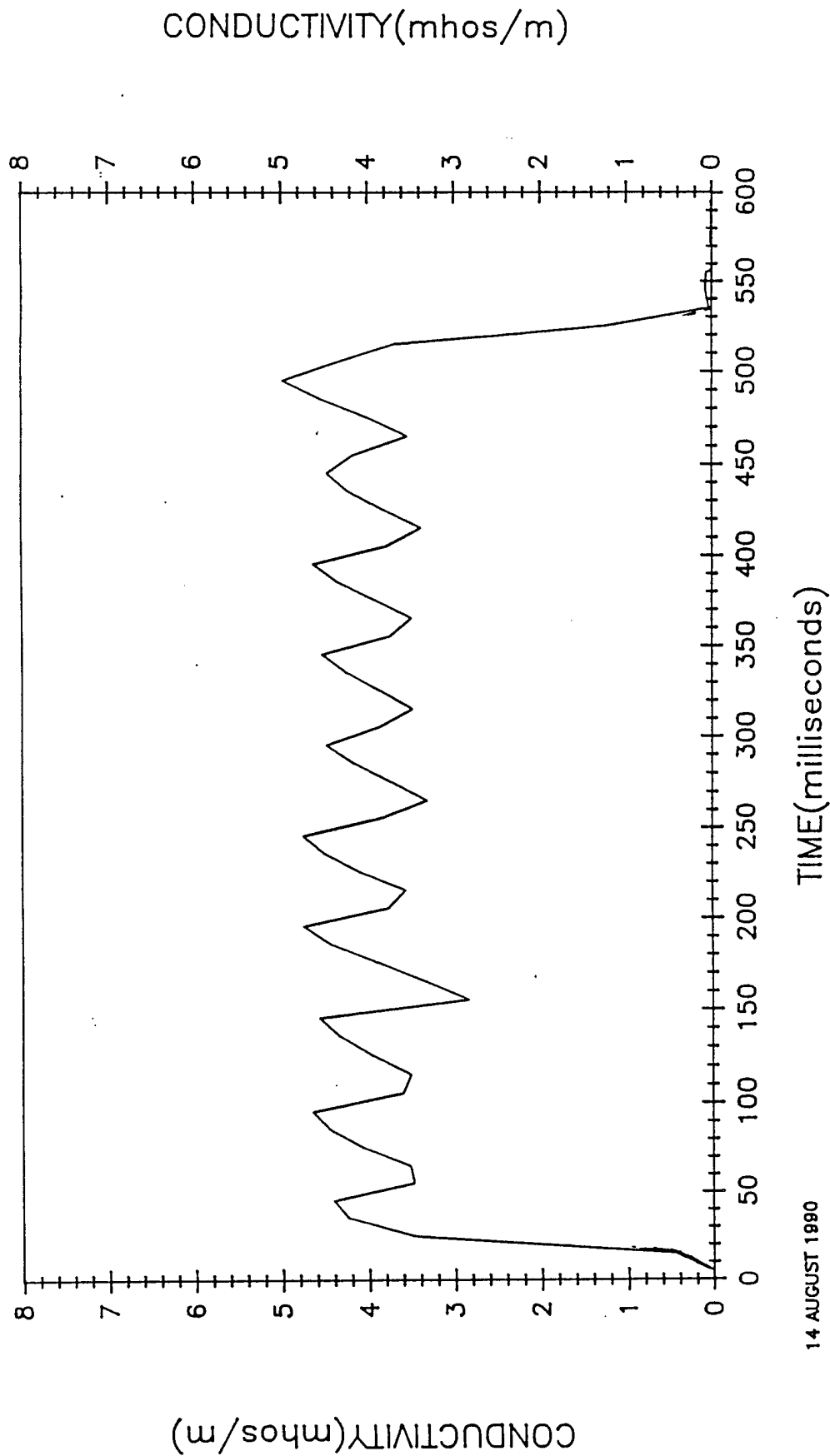


FIGURE E.3. CONDUCTIVITY PROFILE OF EXPANSION NOZZLE PROBE OF 250 gram
MHD HEATER TEST AT FRANKLIN RESEARCH CENTER

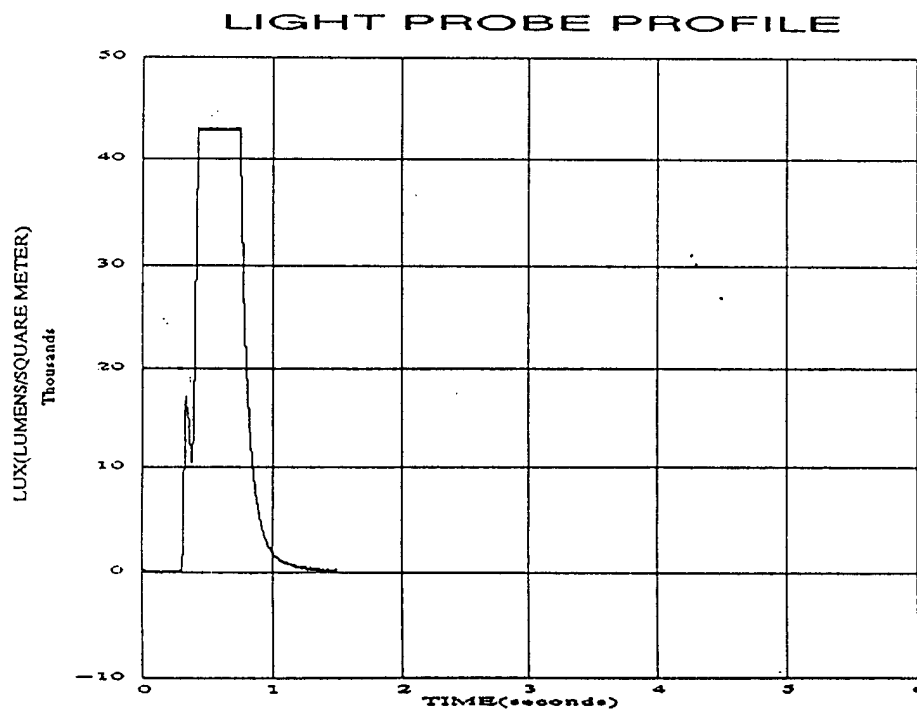
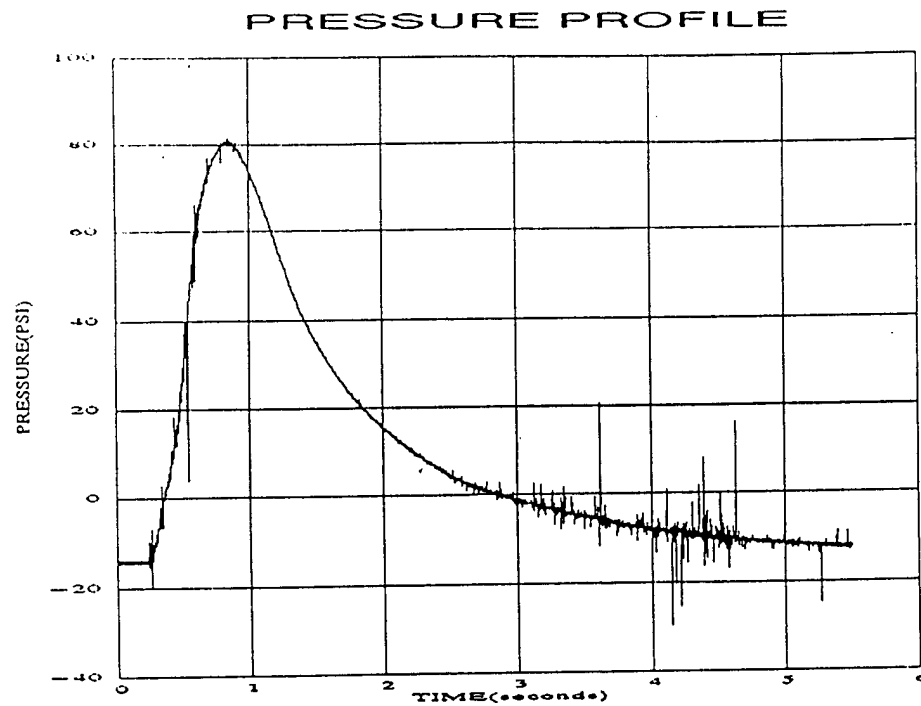


FIGURE E.4. PRESSURE AND LIGHT PROBE DATA OF 250 gram MHD HEATER TEST (MHD #1)

Due to the success of the 250 gram test, the next test was conducted at a charge of 500 grams with a stiffer (i.e. several layers of mylar) diaphragm in an effort to communicate even more energy to the hydride. This test failed to ignite and due to funding and time limitations was not repeated.

The next test, designated MHD #3, we chose to increase the fuel charge to 1 kilogram with a lighter diagram (3 layers of mylar). This was repeated twice (MHD #4 and MHD #5). In MHD #5, the stagnation probe was destroyed and conductivity measurement could not be obtained. The results of MHD #3 and MHD #4 tests are shown in Figure E.5. In test #3, all three probes survived and are designated as follows:

Probe 1 - CENTER OF REACTION CHAMBER

Probe 2 - STAGNATION REGION

Probe 3 - FRONT OF EXPANSION NOZZLE

In test #4, probe 3 failed to record and Probe #1 was nearly destroyed so that the results are not reliable.

Due to time restrictions, the testing was terminated at this point.

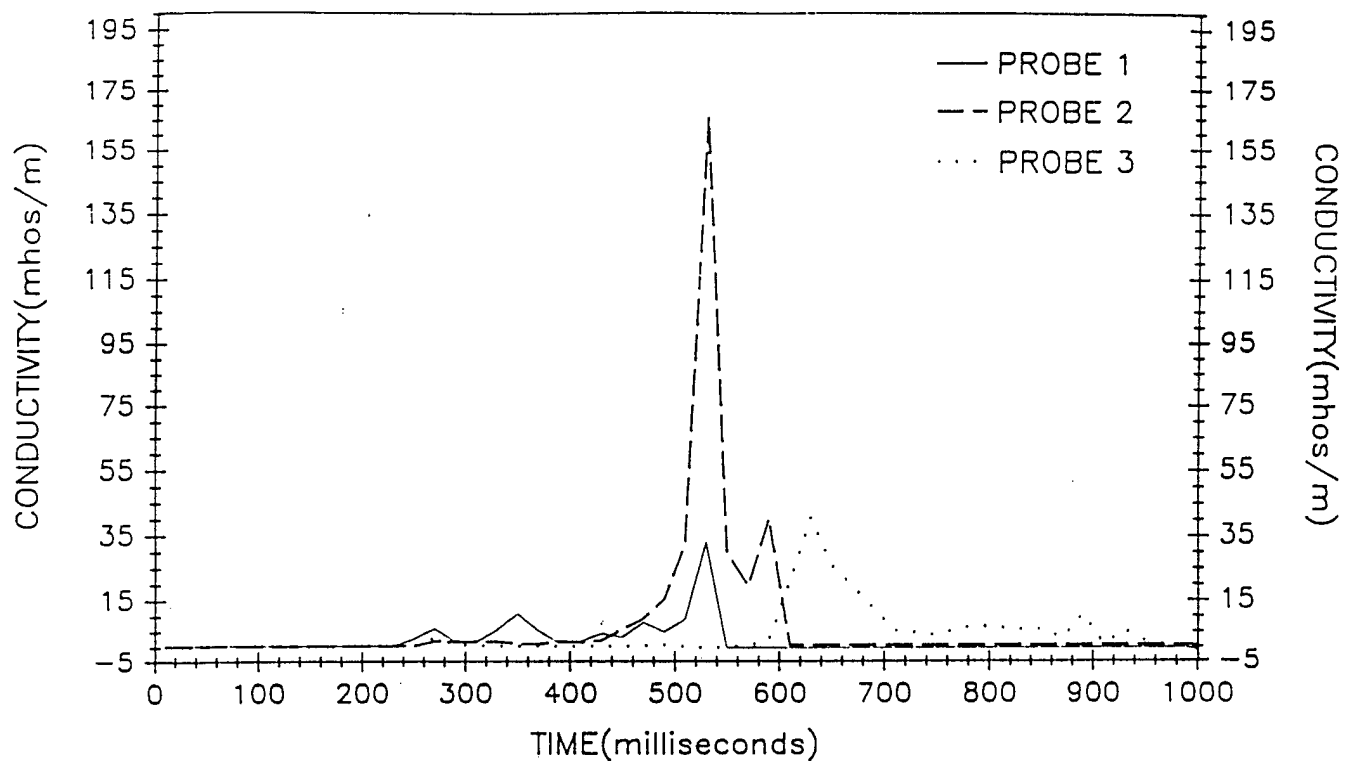
F. CONCLUSIONS AND RECOMMENDATIONS

Although additional testing at the higher fuel weights would have been desirable, the available data indicates that fuel weights cannot be scaled up directly (i.e. single canister holding the higher fuel weight charge). As evidenced from MHD runs #3 and #4 (Figure E.5) the kilogram charges produced spiked flows with very high conductivities while MHD #1 at 250 grams (Figure E.2d) indicated a uniform plasma flow. In addition, the nature of the diaphragm becomes an important developmental parameter as a strong diaphragm holds back the flow too long leading to an explosive discharge. Conversely, if the diaphragm is too weak, the flow is released over a longer period of time leading to lower temperature due to higher radiative cooling effects.

Based on our limited data, we can conclude the following:

1. Higher fuel weights cannot be scaled directly.
2. Type and strength of diaphragm used can determine type of release.
3. Nearly theoretical conductivities can be achieved with Hi-Therm.
4. Weight scaling can be achieved by modular design.
5. In the design of the larger test chamber it was envisioned that the conductivity probe would be located as close as possible to the exit jet of a conveying nozzle, then the flow at the probe would be approximately sonic, see Appendix D, Figure D.3. However, the nozzle "as built", was converging/diverging with an area ratio of about 1.8, see main text Figure E.1, item 5. This area ratio with an isentropic expansion ratio of about 1.16 corresponds to about Mach 3, a temperature ratio of about .58 and a pressure ratio of about .02. While the lower pressure tends to increase conductivity, the temperature effect dominates, see Figure A.2 (b). For example, if stagnation conditions were 3000°K and 10 atmospheres, then at the nozzle exit, the pressure would be about 0.2 atmospheres and the

TEST MHD #3



MHD TEST #4

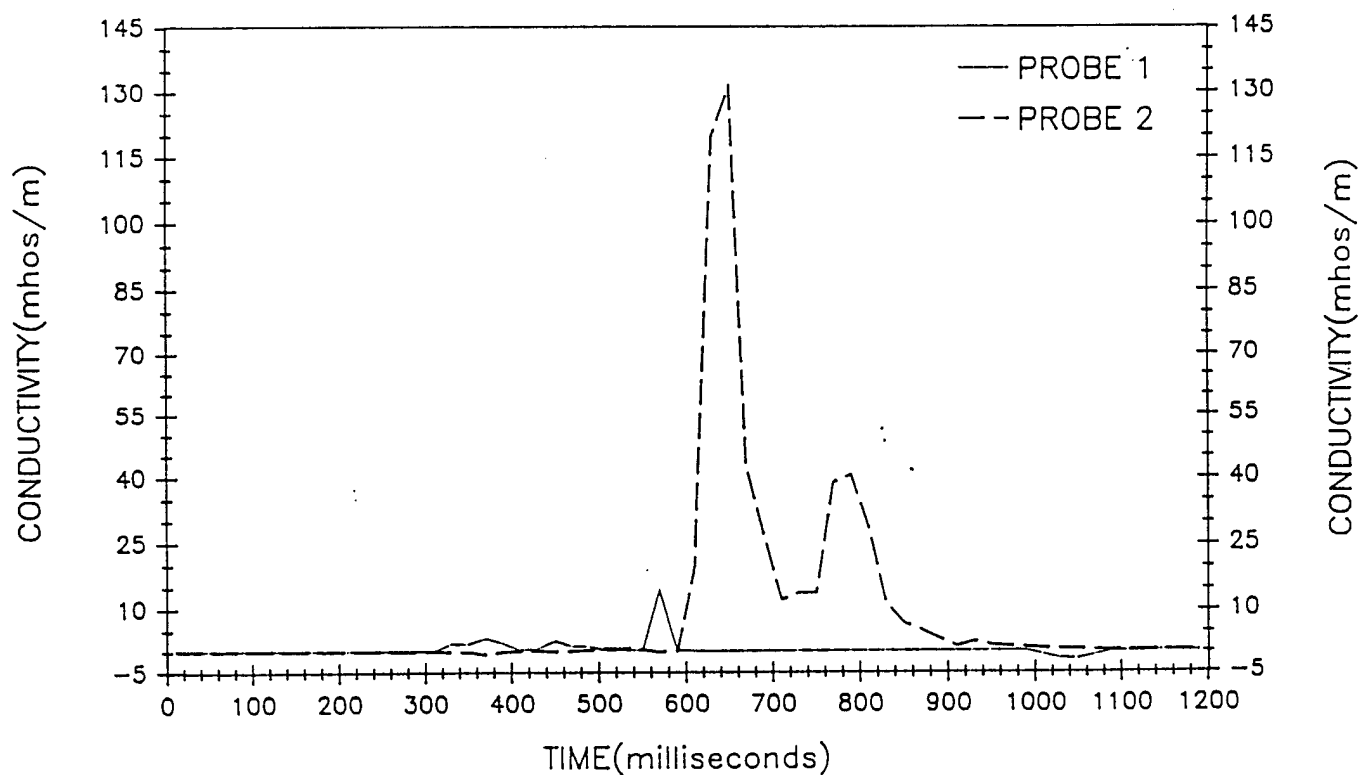


FIGURE E.5. CONDUCTIVITY PROFILES OF MHD TESTS # 3 AND # 4
(1 KILOGRAM FUEL WEIGHT)

temperature about 1740°K. The resulting conductivity, based on Figure A.2 (b) drops from about 100 S/M to about 2 S/M, a factor of 50. These numbers must be taken as quantitative in view of the many complexities involved in the measurements. The drop in conductivity at the exit nozzle as measured, see Figure E.3, is therefore not surprising.

Some expansion of the flow was necessary to cover the probe but in a large scale system an MHD generator would be operated in the range of $0.8 < M < 1.2$, in which case the temperature would be about 90% of its stagnation temperature.

The discussion does not take into account the heat loss but while the magnitude of the heat loss in a larger system would be larger, the greater optical thickness in a larger system should reduce the loss relative to the total energy of the flow.

6. The measurement of a low conductivity at the center of the chamber was surprising as it was expected that conductivity within the chamber should have been more or less uniform. It is possible that some additional chemistry is taking place within the chamber that somehow reduces the temperature. In any future work, this effect will have to be investigated.
7. The effect of velocity on the double probe was an initial concern as the probe was calibrated statically. It was believed that as long as the probe was measuring electron flow and not ionic flow and the velocity of flow relative to the electron velocity is low there will not be an appreciable effect on the probe measurements due to the flow velocity.

As a result of this testing and analysis, the following is recommended for further work.

1. Redesign combustion chamber into modules of 250 grams to produce large volume high conductivity flows.
2. Experiment with different diaphragm materials and thicknesses to control flow uniformity and duration.
3. Experiment with other Hi-Therm materials which can achieve very high temperatures (~4000°K) leading to even higher conductivities (~200 ---> 300 mhos/meter).
4. Experimental program to devise techniques to reduce the energy of reaction transfer to the surroundings (e.g. insulator investigation).

Overall, a plasma source generated by solid intermetallic compounds such as Hi-Therm can provide a pulse of electrical energy for a time period of the order of a few seconds. This system has an indefinite storage life and is instantly available.

While scaling to the magnitudes envisioned for SDI Space Applications faces many obstacles, the technology may well find applications on a smaller scale where the above noted features are advantageous.

G. ESTIMATION OF FUEL WEIGHT REQUIREMENTS FOR SDIO APPLICATIONS

The original intent of this program was to develop a new type of fuel to be used for a pulsed MHD heater to power pulsed space weapons. Typical estimates of requirements are over 100 megawatts of power per pulse (1/2 - 1 sec) for repetitive pulsing of up to 1000 seconds.

The power density that can be generated by a heater source can be written as,

$$P_D \approx 1/4 \sigma v^2 B^2 \quad (G.1)$$

where σ is the conductivity in mhos/meter, v the flow velocity in meters/sec and B the applied magnetic field in Teslas with P_D in watts/meter³. Assuming a 15% extraction efficiency, (G.1) becomes,

$$P_D (\text{extracted}) = .04 \sigma v^2 B^2 \quad (G.2)$$

The volume of the large scale tests were on the order of .05 M³ for a 250 gram fuel weight. Then from (G.2), the power extracted for this volume is,

$$P(\text{watts}) = P_D(\text{extracted}(.05)) \approx .002 \sigma v^2 B^2 \quad (G.3)$$

The average conductivity as measured in this program was about 100 mhos/meter. Assuming flow velocities in the order of 400 meters/sec., (~MACH 1.2) the expected power extracted per module of 250 grams is on the order of 100 kw/(Tesla)².

Assuming in space applications, 5 Tesla can be achieved, a 250 gram charge could be expected to deliver about 0.8 megawatt/charge. For a 100 megawatt power source, approximately 31 Kg would be required per pulse. Assuming the pulses are on the order of 1 second, then for 1000 seconds about 31,000 Kg of fuel would be required (about 34 tons).

These estimates can only be realized when sufficient improvements have been made. The estimates of fuel weight requirements can be halved if higher temperature fuels can be developed using Hi-Therm technologies (in progress at GSI), leading to higher conductivities (~200 - 300 mhos/meter).

ACKNOWLEDGEMENTS

Many people have contributed to this development program and we wish to acknowledge and express our thanks for the contributions of the following:

Mr. Don DeDominicis, Jr., Senior Chemist at GSI, for preparing all the fuel charges for all the tests conducted on this program, preparing all the computer plots from the raw data and carrying out all the calibrations of the tungsten and tantalum probes.

Mr. Dave Rogers. Private Consultant to GSI for designing the electronic curcuitry for the double probe and for his many useful discussions and recommendations regarding the probe measurements.

Mr. Joseph Golden. Private Consultant to GSI for many hours he spent interfacing with the local machine fabricating the MHD heaters and probes.

Mr. Don DeDominicis, Sr., Private Consultant to GSI for designing and preparing the engineering drawings for the MHD heaters and probes.

Dr. Gerald G. Elia, Project Manager at the U.S. Department of Energy for his guidance and encouragement in the early part of this program.

Mr. Leo Makovsky. Project Manager at the U.S. Department of Energy for making substantial recommendations along the way and to his encouragement and guidance in the latter part of this development program.

The success achieved in this very involved and complicated development program can be attributed to the efforts of these people. It is a pleasure to acknowledge their substantial contributions.

REFERENCES

1. Rosa, R. J., "Magnetohydrodynamic Energy Conversion", McGraw-Hill, NY, 1968.
2. Marston, C. H., et. al., "Parametri Study of Potential Early Commercial MHD Power Plants, Task II, Conceptual Design Study", NASA CR-165236 September 1981. See Also NASA Report DEN 3-244-4 Task III-A MHD Cost Analysis, April 1983.
3. Felderman, E. J., et. al., "HPDE Performance in the Faraday Mode", 20th EAMHD Symposium, Irvine CA, June 1982, paper 4, 5.
4. Tarrh, J., Marston, P. G., "A Survey of Magnet Experience Relevant to MHD" 23rd EAMHD Symposium, Somerset, PA, June 1985, pp 215-233.
5. Petrick, M., "Current Status of MHD Technology", U.S. Department of Energy Report ANL/FEP - 1025 (Draft), January 1984.
6. Smith, J. M. and Morgan, J. L., "Results and Comparison of Hall and DW Duct Experiment", 20th EAMHD Symposium, Irvine, CA, June 1982, paper 4.4.
7. Y. C. L. Wu, H. J. Schmidt and M. H. Scott, "Status of Explosive MHD Technology in the Soviet Union, Battelle Columbus Laboratories, Subcontract E-9076, Under Prime Contract F33657-81-C-2070, December 12, 1985.
8. H. J. Schmidt, John B. Dicks, Y. C. L. Wu, M. H. Scott, "The History and Future of Light Weight MHD Power Systems", 20th IECEC, August 1985.
9. P. Zavitsanos, "A Metal Vapor Generator", U. S. Patent #4092-263, May 30, 1978.
10. P. Zavitsanos and J. R. Morris Jr. "Synthesis of TiB_2 by a self-propagating Reaction", Ceramic Eng. and Science Proceedings pp 624-627, July - August 1983.
11. P. Zavitsanos & J. D'Andrea, "Self-Propagating Reaction of Hi-Temp. Materials", AMMRC Final Report Contract No. DAAG46-83-C-0178, June 1985.
12. P. Zavitsanos and J. D'Andrea, "Self-Propagating Condensed Phase Reactions", ARO Final Report Contract DAAG29-83-C-0017, Feb. 1985.
13. Olsen R. A and Larry , E. C., "Electrodeless Plasma Conductivity Apparatus", Review of Scientific Instruments, 1962, Vol. 33, No. 12, p. 1350. (Quoted in Open Cycle

Magnetohydrodynamic Electrical Power Generation, M. Petrick and B. Ya. Sumyatsky, Editors, Argonne National Lab., 1978, Chapter 14).

14. Van Wylen, G. J., and Sonntag, R. G., "Fundamentals of Classical Thermodynamics", 3rd Edition, SI Version, Tables A.11 and A.14, (Both Tables are based on the JANAF Thermochemical Tables).
15. Weatherford, W. D., Tyles, J. C. and Ku, P. M., "Properties of Inorganic Energy Conversion and Heat-Transfer Fluids for Space Applications", WADD Technical Report 61-69, November 1961.

APPENDIX A

EVALUATION OF THE POTENTIAL OF HEATED HYDROGEN AS THE WORKING FLUID IN A LARGE, SPACED BASED, MHD POWER GENERATION SYSTEM

Two parameters of interest in the evaluation of heated hydrogen as a working fluid are energy per unit mass and mass flow rate per unit area.

To obtain an order of magnitude estimate of the energy per unit mass, temperatures of 3000°K and 2400°K were assumed for the generator inlet and exit respectively. At 3000°K and moderate pressure, dissociation is significant so it was taken into account, assuming equilibrium for the reaction



Values for the equilibrium constant and for ideal gas enthalpies of diatomic and monatomic hydrogen were taken from Reference 14. Energy per unit mass was established in two ways. First it was assumed that 70% of the enthalpy change between 3000°K and 2400°K could be converted to useful electric power. Second an enthalpy extraction of 25% was assumed.

Table A.I (text) shows the results of calculations based on these assumptions. The two methods are quite consistent and in line with the extrapolation to very large scale generators shown in Figure A.1. While probably optimistic, they indicate the potential of an order of magnitude improvement over combustion systems.

To calculate mass flow per unit area, choked flow of an ideal gas at a stagnation temperature of 3000°K and stagnation pressures of 1, 10 and 100 atmospheres was assumed. This is not fully consistent with the data in Table A.I but it will indicate the orders of magnitude, molecular weight as calculated from the equilibrium composition. Specific heat ratio at one atmosphere was obtained by extrapolation for 3600°F (2255°K) of data from Reference 15. It was then assumed that at higher pressures with less dissociation the specific heat ratio would approach the value of 1.4 associated with a low temperature diatomic ideal gas.

Table A.II shows the results of that calculation. The low molecular weight of hydrogen tends to reduce mass flow per unit area and argues for operation at higher stagnation pressures. However, this reduces electrical conductivity and thus will tend to limit enthalpy extraction. Optimum operating pressure will require a trade-off between system size - especially magnet size - and generator performance.

Based on the above estimates (i.e. 14 MJ/kg at 10 Atm) and the original requirement of 100 MW-10³ seconds, (which translates to 10⁵ MJ) one estimates a total of 7.14 x 10³ kg of H₂

TABLE A.I

ELECTRICAL ENERGY PER UNIT MASS OF HYDROGEN

Electrical Energy Per Unit Mass of Hydrogen						
PRESSURE (ATM)	TEMPERATURE				0.7 ΔH ₁ (MJ/kg)	0.25H (MJ/kg)
	3000K		2400K			
	(1)	(2)	(1)	(2)		
1.0	.146	77384	.016	36776	28.4	19.3
10.0	.049	55156	.005	34331	14.6	13.8
100.0	.016	47602	.002	33553	9.8	11.9

NOTES: (1) Mole fraction monatomic hydrogen
(2) Enthalpy KJ/kg

TABLE A.II

MAXIMUM MASS FLOW RATE (CHOCKED FLOW)

PRESSURE (ATM)	MOL WT	C_p/C_v	FLOW RATE (kg/s-m ²)
1.0	1.868	1.29	18.4
10.0	1.967	1.35	192.3
100.0	2.000	1.40	1964.

required (i.e. about 7 tons) to be generated, at an average rate of 7.14kg/sec. The amounts of different fuels required to heat all the hydrogen to the desired temperature ($\sim 3000^\circ\text{K}$, $55 \times 10^3\text{KJ/kg}$) are shown in Table A.III.

TABLE A.III.

Reaction System	Energy	Minimum Total Weight (Fuel and Oxidation)
Ti + 2B (or Ti + C)	5 KJ/g	$78.54 \times 10^3 \text{ kg}$
B/O ₂	18.4 kj/g	$21.34 \times 10^3 \text{ kg}$
Ti/2B/Li/O ₂	17.5 kj/g	$22.44 \times 10^3 \text{ kg}$
Ti/2B/8B/O ₂	17.2 kj/g	$22.83 \times 10^3 \text{ kg}$

In conclusion it is interesting to note that one requires H₂ - flow rates in the vicinity of 7 kg/sec and corresponding reactants of the order of (23 - 78) kg/sec.

APPENDIX B.

CALCULATION OF CONDUCTIVITY AND PROGRAM LISTING

One of the tasks under this program was the development of a method for screening candidate solid fuels. A simple inexpensive experimental setup can be used to identify promising candidates for large scale testing was desired.

1.0 Electrical Conductivity

The primary property of interest is electrical conductivity and initial work was devoted to developing a capability for theoretical calculation of conductivity. The equations discussed below were programmed using Turbo Basic (B.I) on an IBM compatible desktop computer. The program listing is included as Appendix B.I.

Rosa (B.2) gives the following equation for scalar electrical conductivity, including expression for electron-ion cross-section

$$\sigma = \frac{n_e e^2}{m_e V_e} \left[\frac{1}{\sum_k n_k Q_k + 3.9 n_i \left(\frac{e^2}{8\pi \epsilon_0 K T} \right) \ln \Lambda} \right]$$

$$\Lambda = \frac{12\pi}{\sqrt{n_e}} \left(\frac{\epsilon_0 K T}{e^2} \right)^{3/2}$$

where

n_e	Electron number density (#/m ³)
e	electron charge (1.60219E-19 Coulomb)
m_e	electron mass (9.10956E-31 kg)
V_e	mean random electron thermal velocity (m/s)
n	particle concentration (#/m ³)
Q	collision cross-section (m ²)
ϵ_0	permittivity of free space (8.85419E-23 J/K)

k	Boltzmann constant (1.38062E-23 J/K)
π	3.14.....
T	temperature (Kelvin)
λ	Debye shielding length

Electron concentration was calculated from the Saha Equation (B.2, B.3)

$$\frac{n_e n_i}{n_s} = \frac{(2\pi m_e k T)^{3/2}}{h^3 g_o} \frac{2 g_i}{e^{-\left(\frac{\epsilon_i}{kT}\right)}}$$

where

n_s	concentration of seed atoms
n_e	electron concentration (#/m ³)
n_i	ion concentration (#/m ³)
h	Planck's constant (6.6260E-34 J-s)
ϵ_i	ionization potential of the seed atom (3.89 eV for Cs)
g_i	statistical wt of ground state of ion (1 for Cs)
g_o	statistical wt of ground state of neutral (2 for Cs)

Rosa (B2) gives a convenient form for calculation which was used directly (after some effort to evaluate units consistency).

$$\text{Log}_{10}\left(\frac{n_e n_i}{n_{os} - n_i}\right) = \frac{-5040}{T} \epsilon_i - \frac{3}{2} \text{Log}_{10} \frac{5040}{T} + \text{Log}_{10} \frac{2 g_i}{g_o} + 26.9366$$

in which n_{os} is the original concentration of seed atoms.

A mixture of hydrogen and cesium was assumed. The hydrogen was assumed to be dissociated but not ionized. Equilibrium constant for dissociated was interpolated from values tabulated in VanWylen and Sonntag (B.4). Hydrogen dissociation and cesium ionization were assumed to be independent.

Results are shown in Figure B.1 a. If conductivity in the range of 10 to 100 S/m is to be

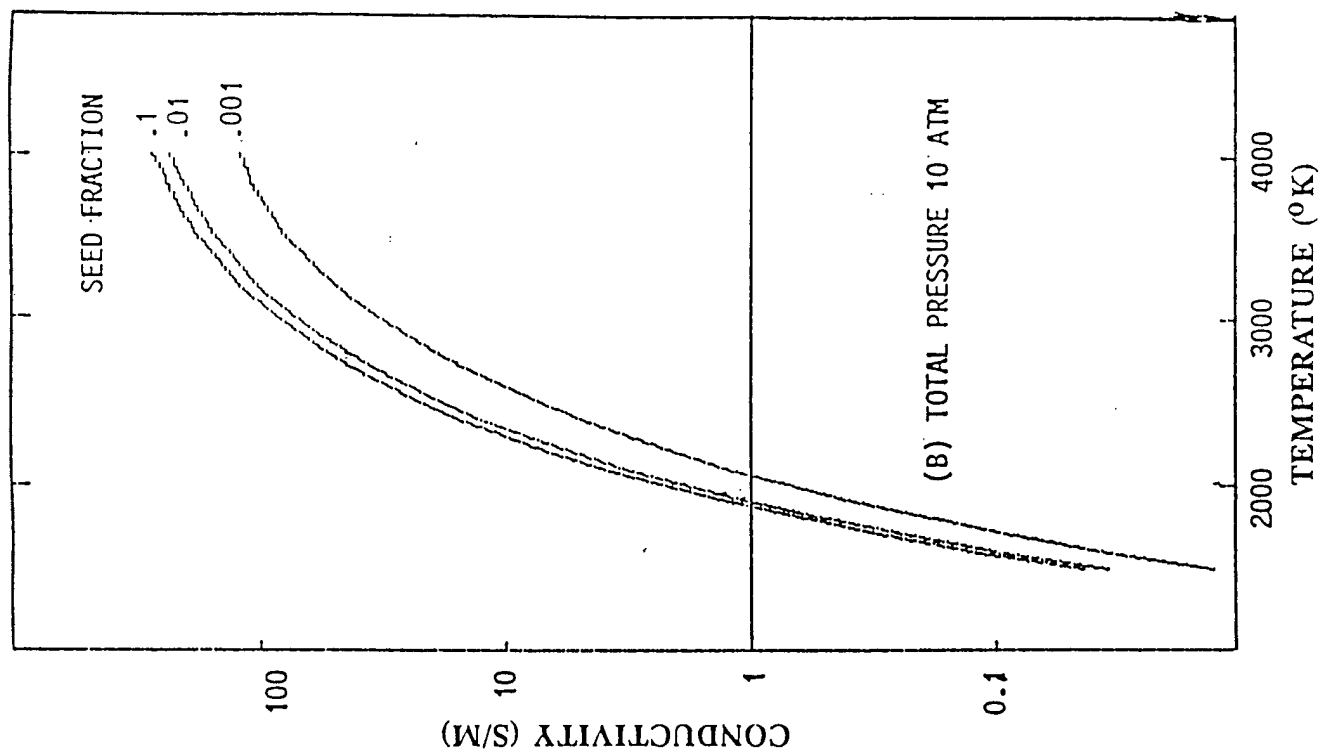
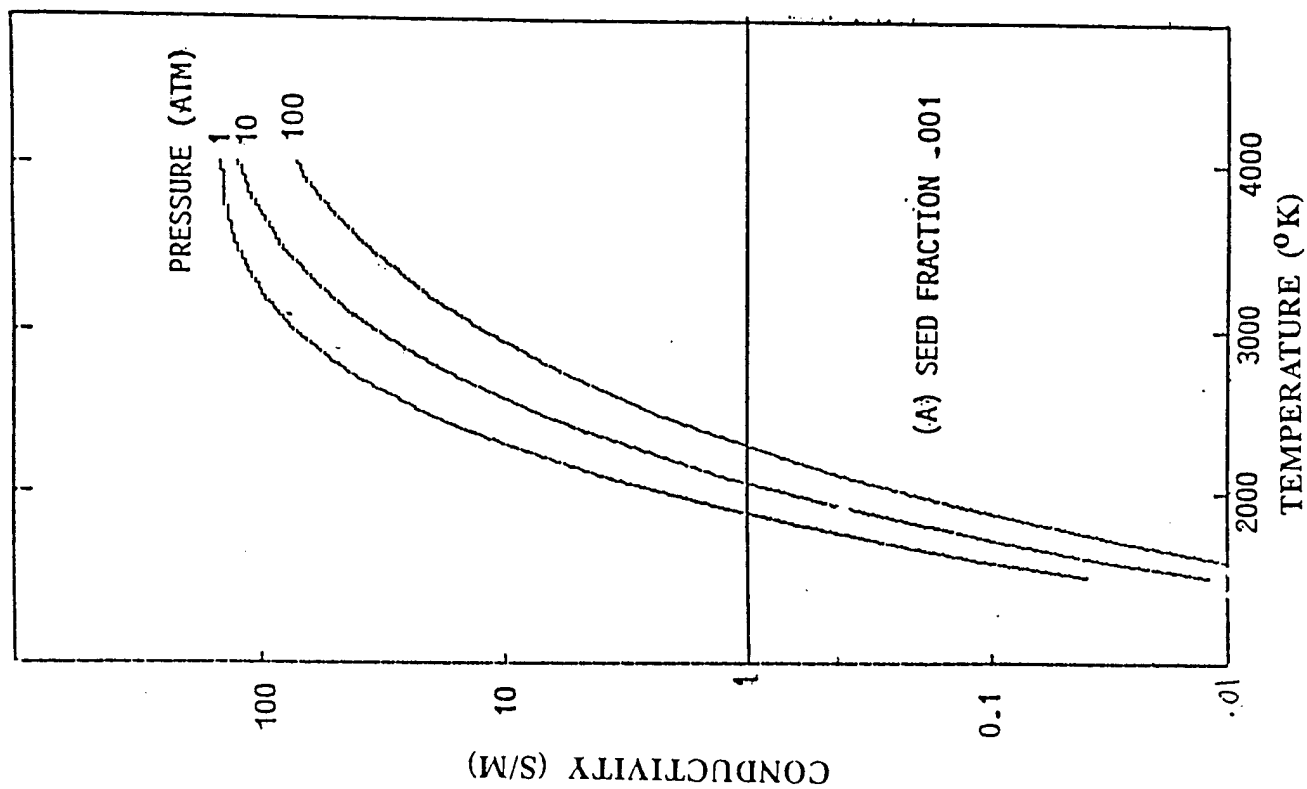


FIGURE B.1. ELECTRICAL CONDUCTIVITY OF CESIUM-SEEDED HYDROGEN PLASMAS.

achieved at a pressure of order 10 atmospheres, temperatures of order 3000 K will be necessary. Figure B.1b. indicates that seeding in excess of 1% (seed fraction 0.1) produces little additional conductivity. this effect is a consequence of the large collision cross-section of the cesium atoms.

Appendix B.1. gives detailed particle concentrations at 3000° Kelvin and Table B.1 gives the program listing.

Since these calculations do not take into account the effect of the presence of other, possibly electronegative, species, the curves of Figure B.1. are probably optimistic.

REFERENCES

- B.1. Turbo BASIC, Borland International, Inc. Scotts Valley CA.
- B.2. Rosa, R. J., Magnetohydrodynamic Energy Conversion, McGraw-Hill, N.Y., 1968.
- B.3. Frost, L. S., "Conductivity of Seeded Atmospheric Pressure Plasmas", Journal of Applied Physics, Vol. 32, No. 10, Oct 1961, pp 2029-2036.
- B.4. VanWylen, G. J. and R. E. Sonntag, Fundamentals of Classical Thermodynamics, 3rd SI Version, Wiley, 1985.

APPENDIX B.1

CONDUCTIVITY AND PARTICLE CONCENTRATIONS FOR A CESIUM- SEEDED HYDROGEN PLASMA AT 3000°K.

PTOT= 1.00 SEED FRACTION=0.0010

T= 3000K H2<=>2H: MOLE FR H=0.1464

KS=1.157E+20

NH2=2.085E+24 NH=3.578E+23 NCS=1.824E+21
NE-=4.423E+20 NCS+=4.423E+20 NTOT=2.446E+24

SIGMA= 71.2 S/M

PTOT= 10.00 SEED FRACTION=0.0010

T= 3000K H2<=>2H: MOLE FR H=0.0489

KS=1.157E+20

NH2=2.324E+25 NH=1.194E+24 NCS=2.227E+22
NE-=1.586E+21 NCS+=1.586E+21 NTOT=2.446E+25

SIGMA= 32.6 S/M

PTOT= 100.00 SEED FRACTION=0.0010

T= 3000K H2<=>2H: MOLE FR H=0.0157

KS=1.157E+20

NH2=2.405E+26 NH=3.842E+24 NCS=2.374E+23
NE-=5.221E+21 NCS+=5.221E+21 NTOT=2.446E+26

SIGMA= 11.9 S/M

PTOT= 1.00 SEED FRACTION=0.0100

T= 3000K H2<=>2H: MOLE FR H=0.1470

KS=1.157E+20

NH2=2.066E+24 NH=3.561E+23 NCS=2.116E+22
NE-=1.506E+21 NCS+=1.506E+21 NTOT=2.446E+24

SIGMA= 130.9 S/M

PTOT= 10.00 SEED FRACTION=0.0100

T= 3000K H2<=>2H: MOLE FR H=0.0491

KS=1.157E+20

NH2=2.303E+25 NH=1.189E+24 NCS=2.334E+23
NE-=5.134E+21 NCS+=5.134E+21 NTOT=2.446E+25

SIGMA= 72.4 S/M

PTOT= 100.00 SEED FRACTION=0.0100

T= 3000K H2<=>2H: MOLE FR H=0.0158

KS=1.157E+20

NH2=2.383E+26 NH=3.825E+24 NCS=2.410E+24
NE-=1.663E+22 NCS+=1.663E+22 NTOT=2.446E+26

SIGMA= 29.7 S/M

TABLE B.1.

PROGRAM LISTING FOR THE CONDUCTIVITY AND PARTICLE
CONCENTRATIONS FOR A CESIUM-SEEDED HYDROGEN PLASMA.

```

REM ELECTRICAL CONDUCTIVITY OF HYDROGEN CESIUM MIXTURES
REM DISSOCIATION BUT NO IONIZATION OF HYDROGEN
REM DISSOCIATION AND IONIZATION EQUILIBRIA ASSUMED INDEPENDENT
REM CONSTANT TOTAL PRESSURE
REM PRESSURE CORRECTED FOR DISSOCIATION OF H2
REM AND FOR CESIUM IONIZATION

```

```

      DIM PATM(10), XSECT(10), NP(10), TKHDIS(20), LNKHDIS(20)
      DIM TPL0T(50), SIGPLOT(50)

```

```

REM EQUILIBRIUM CONSTANT FOR HYDROGEN DISSOC (VAN W & S TABLE A.14)

```

```

      DATA 1000, -39.803, 1200, -30.874, 1400, -24.463
      DATA 1600, -19.637, 1800, -15.866, 2000, -12.840
      DATA 2200, -10.353, 2400, -08.276, 2600, -06.517
      DATA 2800, -05.002, 3000, -03.685, 3200, -02.534
      DATA 3400, -01.516, 3600, -00.926, 3800, 00.202
      DATA 4000, 00.934, 4500, 02.486, 5000, 03.725
      DATA 5500, 04.743, 6000.001, 05.590

```

```

      FOR I=1 TO 20
      READ TKHDIS(I)
      READ LNKHDIS(I)
      NEXT I

```

```

REM PHYSICAL CONSTANTS

```

```

      C1=6212.39      '[(8*k)/(PI*me)]^0.5, MAXWELL VEL
      C2=7.3373E27    '[1.013E5/k], PARTICLE CONCENTRATION
      C3=5040         '[(e/k)/(ln10)], CONST IN SAHA EQUIL EQ
      C4=26.9366      'ANOTHER CONSTANT IN EQ 2.3, ROSA
      C5=1.23886E7    '12*PI*(eps0*k/e^2)^1.5, DEBYE LENGTH
      C6=6.9812E-11   'e^2/(8*PI*eps0*k), FOR FQION
      C7=2.81793E-8   'e^2/me, FOR CONDUCTIVITY

```

```

REM THREE SPECIES H2, H, CS PLUS ELECTRONS AND IONS

```

```

      KMAX=3
      EI=3.89
      GI=1
      GO=2
      EPS=.0001

```

```

REM CROSS-SECTIONS: 1=H2, 2=H, 3=CS
      XSECT(1)=13.8E-20

```

```

REM IN ABSENCE OF DATA XSECT OF H ASSUMED SLIGHTLY LARGER THAT
REM THAT OF H2. COMPARE O2 AND O OR N2 AND N, SUTTON & SHERMAN PG 139
      XSECT(2)=15E-20
      XSECT(3)=300E-20

```

```

      CLS

```

```

REM DEFAULT VALUES (SEED FIRST)

```

```

      PTOT=1.0
      SEEDFR=.001

```

```

START:

```

```

REM TOTAL PRESSURE AND PARTIAL PRESSURES
REM WITH NO DISSOCIATION OF H2 OR IONIZATION OF CS
      PRINT

```

```

PRINT "PTOT=";
PRINT USING "###.##";PTOT;
PRINT " ATM";
PRINT " SEED FRACTION=";
PRINT USING "#####";SEEDFR
INPUT " CHANGE PRESSURES? (Y, N OR Q) : ",CH$
IF CH$="Y" THEN
  INPUT " TOTAL PRESSURE (ATM) : ",PTOT
  IF PTOT <= 0 GOTO START
  INPUT " SEED FRACTION : ",SEEDFR
  IF SEEDFR <= 0 GOTO START
ELSEIF CH$ = "Q" THEN
  GOTO QUIT
ELSEIF CH$ <> "N" THEN
  GOTO START
END IF
POH2=PTOT*(1-SEEDFR)
POCS=PTOT*SEEDFR

REM PLOT FILES OR INDIVIDUAL OUTPUTS (NEED DECISION BEFORE TEMPERATURE)
INPUT " WRITE FILES TO PLOT? (Y OR N) : ",WF$
IF WF$ = "N" THEN
  GOTO SINGLE
ELSEIF WF$ = "Y" THEN
  TK=1400
  NPLF=0
  NMAX=26
  GOTO WFILE
ELSE
  GOTO START
END IF

WFILE:
REM SET UP OUTPUT FILE AND WRITE RESULTS TO IT
NPLF=NPLF+1
TK=TK+100
IF NPLF > NMAX THEN
  INPUT " FILENAME : ",F$
  OPEN F$ FOR OUTPUT AS #1
  FOR NP=1 TO NMAX
    PRINT #1, USING " +###.#####^ ^ ^ ^"; TPLOT(NP); SIGPLOT(NP)
  NEXT NP
  CLOSE 1
  GOTO START
ELSE
  GOTO DISSOC
END IF

SINGLE:
REM SINGLE ENTRY WITH OUTPUT TO SCREEN AND PRINTER
INPUT " HARD COPY? (Y OR N) : ", HC$
IF HC$ <> "Y" AND HC$ <> "N" GOTO SINGLE
INPUT " ENTER TEMPERATURE (0 TO QUIT) : ",TK
IF TK = 0 GOTO QUIT

DISSOC:
REM DISSOCIATION EQUILIBRIUM
FOR I=1 TO 20
  IF TK < TKHDIS(I) THEN
    IF I = 1 THEN

```

```

      PRINT "TEMPERATURE LESS THAN 1000 K"
      STOP
    END IF
    INTERP=(TK-TKHDIS(I-1))/(TKHDIS(I)-TKHDIS(I-1))
    LNK=LNKHDIS(I-1)+INTERP*(LNKHDIS(I)-LNKHDIS(I-1))
    KHDIS=EXP(LNK)
    GOTO MOLEFR
  END IF
NEXT I
MOLEFR:
  XH=SQR((KHDIS/POH2)/(4+(KHDIS/POH2)))
  MLFH=(2*XH)/(1+XH)

REM SAHA EQUIL CONST, ROSA, EQUATION 2.3 (#/M3)
  FKS1=-(C3/TK)*EI
  FKS2=-1.5*LOG10(C3/TK)
  FKS3=+C4
  FKS4=LOG10(2*GI/GO)
  LOGKS=FKS1+FKS2+FKS3+FKS4
  KS=10^LOGKS

REM ELECTRON DENSITY RELATIVE TO UNDISSOCIATED H2 (#/M3)
  NOCS=C2*POCS/TK
  F1=KS/(4*NOCS)
  F2=KS/NOCS
  XE=SQR(F2)*(SQR(1+F1)-SQR(F1))
  NE=XE*NOCS

REM CORRECTED PARTIAL PRESSURES (ATM) AND PARTICLE CONCENTRATIONS (#/M3)
  DEN=(1+XH)*(1-SEEDFR)+(1+XE)*SEEDFR
  PP(1)=(1-XH)*POH2/DEN
  PP(2)=2*XH*POH2/DEN
  PP(3)=(1-XE)*POCS/DEN
  PP(4)=XE*POCS/DEN
  PP(5)=PP(4)
  PCHECK=0
  NTOT=0
  FOR N = 1 TO 5
    PCHECK=PCHECK+PP(N)
    NP(N)=C2*PP(N)/TK
    NTOT=NTOT+NP(N)
  NEXT N
  NECORR=NP(5)
  IF ABS((PCHECK-PTOT)/PTOT) > EPS THEN
    PRINT "PARTIAL PRESSURES DON'T CHECK"
    STOP
  END IF

REM
REM DEBYE LENGTH
  LAMBDA=C5*(TK^1.5)/NECORR^(1/3)

REM n*Q FOR ELECTRON-ION COLLISIONS
  FQION=C6/(TK^2)
  NI=NECORR
  NQION=3.9*NI*FQION*LOG(LAMBDA)

REM CROSS SECTION (KMAX=3, FOR THREE UNCHARGED SPECIES: H2, H, CS)
  FQ=0
  FOR K=1 TO KMAX

```

```

      FQ=FQ+NP(K)*XSECT(K)
    NEXT K
    FQ=FQ+NGION
    FQR=1/FQ

```

```

EM MAXWELL VELOCITY (M/SEC)
  CE=C1*SQR(TK)

```

```

EM CONDUCTIVITY
  SIGMA=C7*(NECORR/CE)*FQR
  IF WF$ = "Y" THEN
    TPLOT(NPLF)=TK
    SIGPLOT(NPLF)=LOG10(SIGMA)
    GOTO WFILE
  END IF

  IF HC$ = "Y" GOTO HARD

```

```

EM OUTPUT TO SCREEN
  PRINT
  PRINT "      T=";
  PRINT USING "####.";TK;
  PRINT "K";
  PRINT "      H2<=>2H: MOLE FR H=";
  PRINT USING "#.####";MLFH;
  PRINT "      KS=";
  PRINT USING "#.###^^^^";KS
  PRINT
  PRINT "      NH2=";
  PRINT USING "#.###^^^^";NP(1);
  PRINT "      NH=";
  PRINT USING "#.###^^^^";NP(2);
  PRINT "      NCS=";
  PRINT USING "#.###^^^^";NP(3);
  PRINT "      NE-=";
  PRINT USING "#.###^^^^";NP(4);
  PRINT "      NCS+=";
  PRINT USING "#.###^^^^";NP(5);
  PRINT "      NTOT=";
  PRINT USING "#.###^^^^";NTOT;
  PRINT "      SIGMA=";
  PRINT USING "####.#";SIGMA;
  PRINT " S/M"
  GOTO START

```

EM HARD COPY

HARD:

```

  LPRINT " PTOT=";
  LPRINT USING "####.##";PTOT;
  LPRINT " SEED FRACTION=";
  LPRINT USING "#.####";SEEDFR
  LPRINT
  LPRINT "      T=";
  LPRINT USING "####.";TK;
  LPRINT "K";
  LPRINT "      H2<=>2H: MOLE FR H=";
  LPRINT USING "#.####";MLFH;
  LPRINT "      KS=";
  LPRINT USING "#.###^^^^";KS
  LPRINT

```

```

LPRINT "    NH2=";
LPRINT USING "#.###^"; NP(1);
LPRINT "    NH=";
LPRINT USING "#.###^"; NP(2);
LPRINT "    NCS=";
LPRINT USING "#.###^"; NP(3);
LPRINT "    NE-=";
LPRINT USING "#.###^"; NP(4);
LPRINT "    NCS+=";
LPRINT USING "#.###^"; NP(5);
LPRINT "    NTOT=";
LPRINT USING "#.###^"; NTOT;
LPRINT "    SIGMA=";
LPRINT USING "####.#"; SIGMA;
LPRINT " S/M"
LPRINT
LPRINT
GOTO START

```

```

IT:
PRINT "PROGRAM EXITS"

END

```

APPENDIX C

PROGRAM LISTING FOR CALCULATING TEMPORAL CONDUCTIVITY FROM VOLTAGE VS. CURRENT DATA

This data reduction program is designed to operate automatically when used properly. Make sure that your data file is in two columns (A and B), with 1220 row in each column, and in an existing lotus file on a floppy disk.

NOTE: THE DATA SHOULD BE IN TWO COLUMNS WITH V AND I

Answer the questions properly and the program should output your calculated data file on the C: drive in the Sigmaplot files directory under the filename you choose.

Please do not give the output data file a name that already exists in that directory!

Do you want to continue? (Y or N) Y

MACRO AREA

```
VO          {GOTO} I1~{goto} N18~{?}~
            {IF @CELLPOINTER("CONTENTS")="Y"}{BRANCH BEGIN}
            {IF @CELLPOINTER("CONTENTS")="y"}{BRANCH BEGIN}
            /QY

BEGIN       {GOTO}I38~
            {WINDOWSOFF}{GOTO}AA1~
            /FCCNA1. .B1200~{esc}a:~{?}~
            {CALC}{GOTO}I38~{WINDOWSON}:
            {BRANCH XTRACT}

/C          /C~{PGDN}~

XTRACT     {goto}i58~{WINDOWSOFF}{GOTO}AP10~
            /FXV{ESC}{ESC}A:~{?}~
            {RIGHT}{PGNDN}{PGDN}~
            {GOTO}I78~{WINDOWSON}{BRANCH EXIT}

EXIT       {goto}I78~{q}/QY
```

APPENDIX D

LARGER SCALE TEST FACILITY DESIGN

The design of the small scale test facility was based on a model which assumed a steady-state flow, that is, for the estimated burning rate of the solid, it was assumed that gas flow rate out of the chamber was equal to the rate of gas generation.

The data seems to have indicated that the steady-state assumption is not valid. More likely, the solid burns in a small fraction of the run time, during which pressure and flow rate build up, followed by a more or less exponential pressure decay as the remaining gas discharges.

Analyzing the flow on this basis, "it was assumed that the gas temperature in the chamber is constant at the nominal stagnation value during the buildup phase and that the subsequent decay phase is isentropic. Both assumptions are obviously very rough but they do lead to a qualitative pressure trace which is a reasonable representation of the actual data.

There are uncertainties in the data, considerable run-to-run variation and some question regarding the effect of the blowout diaphragm, so the results must be considered very approximate.

Reference 1 (below) was used as the source for molecular weight and for the expansion coefficient (i.e. the value of k for the isentropic relation between pressure and density). At 3000 Kelvin they are equal to 1.97 and 1.16 respectively.

Based on a previous analysis, it was implicitly assumed a burning rate such that 1 kilogram of mixture would burn in 1/2 second. However, shorter burn times at fixed chamber volume and fixed maximum pressure then means smaller total mass flows.

Table D.I shows a new reference case designated ND1 (for New Design 1). The calculated performance is based on the model discussed above.

-
1. Patch, R. W., "Thermodynamic Properties and Theoretical Rocket Performance of Hydrogen to 100,000 K and $1.013\text{E}+08 \text{ N/m}^2$ ", NASA Lewis Research Center, NASA SP-3069, 1971.

PRESS RETURN :

GAS CONSTANT= 4220.3 FLIEGNER CONSTANT=0.00986
ZPMAX= 1.0000 ZASTR= 0.2000 ZH2FLOW= 1.0000 ZVOL= 0.0080
CHBRDIA(IN)=14.89 L/D= 2.50 CHERLEN(IN)=37.23
PMA(ATM)= 10.0 ASTR(M2)=7.300E-05 NOZDIA(IN)=3.796E-01 VOL(M3)=0.106250
ZTOI= 1.00 TOI(K)=3000 TAU(SEC)=0.638 TIME TO PEAK(SEC)=0.412
H2 FLOW RATE(KG/S)=0.02800 H2 MASS(KG)=1.154E-02 TOTAL MASS(KG)=8.134E-01

TIME	P1	P2
0.00	0.000	21.567
0.10	3.049	17.830
0.20	5.655	14.776
0.30	7.884	12.275
0.40	9.790	10.221
0.50	11.420	8.531
0.60	12.813	7.135
0.70	14.004	5.981
0.80	15.023	5.025
0.90	15.893	4.230
1.00	16.638	3.568
1.10	17.275	3.015
1.20	17.819	2.553
1.30	18.285	2.166
1.40	18.683	1.841
1.50	19.023	1.568
1.60	19.314	1.337
1.70	19.563	1.143
1.80	19.775	0.978
1.90	19.957	0.838
2.00	20.113	0.720
2.10	20.246	0.619
2.20	20.359	0.533
2.30	20.457	0.460
2.40	20.540	0.398
2.50	20.611	0.344

The total mass of reactants for Case ND1 is approximately 0.8 kg. Two sets of variations about this reference case was calculated.

Figure D.1 shows comparison of the reference case (Curve 1) with cases where the chamber volume is halved (Curve 4) and doubled (Curve 5) holding nozzle area constant. The larger volume can accommodate a larger charge of reactants without exceeding 10 atmospheres and results in a slower pressure decay.

Figure D.2, volume is held constant and nozzle exit is halved (Curve 6) and doubled (Curve 7). The mass of the reactant charge does not stay constant. A larger nozzle opening results in a longer rise time because the difference between rate of gas production and gas discharge is smaller. Moreover the difference in these rates is reduced as flow rate increases with pressure so the rate of pressure rise increases. Thus, assuming a constant burning rate, more mass is needed. The larger nozzle also results in a more rapid pressure decay.

Data for these variations is shown in Table D.II. For all cases the chamber is assumed cylindrical. Chamber size is shown for three values of the ratio of length to diameter (L/D). Choice of L/D will partly depend on length needed for instrumentation and on space or structural limitations. From a fluid dynamic standpoint, L/D should be a minimum of 1.5 and preferably 2 or more.

As a result of this analysis, an L/D of 2.5 was chosen for the design of the MHD heater for the large scale testing (case ND 4).

The downstream conductivity probe was mounted (Probe #3) in the jet from a converging nozzle, Figure D.3. Expanding the flow in a supersonic nozzle would have lowered the temperature significantly.

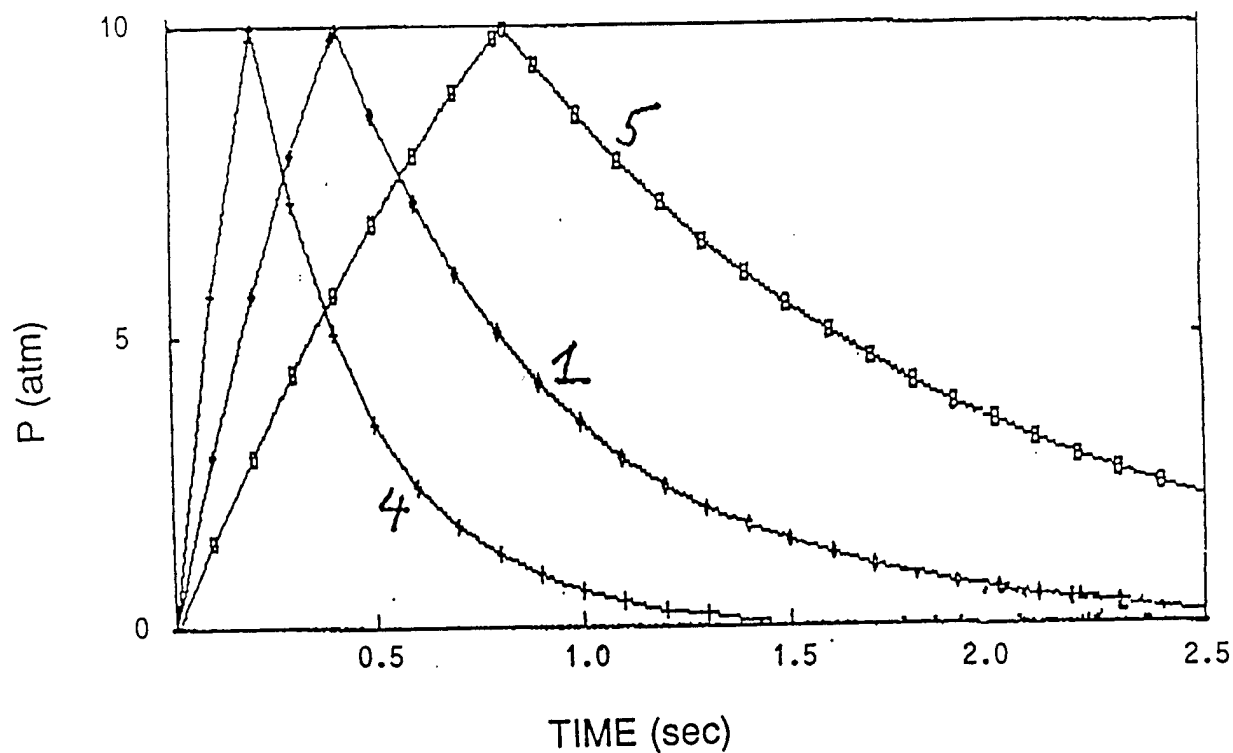


FIGURE D.1. PRESSURE VS. TIME FOR THREE DIFFERENT CHAMBER VOLUMES, NOZZLE AREA CONSTANT. 1=REFERENCE CASE; 4=VOL/2; 5=VOL X 2. SEE TABLE D.II FOR DETAILS.

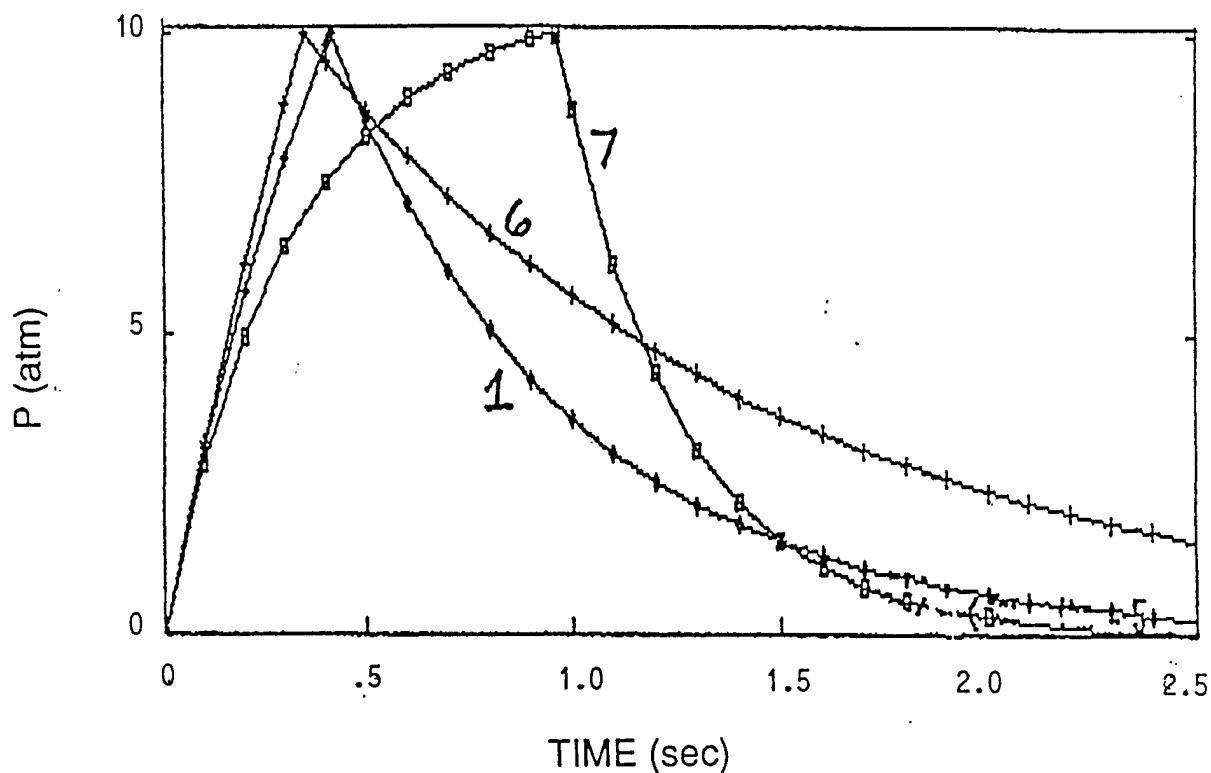
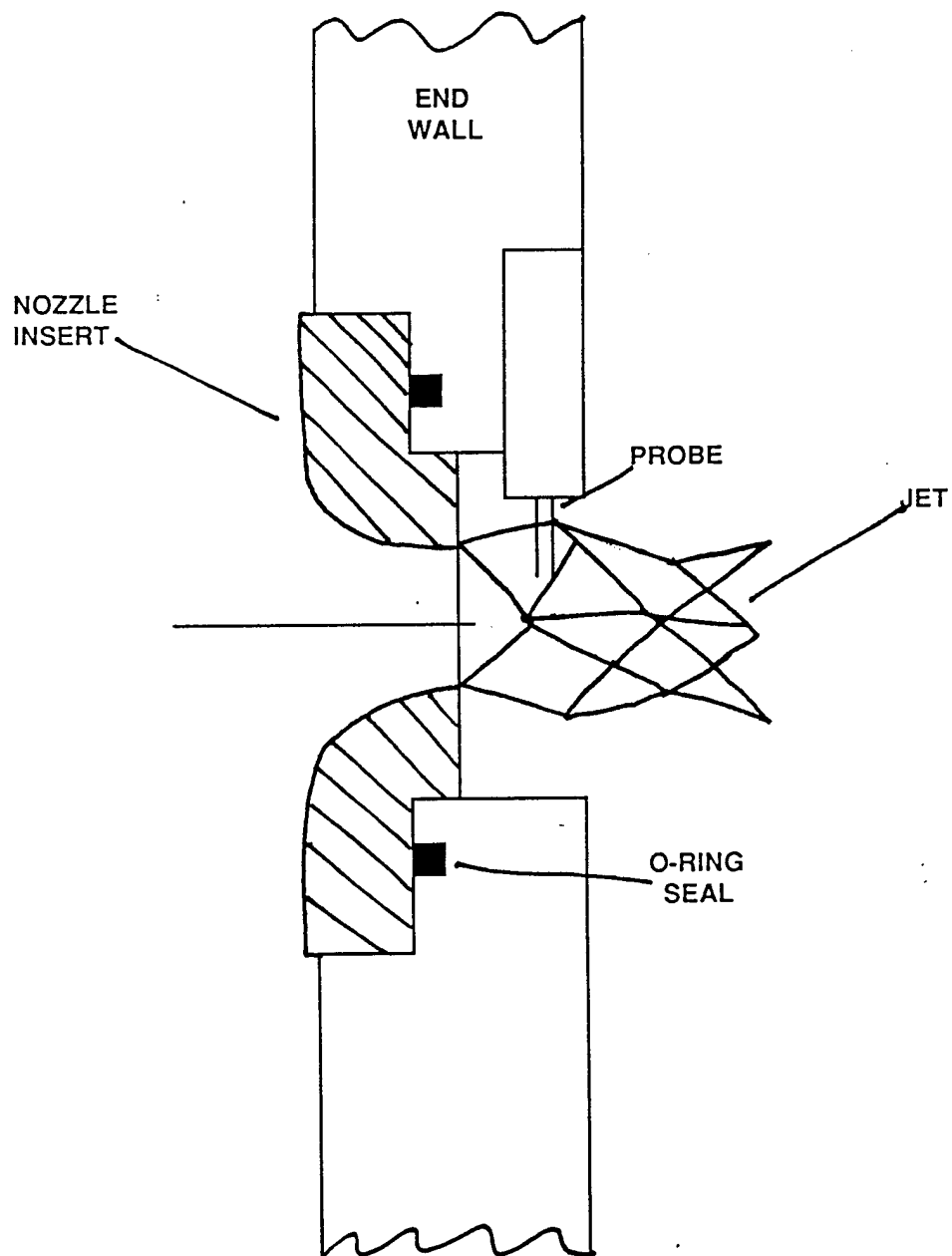


FIGURE D.2. PRESSURE VS. TIME FOR THREE DIFFERENT NOZZLE CROSS-SECTIONS. 1=REFERENCE CASE; 6=AREA/2; 7=AREA X 2. SEE TABLE D.II FOR DETAILS.

TABLE D.II.
GSI MHD HEAT SOURCE LARGE SCALE SCREENING TEST FACILITY

CASE	RELATIVE NOZZLE AREA	RELATIVE CHAMBER VOLUME	CHAMBER SIZE						NOZZLE DIA (in)	TIME TO PEAK PRESSURE (sec)	REACTANTS MASS (kg)	REMARKS
			L/D = 2.5		L/D = 2.0		L/D = 1.5					
			L (in)	D (in)	L (in)	D (in)	L (in)	D (in)				
ND 1	1	1	37.2	14.9	32.0	16.0	16.0	26.5	0.38	0.41	0.81	Reference Case Vary Vol. Vary Vol.
ND 4	1	0.5	29.6	11.8	25.5	12.7	21.1	14.0	0.38	0.41		
ND 5	1	2	26.9	18.8	40.4	20.2	33.4	22.3	0.38	1.63		
ND 1	1	1	37.2	14.9	32.0	16.0	16.0	26.5	0.41	0.81		Reference Case Vary Nozz. Area Vary Nozz. Area
ND 6	0.5	1	37.2	14.9	32.0	16.0	16.0	26.5	0.35	0.68		
ND 7	2	1	37.2	14.9	32.0	16.0	16.0	26.5	0.96	1.9		



~2 x Full Scale

Nozzle Detail
3/25/90
C. Marston

FIGURE D.3. NOZZLE DETAIL

APPENDIX E

PHOTOMETRIC MEASUREMENT OF TEMPERATURE

Hydrogen gas at 3000°K does not radiate appreciably. In order to measure temperature within the reaction chamber, it was necessary to measure the particle temperature and assume it was nearly the same as the gas temperature to support the conductivity measurements.

It was decided to measure the particle temperature by measuring its visible output. The visible output can then be correlated to blackbody temperature (see Figure D.1.). The Hi-Therm material generates particles that are nearly black (emissivity of the order of .9) allowing a direct measurement of particle temperature. The advantage in using the visible output is the strong dependence on temperature (i.e. visible output is proportional to about T^{10}). As a result even a larger error in visible intensity measurement has a much smaller error in the temperature measurement.

The photometer used was designed and fabricated at GSI. It consisted of a silicon photodiode detector fitted with a photopic filter (i.e. filter/detector combination that has a spectral response resembling the eye spectral response). The detector was fitted with a fiber-optic cable which was used to interface with the chamber. For the large scale tests, a window placed at the stagnation region of the chamber with a right angle prism interface to a 6 foot long fiber-optics cable which then interfaced to the outside port of the Franklin Research vacuum tank. The entire fiber optics/photometer system was then calibrated using a visible light source against a NBS calibrated United Detector Technology Photometer.

The measurement is based on the following photometric relationship,

$$\phi = B \Omega_{FOV}$$

where ϕ is the flux density measured at the entrance to the fiber-optic cable (units of lumens/meter² - LUX), B, is the source brightness (units of lumens/meter² steradian) and Ω_{FOV} is the solid angle formed by the field-of-view of the fiber-optic system, right angle prism, window and limiting apertures. For the measurements made in the large scale tests, the Ω_{FOV} was approximately .013 steradians. Consequently a measurement of ϕ divided by Ω_{FOV} is a measure of the source brightness.

For example in the 250 gram test, Figure E.4, the flux measured was in excess of 42,000 LUX. Dividing by the Ω_{FOV} gives a brightness in excess of 2.8×10^6 LUX/steradian. Converting to cm² yields a brightness in excess of 320 candles/steradian (STILBS). Referring to Figure D.1 yields a particle temperature in excess 2400°K. This value is a minimum temperature for two reasons:

- (1). The sensor saturated (note flat top of curve E.4). It is estimated that the flux was at least twice this value based on the sharp use and decay leading to a minimum temperature of at least 2600°K.
- (2). The particle cloud is not optically thick. Based on previous tests it is estimated that the particle cloud emissivity is about 0.5 leading to a brightness of at least 1200 stilbs. This is equivalent to a brightness temperature of about 2700°K.

Based on a pressure of about 6 atmospheres for this test, the expected conductivity should be about 80 S/M (see Figure B.1). The measured conductivity was about 100 S/M. The correlation of measured temperature and conductivity are seen to be within the experimental errors noting the many assumptions that have been made.

It might have been useful to have incorporated a fiber optic photometer at the center of the reaction chamber to see how the temperature correlated with the low conductivity measured there. However, due to the complexity of the instrumentation used it would have required extensive modifications to the reaction chamber.